INAUGURAL-DISSERTATION

submitted to the
Combined Faculties for the Natural Sciences and for Mathematics
of the Ruperto-Carola University of Heidelberg, Germany
for the degree of
Doctor of Natural Sciences

Presented by
Master of Science: Geok Choo, Sim
born in Johor, Malaysia

Dysfunctional Plasmacytoid Dendritic Cells but not NK cells in the Peripheral Blood of Stage IV Melanoma Patients

Referees: Prof. Dr. Rainer Zawatzky
PD. Dr. Annette Paschen

The present work was performed in the research group led by PD. Dr.Annette Paschen, clinical cooperation unit for Dermato-Oncology, German Cancer Research Center (DKFZ) and University Hospital Mannheim.

Publications during PhD work:

1. Annette Paschen, Antje Sucker, Bettina Hill, Iris Moll, Marc Zapatka, Xuan Duc Nguyen, Geok Choo Sim, Isabelle Gutmann, Jessica Hassel, Jürgen C. Becker, Alexander Steinle, Dirk Schadendorf and Selma Ugurel. Differential clinical significance of individual NKG2D ligands in melanoma: soluble ULBP2 as an indicator of poor prognosis superior to S100B. **Clin Cancer Res 2009;15(16):5208–15**

2. Geok Choo Sim, Xuan Duc Nguyen, Christine Falk, Drik Boorken, Dirk Schadendorf and Annette Paschen. **Regulation of TLR9 responses in plasmacytoid dendritic cells of melanoma patients. 2010** (Maunuscript in preparation).

Work presented in conferences:

3. G.C. Sim, D. Schadendorf, A. Paschen. The influence of tumour cells on the crosstalk between activated or resting natural killer and dendritic cell. **Abstract in the proceedings of DC2007; P080, 2007.**

4. Geok Choo Sim, Dirk Schadendorf and Annette Paschen. Differential Influence of Tumor Cells and IFN-α on the Crosstalk between Activated or Resting Natural Killer Cells and Dendritic Cells. **Abstract in the proceedings of Natural Killer cells symposium 2008; C23, 2008.**

5. Geok Choo Sim, Dirk Schadendorf, Christine Falk, Annette Paschen. Serum Cytokine, Chemokine and Growth Factor Profiles of Stage IV Melanoma Patient: Defining Combinatorial Patterns. **Abstract in the Keystone symposia: Mobilizing Cellular Immunity for Cancer therapy, Utah; Jan 2009.**

6. Geok Choo Sim, Dirk Schadendorf, Christine Falk, Annette Paschen. Defining combinatorial patterns of chemokines, cytokines and growth factors in sera from stage IV melanoma patients. **Abstract in the proceedings of Cancer Imunotherapy CIMT, P75; 2009.**

Table of contents

ACKNOWLEDGEMENTS

First and foremost, the author would like to take this opportunity to express her profound gratitude to the supervising committee members, PD. Dr. Annette Paschen from clinical cooperation unit for Dermato-Oncology of the German Cancer Research Center (DKFZ) and University Medicine Mannheim (UMM) for her patience and encouragement throughout the completion of the research. I thank very much also Prof. Dirk Schadendorf, Dr. Dirk Booken, Dr. Lisa Zimmer, Dr. Wolfram Fink and Dr. Xuan Duc Nguyen who have supported the work by providing valuable healthy donor and patient materials. Without their assistance and valuable contribution, this work would have been impossible. I am especially grateful to DKFZ for the financial support of this research.

My special appreciations to Prof. Dr. Rainer Zawatzky (DKFZ), Prof. Dr. Victor Umansky (DKFZ) and Prof. Dr. Gernot Geginat (UMM), who generously provided their insightful scientific expertise and suggestions during the course of this project. In addition, I would like to thank Prof. Dr. Rainer Zawatzky for supplying me with cytokine and UV-inactivated Newcastle virus (NDV) for my work.

My appreciations to Dr. Steffen Schmidt from the core facility of flow cytometry (DKFZ) and Melanie Ficht (UMM core facility of flow cytometry) for their technical assistance in flow cytometry and in cell sorting during the course of my study. I also would like to thank Dr. Christine Falk for her assistance in multiplex cytokine and chemokine assay. I thank also Dr. Felix Bestvater and Manuela Brom from the light microscopy facility (DKFZ) for their great assistance in the confocal microscopy analysis. Thanks also to Dr. Jessica Hassel and Silvia Pustal for their assistance in my study, my research group, and everybody in the clinical cooperation unit for Dermato-Oncology (DKFZ) and department of dermatology (UMM). My appreciation also extends to my friends especially Cleopatra Gkianatsuo, Kevin Richler, Marta Galach, Francis Peyre, Lydia Tome and Astrid Schmieder for bringing good memorial time during my course of study.

Last but not least, I would like to express my heartiest appreciation and thanks to my family member and Vladimir Riabov. Thanks for all your understanding and support throughout my studies.

Abstract

Dendritic cells (DCs) and Natural Killer (NK) cells are two key innate immune effectors that are of importance in the initiation and linkage of both innate and adaptive immune responses for preventing growth and spreading of malignant tumours. Immune dysfunction of DCs and NK cells in cancer patients apparently has a critical role in promoting tumour progression and limiting the efficacy of various immunotherapies. Therefore, identification of the mechanisms underlying this impairment and the molecules involved could facilitate the design of effective cancer therapies.

In the current work, the integrity of the number and functions of peripheral blood DC subsets, mDC1, mDC2 and pDCs from stage IV melanoma patients were analysed. We found a significant decrease in the absolute numbers of circulating pDCs and mDC2 in melanoma patients compared to aged-matched healthy controls. This change led to alterations of the mDC1/pDC and mDC2/mDC1 balance. Co-incubation experiments revealed an impairment of the mDC/pDC interaction upon CpG A stimulation, with little or no enhancement of surface CD40 expression on mDC1 from melanoma patients. This was in contrast to an up-regulation of CD40 expression on mDC1 from healthy donors under similar condition.

The activation of TLR9 signalling in pDCs by CpG A typically induces the production of various pro-inflammatory cytokines and chemokines. Interestingly, purified pDCs and PBMCs from melanoma patients when stimulated with CpG A produced lesser amounts of IFN-α than healthy controls. Furthermore, PBMCs from melanoma patients showed lower CCL5, CCL3 and CCL4 fold change compared to healthy controls, suggesting an impairment of TLR9 signalling in pDCs in response to CpG A stimulation. Interestingly, a dysregulated profile of cytokines and chemokines including IL-6, IL-8, CXCL10, CCL2, CCL4, CCL5 and IL-10 was also observed in the sera of patients.

Further analysis revealed a significantly stronger up-regulation of MyD88 and both IRF7 mRNA and protein expression in pDCs from healthy controls compared to patients upon TLR9 activation. Using flow cytometry and immunoblot analysis, it was demonstrated

that phosphorylation levels of the 4E-BP1 protein, controlling IRF7 mRNA translation, remained constant in CpG A stimulated pDCs and PBMCs from melanoma patients in contrast to healthy donors. Besides, the impairment of IRF7 up-regulation in pDCs from melanoma patients was accompanied by a reduced IRF7 translocation into the nucleus. Taken together, these data indicate that an impairment of the TLR9 downstream signalling cascade is responsible for the reduced IFN-α production by pDCs from melanoma patients.

Next, enumeration of NK cells in whole blood from melanoma patients revealed a significant reduction in $CD56^{+}CD16^{+}$ NK cell numbers. Interestingly, we found a significantly higher percentage of NKp30 and NKp46 receptor expressing NK cells accompanied with a higher expression level of both activating receptors on the peripheral blood NK cells from melanoma patients. Furthermore, patient NK cells exhibited comparable functional activity to healthy controls.

In conclusion, the data of this study provide evidences for an alteration in the function of circulating pDCs but not of NK cells from melanoma patients. An aberrant IFN-α production by pDCs is due to an impaired TLR9 signaling. This provides new insights in designing and improving melanoma therapy.

Zusammenfassung

Dendritische Zellen (DCs) und Natürliche Killer (NK) Zellen sind Immuneffektoren, die eine essentielle Rolle in der Initiierung und Verknüpfung von Immunantworten des angeborenen und adaptiven Immunsystems im Rahmen der Abwehr von Tumoren übernehmen. Eine Fehlfunktion von DCs und NK Zellen in Tumorpatienten scheint das Tumorwachstum zu fördern und die Effizienz von Immuntherapien zu beeinträchtigen. Daher ist es wichtig, Mechanismen, die zur Beeinträchtigung der Funktion dieser Effektoren führen, zu identifizieren, um somit eine Entwicklung effizienter Tumortherapien zu ermöglichen.

In der vorliegenden Arbeit wurde die Integrität der Zahl und Funktion von DC Subgruppen, mDC1, mDC2 und pDCs, aus dem peripheren Blut von Stadium IV Melanompatienten untersucht. Es konnte eine signifikante Reduktion in der absoluten Zahl der zirkulierenden pDCs und mDC2 in Melanompatienten im Vergleich zu gesunden Kontrollpersonen entsprechenden Alters gemessen werden. Diese Reduktion führt zu Veränderungen in der mDC1/pDC und mDC2/mDC1 Balance. Weiterhin konnte im Rahmen einer mDC/pDC Koinkubation mit CpG A gezeigt werden, dass eine Störung der mDC/pDC Interaktion in Melanompatienten vorliegt. So führte die Koinkubation auf den mDC1 von Melanompatienten zu keiner oder nur zu einer sehr schwachen Hochregulation der CD40 Oberflächenexpression, während im Falle der mDC1 gesunder Spender eine deutliche Verstärkung der CD40 Expression detektiert werden konnte.

Die Aktivierung der TLR9 Signalkaskade in pDCs durch CpG A induziert typischerweise die Synthese und Freisetzung verschiedener pro-inflammatorischer Zytokine und Chemokine. Interessanterweise zeigten PBMCs und aufgereinigte pDCs von Melanompatienten nach Stimulation mit CpG A eine geringere Produktion von IFN-α im Vergleich zu den Zellen gesunder Spender. Außerdem produzierten PBMCs aus Patienten nach CpG A Stimulation geringere Mengen an CCL5, CCL3 und CCL4, was darauf hindeutet, dass die TLR9 Signalgebung in pDCs von Melanompatienten beeinträchtigt ist. Interessanterweise konnte auch ein verändertes Profil von Zytokinen

und Chemokinen wie IL-6, IL-8, CXCL10, CCL2, CCL4, CCL5 und IL-10 in Seren von Melanompatienten nachgewiesen werden.

Weitere Analysen ergaben, dass die Induktion von MyD88 sowie IRF7 mRNA und Protein infolge TLR9 Stimulation in den pDCs gesunder Spender im Vergleich zu Patienten pDCs signifikant erhöht war. Mittels Durchflusszytometrie und Immunoblot, konnte gezeigt werden, dass der Phosphorylierungsstatus der 4E-BP1 Proteins, welches die IRF7 mRNA Translation kontrolliert, nach CpG A Stimulierung in pDCs and PBMCs von Melanompatienten im Gegensatz zu gesunden Spendern konstant blieb. Neben einer verminderten IRF7 Hochregulation wurde auch eine verringerte Translokation von IRF7 in den Nukleus von pDCs aus Melanompatienten beobachtet. Zusammenfassend deuten diese Daten auf eine Beeinträchtigung des TLR9 nachgeschalteten Signalwegs hin, welche für die verringerte Produktion von IFN-α durch pDCs aus Melanompatienten verantwortlich ist.

Im Anschluss wurde die Zahl von NK Zellen im Gesamtblut von Melanompatienten bestimmt. Es zeigte sich, dass diese im Vergleich zu gesunden Spendern signifikant reduziert ist. Allerdings konnte in Melanompatienten ein signifikant erhöhter prozentualer Anteil von NKp30 und NKp46 Rezeptor-exprimierenden NK Zellen detektiert werden, einhergehend mit einem erhöhten Expressionslevel beider Rezeptoren. Interessanterweise zeigten NK Zellen aus Patienten und gesunden Spendern eine vergleichbare Aktivität.

Die Daten dieser Arbeit beweisen, dass in Melanompatienten die Funktion von zirkulierenden pDCs, aber nicht von NK Zellen, beeinträchtigt ist. Die aberrante IFN-α Produktion durch pDCs der Patienten wird durch eine Beeinträchtigung des TLR9 Signalwegs verursacht. Somit konnten neue Erkenntnis für die Verbesserung und Entwicklung gewonnen werden.

Abbreviations:

All abbreviations employed in this research report are those accepted by the Biochemical Journal. (Biochemical Journal; 1978, 169, 1-27). Other abbreviations used are as listed.

APC	antigen-presenting cell
APC	allo-phycocyanin
Ab	antibody
BCR	B cell receptor
BDCA	blood dendritic cell antigen
BSA	bovine serum albumin
bp	base pair
CCL	chemokine ligand
CCR	chemokine receptor
CD	cluster of differentiation
cm	centimeter
CTL	cytotoxic T lymphocyte
CTLA	cytotoxic T Lymphocyte antigen
CO_2	carbon dioxide
cDNA	complementary DNA
(CpG DNA)	unmethylated CpG motifs
c_T	threshold cycle
°C	degree Celsius
DC	dendritic cell
DNA	deoxyribonucleic acid
DMSO	dimethylsulfoxide
dNTP	deoxynucleoside triphosphate
ECL	enhanced chemiluminescence
EDTA	ethylenediaminetetraacetic acid
ELISA	enzyme-linked immunosorbent assay
ER	endoplasmic reticulum
FACS	fluorescent activated cell sorting
FAM	6-Carboxy-fluorescein
FCS	fetal calf serum
FITC	fluorescein-5-isothiocyanate
Flt-3L	Fms-like tyrosine receptor-3 ligand
FSC	forward scatter
g	gramm
g	centrifugal force/gravity
GM-CSF	granulocyte/macrophage colony stimulating factor
h	hour
HRP	horseradish peroxidase
H_2O	water
H_2SO_4	acid sulphuric
HNSCC	head and neck squamous cell carcinoma
IDO	indoleamine 2,3-dioxygenase

IFN	interferon
IFNAR	intereferon alpha receptor
Ig	immunglobulin
IL	interleukin
IMDM	Iscove's Modified Dulbecco's medium
IRFs	IFN regulatory factors
IRAK	Interleukin-1 receptor-associated kinase
ISGF3	Interferon-stimulated gene factor 3
ISRE	Intereferon stimulated response element
IU	International units
L	Liter
LPS	lipopolysaccharides
LRR	leucine rich repeat
MACS	magnetic cell sorting
MDA5	melanoma differentiation-associated gene 5
MDCs	myeloid dendritic cells
MHC	major histocompatibility complex
Mo-DC	monocyte-derived dendritic cells
min	minute
MIP	macrophage inflammatory protein
M	molar (mol/l)
mM	millimolar
mL	milliliter
mg	milligramm
mm	millimeter
µL	microliter
µg	microgramm
MEF	mouse embryonic fibroblast
MFI	median fluorescence intensity
mRNA	messenger RNA
MyD88	myeloid differentiation primary-response protein 88
NK cells	natural killer cells
NKT	natural killer T cells
nm	nanometer
NDV	newcastle disease virus
NF-κB	nuclear factor kappa B
Oligo	oligonucleotide
ODN	oligodeoxynucleotide
OAS1a	2'-5' Oligoadenylate synthetase 1A
%	percentage
PAGE	polyacrylamide gel electrophoresis
PAMP	pathogen-associated molecular pattern
PBMC	peripheral blood mononuclear cells
PBS	phosphate buffered saline
PCR	polymerase chain reaction
PE	phycoerythrin

Pen/Strep	penicillin/streptomycin
pDCs	plasmacytoid dendritic cells
pg	pikogramm
PGE_2	prostaglandin E2
poly (I:C)	polyriboinosinic polyribocytidylic acid
PKR	protein kinase PKR
PRR	pattern recognition receptor
RNA	ribonucleic acid
rpm	revolutions per minute
RPMI	Roswell Park Medical Institute
RIG-I	retinoic acid-inducible gene I
RT	reverse-transcriptase
RT	room temperature
SSC	side scatter
SD	standard deviation
SDS	sodium dodecyl sulphate
ssRNA	single-stranded RNA
STAT	signal transducer and activator of transcription
TCR	T-cell receptor
TGF-β	transforming growth factor-β
TLR	Toll-like receptor
TIR	Toll/IL-1 receptor
TRAIL	TNF-related apoptosis-inducing ligand
TRAF	TNF receptor-associating factor
TRIF	TIR-domain-containing adaptor protein inducing IFN-β
Tris	tris-hydroxymethyl-aminomethane
TYK2	tyrosine kinase 2
TEMED	tetramethylethylenediamine
TNF	tumor necrosis factor
Treg	regulatory T cell
Tr	T regulatory cell
U	Unit
VEGF	vascular endothelial growth factor
V	volt
v/v	volume per volume
w/v	weight per volume

1.0 INTRODUCTION

1.1 Cancer

Cancer is not a modern disease as the awareness of cancer has been documented since a few thousand years ago. The use of the term “cancer” to describe this “incurable” disease can be found in the oldest description of human breast tumour written on Egyptian papyrus between 3000-1500 BC (1). Today, cancer is the leading cause of death worldwide. The formation of cancer is initiated with transformation of a normal cell into pre-cancerous cells with predisposed genetic defects or under influence of external agents of carcinogenesis. Tumours that arise from single transformed cells further evolve into a heterogenous population with different genetic signatures. The transformed cancer cells usually possess genetic alterations that govern cell physiology including cell proliferation, insensitivity to growth-inhibitory signals, evasion of apoptosis, tissue invasion and metastasis and sustained angiogenesis (2). Accumulation of genetic alterations along the tumour development equips cancer cells with various mechanisms that confer protection against recognition and elimination by immune cells.

1.1.1 Melanoma

Melanoma is a malignant tumour mainly originating from melanocytes in the skin and thus is generally recognized as type of skin cancer. Indeed it represents a neuroectodermal neoplasm that could arise from pigmented cells and is therefore detectable in skin, brain, mucous membranes and other organs. Melanoma accounts for >76% of skin cancer-related death and the incidence increases fastest among all cancers over recent years. Yet, it is one of the cancer types that is highly preventable if discovered at early stages and could achieve remission even in advanced stages for some instances. Survival of the disease depends on the vertical depth of invasion of the primary tumour into the dermis, which is measured as Breslow depth (3). Primary tumour thickness of < 1 mm Breslow depth (stage I) at the time of diagnosis gives excellent prognosis. Patients having tumours with a Breslow depth > 4 mm (Stage IIB), ulceration and metastasis at sentinel lymph node may have intermediate-to-high risk of relapse from

treatment. Patients with stage IV melanoma represents those with distant metastases and the 5 year survival rate is <10% (4).

Melanoma arises due to predisposed or acquired genetic alterations within the melanocytic system. These mutations affect signal transduction pathways that govern cellular proliferation, expression of tumour oncogenes and inactivation of tumour-suppressor genes. One of such genes is B-RAF that acts as a regulator of the MEK-ERK1/2 pathways. It has been found mutated in over two-thirds of human malignant melanoma (5). Mutation up-stream of RAF, exclusively affecting the NRAS gene, have also been discovered in human melanoma (6). Furthermore, alteration of PTEN, a tumour suppressor gene was detected in approximately 10% of melanomas (7). PTEN is one of the phosphatases critical for suppressing the PI3K pathway, its constitutive activation is frequently associated with tumorigenesis. Dysregulated PTEN could thus lead to an activation of AKT1/2/3, the downstream molecules of the PI3K signaling pathway (8) that participate in the cellular proliferation.

1.1.2 Melanoma therapies

Chemotherapy/chemoimmunotherapy

Chemotherapy is currently the standard treatment for the majority of melanoma patients with advanced disease. There are various cytotoxic drugs including Dacarbazine (DTIC), Taxanes (including paclitaxel and docetaxel), Temozolomide and Cisplatin, which have been used as single chemotherapeutic agents to treat melanoma patients in the early time. DTIC is so far the only US Food and Drug Administration (FDA) approved chemotherapy agent for metastatic melanoma and the objective response rates are between 15-20% (9). Cisplatin, another potential chemotherapeutic agents has modest activity with partial responses are observed in about 10% of patients (10,11) On the other hand, treatment with Temolozomide in phase III clinical study revealed a median survival of 7.7 months in patients with advanced disease and demonstrated efficacy equal to that of DTIC (12). Apart from using cytotoxic drugs as single agent, combined chemotherapy has been performed in different phase of clinical trials including the combination of Cisplatin, Vinblastine and DTIC and the combination of Thalidomide and Temolozomide

(13, 14). The combination of DTIC and IFN-α as form of chemoimmunotherapy was evaluated in phase III trial and revealed a comparable median survival compared with DTIC alone (15).

Surgery

Surgical excision has been widely used and considered for melanoma patients who have residual respectable disease after systemic therapy. Metastasectomy has been associated with prolonged survival for recurrent melanoma if all disease could be resected. The median survival of patients that underwent complete metastasectomy was 18.2 months in comparison to 5.9 months in nonsurgical treatment (16).

Radiotherapy

Radiotherapy is the usage of ionizing radiation to damage DNA and to arrest the growth of malignant cells. Primary radiation is applied as a second-line treatment for non-resectable lentigo maglina in the skin while it is often used for ocular melanoma (17). Radiotherapy has been shown to be effective for the palliation of brain and bone metastases. A study by Lavine *et al.* demonstrated that patients who underwent radiosurgery using gamma knife for brain lesion resection achieved a median survival of 8 months and 77.8% of treated patients experienced either improved or stable neurological symptomatology (18).

Immunotherapy

Cytokine immnnotherapy

IFN-α2b was the first exogenous cytokine approved by the FDA and demonstrated to have modest activity as single agent in treating melanoma. This cytokine has been proven to exert immunoregulatory effects, anti-proliferative, pro-apoptotic and anti-angiogenic activities in multiple maglinancies (19). The use of IFN-α2b in phase I/II trials revealed a rate of objective responses at an average of 10-15% for metastatic disease (20). As the only cytokine approved for adjuvant therapy, IFN-α2b has been proven to significantly reduce the risk of recurrence in melanoma patients (21). Furthermore, high-dose IL-2 was

also approved for melanoma treatment and long term analysis of the phase II trials showed an objective response rate of 16% (22).

Vaccination

Tumour vaccines have been applied in several clinical studies, which were designed to either enhance the immunogenicity of tumour cells or to enhance the antitumour immune response via lymphocyte activation. Cancer vaccines for treating melanoma involve the application of mixed antigens or single antigens specific for the tumour target. Antigens are delivered as single agents or loaded on monocyte-derived DCs (mo-DCs), which are generated i*n vitro* using GM-CSF and IL4 and further matured with cytokine cocktails (23, 24). Among these antigens that have been used in clinical trial are melanocyte lineage antigens (MART-1/melan-A, tyrosinase or gp100) (24), or those over-expressed in tumour tissues such as p53 and survivin.

Novel approaches

Several new approaches for improving cancer immunotherapy including CTLA4 blockade and adoptive T cell transfer have shown some promises for treating melanoma. The CTLA4 molecule is expressed by T cells upon their activation and its binding to CD80/CD86 on antigen presenting cells (APC) delivers inhibitory signals to limit excessive T cell activation. CTLA4 blockade is the application of anti-CTLA4 mAbs to block inhibitory signals by preventing the CTLA4-CD80/CD86 engagement with the aim to prolong T cell activation (25, 26). Adoptive T cell transfer is based on the *in vitro* expansion of autologous anti-tumour lymphocytes and the subsequent re-infusion into the patient to boost adaptive immunity of cancer patients. Both approaches are currently undergoing further evaluation in clinical trials (27).

1.2 The immune system

The human immune system is complex and composed of diverse cells and soluble mediators that interact in a dynamic network to protect the host from the invasion of foreign pathogens and to maintain self tolerance. A large variety of immune cells that patrol in the blood and reside in peripheral tissues render the generation of a rapid

immune response when encountering ‘danger’ signals. The mammalian immune system has evolved in a way that two subsets of immunity can be classified, the innate and the adaptive immunity.

1.2.1 Innate immunity

The innate immune system is the first line of immune defence against infection or pathogen invasion. Immune cells that serve in initiating innate immune responses are dendritic cells, natural killer cells, macrophages, mast cells and granulocytes (neutrophils, basophils, and eosinophils). Together with soluble factors such as cytokines and complements, the innate immune sytem cooperates with the adaptive immune system to generate protective immune responses. Innate immune cells are generally equipped with additional pathogen sensing receptors, such as germline encoded Toll like receptors (TLRs) to allow the recognition of conserved pathogen associated molecular patterns (PAMPs), uniquely found in microbes and viruses but not in self-tissue.

Cellular-mediated innate immunity

Macrophages are phagocytes, very efficient in engulfing pathogens. They reside in the lymphoid and non-lympohid tissues and maintain tissue homeostasis in steady state. Expression of a broad range of TLRs by macrophages including TLR4, allow macrophages to respond to bacterial insult. Activation of macrophages is typically characterized by the secretion of nitric oxide, pro-and anti-inflammatory cytokines depending on the stimulus.

Polymorphonuclear leukocytes comprise neutrophils, eosinophils and basophils, which make up approximately 50-70 % of all white blood cells. These cells play an important role in acute and chronic inflammation and are essential for host defence. They are also involved in the regulation of immune responses, participate in angiogenesis, and play a role in tumour biology (28, 29). Mast cells are another cell subtypes found resident in tissues throughout the body and appear to play vital roles in innate immunity with multiple critical biological functions (30). Dendritic cells (DCs) and natural killer (NK)

cells are two major innate immune cell types. Their characteristics are described in detail in section 1.3 and 1.4.

1.2.2 Adaptive immunity

Adaptive immunity is a more specialized immunity than innate immunity in such that it supplements the protection rendered by innate immunity. B and T lymphocytes are the two major immune cells responsible for the adaptive immunity in which B cells mediate humoral immunity while T cells provide cellular-mediated immune responses. Unlike innate immune cells, both B and T cells express antigen-specific receptors generated somatically, the BCR and TCR, respectively. Both TCR and BCR are highly diverse and are generated by random rearrangement of TCR and immunoglobulin (Ig) gene segments, respectively, thereby contributing to the diverse lymphocytes repertoire, which is able to recognise a broad range of antigens. Since the TCR and BCR are randomly rearranged, 'education' on specific antigens is a pre-requisite to achieve safe and efficient immunity and to prevent auto-reactivity. Another characteristic of adaptive immunity is the immunological memory of T and B cells, which allows an instant and vigorous response to a particular antigen.

T lymphocytes

There are two major subsets of T cells that have been identified based on the expression of the co-receptor molecules CD4 and CD8 on the cell surface. $CD4^+$ T cells can act as helper T cells that play a role in the activation of other cells such as $CD8^+$ T cells and B cells. Activation of $CD4^+$ T cells requires interaction of the TCR with the antigen presented on MHC II that are expressed by professional antigen presenting cells such as DCs (30). It has been established that various types of cytokines, which have biological impact on other immune cells are secreted by $CD4^+$ T cells upon activation. The distinct cytokine profiles secreted by $CD4^+$ T cells are further classified into T helper 1 (Th1) and T helper 2 (Th2) cytokines. Generation of Th1 $CD4^+$ T cells relies on the presence of pro-inflammatory cytokines such as IFN-γ and IL-12 during T cells stimulation, while Th2 differentiation is promoted by IL-4. Differentiated Th1 cells in turn have been shown to secrete IFN-γ, TNF-β, GM-CSF and IL-2 and mediate cell-activated immune responses

while Th2 cytokines secreted by Th2 cells including IL-4, IL-10, IL-13, and IL-5 play important roles in inducing humoral immune responses (30).

The other major T cell population consists of $CD8^+$ T cells which function in mediating lysis of tumour cells or virus infected cells and thus are frequently referred to as cytotoxic T cells (30). Naïve $CD8^+$ T cells activated via peptide-MHC I complex-TCR interaction, co-stimulatory signals, IL-2 secreted by $CD4^+$ T cells and signals from IL-12 and IFN-α further undergo robust expansion and differentiation into effector $CD8^+$ T cells. The effector $CD8^+$ T cells recognise targets carrying specific antigens and mediate cytolytic activity via the release of perforin, granzymes, IFN-γ and through the FAS/FASL pathway (30). The rapid expansion of effector cells is then followed by a phase called contraction where most of the cells undergo apoptosis when infection or inflammation is resolved. The remaining antigen specific T cells survive and differentiate into long-lived memory T cells, which allow a rapid response in subsequent exposure with the same antigen.

B lymphocytes

B lymphocytes are the key cells responsible for generating humoral immune responses. B cells are known to recognise soluble antigens specifically via their BCR and additional signals derived from T helper cells contribute to their full activation. Upon activation, B cells have been shown to secrete antibodies that bind to specific antigens on the surface of invading microbes (such as viruses or bacteria), which flags them for destruction by phagocytes (30, 31). Similar to T cells, antigen-specific B cells are found to develop into memory B cells, which enable them to live for a long time and generate rapid responses following a second exposure to the same antigen.

1.3 Dendritic Cells

Dendritic cells (DCs) are key effector cells in initiating and linking both innate and adaptive immune responses. They were first described by Ralph Steinmann and colleagues as a rare subset of accessory cells with unique T-cell stimulatory capacity in contrast to macrophages (32). Further investigations unveiled the unique capability of

DCs to take up, retain, process and to present antigens to T cells. Accompanied by Th1-driven cytokines e.g IFN-γ and IL-12p70, the interaction of mature DCs and T cells could lead to an efficient Th1 immune response that is crucial for protecting the host from infection and tumors. To date, DCs are widely accepted as the only APCs capable of eliciting primary and boosting secondary immune responses (33, 34). Many different subtypes of DCs widely distribute throughout the body. In steady state, DCs can be found in trace amounts in the blood, lymphoid tissue, thymus, skin, gastrointestinal and respiratory system (34). Each of the DC subtypes exhibits specialized functions depending on their anatomical location. For instance, thymic DCs are involved in initiating tolerance of developing T cells to prevent reactivity with self antigens (35). Whereas, follicular DCs are mainly present within the primary B-cell follicles and play a central role in humoral immunity (34).

1.3.1 DC development

DCs are commonly believed to derive from separate haematopoietic precursors namely myeloid and lymphoid precursors. The conventional or myeloid DCs including mo-DCs, interstitial DCs and Langerhans DCs are proposed to differentiate from the myeloid lineage expressing myeloid makers such as CD33 (33). On the other hand, pDCs are believed to derive from a common lymphoid progenitor that is distinct from myeloid DCs as pre-pDCs lack most of the myeloid markers (36) and the differentiation of immature pDCs depends on IL-3 but not GM-CSF, which is required for mDC differentiation. The development of pDCs from haematopoietic progenitors appears to depend on FLT-3 ligand as injection of FLT-3 ligand *in vivo* dramatically increases the numbers of pDCs in human and mice (37). A recent report by ChiCha *et al*. however, suggested that pDCs can arise from both common lymphoid and common myeloid progenitors (38). *In vitro*, using distinct growth factor and cytokine combinations, different DCs can be generated from $CD34^+$ precursor cells, cord blood and monocytes in human whereas bone marrow serves as major source for generating murine DCs.

1.3.2 Antigen uptake and processing by DCs

DCs present in the periphery are in a state called immature stage and are highly potent to capture and internalize antigens from the surrounding, which may trigger their activation. DCs efficiently engulf antigens through pinocytosis and receptor-mediated endocytosis. There are many receptors expressed by DCs that appear to have crucial function in antigen up-take, among these are the Fc receptors, DEC205/CD205 in mouse, DC-SIGN/CD209, mannose-receptor/CD206 and langerin/CD207 (39). Meanwhile, expression of pattern recognition receptors (PRRs) such as TLRs, retinoic acid-inducible gene I (RIG-I) and intracellular oligomerization domain (NOD)-like receptors (NLRs) facilitate the recognition of microbes by conserved pathogen associated molecular patterns (PAMPs).

Antigens taken up by DCs in peripheral organs are delivered to the cellular antigen processing compartment. Extracellular antigens are endocytosed by cells and degraded by proteases in endosomes to generate immunogenic peptides. The late endosome containing the endocytosed and degraded proteins are then fused with vesicles carrying MHC class II molecules that export from endoplasmic reticulum (ER) and allowing the assembly of MHC class II molecules with antigenic peptides to form the peptide-MHC II complexes (30). On the other hand, cytoplasmic antigens derived from different sources like viruses are processed by the proteasome into peptides and transferred by TAP proteins into the ER. The peptides are then loaded onto MHC class I molecules and peptide-MHC complexes are transported to cell surface via the Golgi apparatus (30). A process called cross-presentation occurs when extracellular antigens derived from viruses and bacteria were transferred into the MHC class I pathway for triggering $CD8^+$ cytotoxic T cell (CTL) activation. Furthermore, DCs express CD1d, another antigen presenting molecule that is similar to MHC class I but specialised in presenting lipid instead of protein antigens to NKT cells.

1.3.3 DC as Antigen Presenting Cell

Immature DCs with low expression of MHC, co-stimulatory and adhesion molecules are less motile and unable to form conjugates with T cells for priming until they undergo

maturation. After the up-taking and processing of antigens and in the presence of inflammatory cytokines (e.g. TNF-α), the 'licenced' or immunogenic DCs lose the capability of antigen acquisition and antigen processing. But, they up-regulate adhesion molecules (CD54), chemokine receptors (e.g. CCR7) and co-stimulatory molecules including CD40, CD80, CD86 and CD83 (for human DCs) that increase their ability to home to lymph nodes and to activate T cells. DCs migrate through lymphatic vessels and high endothelial venules to regional lymph nodes or home to T cells zones of lymphoid organs for optimal interaction with T and B cells. It has been described that DC-T cell interactions in T cell rich areas facilitate engagement of peptide-MHC complexes to TCRs, which serve as first signal to educate T cells to specific exogenous antigens (30).

Priming of naïve T cells requires second signals provided by CD80/CD86 expressed on mature and immunogenic DCs that are delivered via CD28 to T cells. This signal is essential for stabilising IL-2 mRNA (40) and promoting the T cell survival, proliferation and antigen-specific clonal expansion (30). Moreover, interaction of CD40, up-regulated on DCs, with its ligand expressed predominantly on T cells has shown to stimulate IL-12p70 production (41), thereby skewing $CD4^+$ T cell priming towards Th1 differentiation. In contrast, in the presence of IL-10, priming of $CD4^+$ T cell by DCs is skewed to the generation of regulatory T cells (Treg). There are evidences that DCs in the steady state or absence of maturation signals can tolerize peripheral $CD4^+$ and $CD8^+$ T cells by inducing T cell deletion and anergy (42, 43). Furthermore, tolerogenic DCs that express substantial levels of co-stimulatory molecules (44, 45) and other maturation markers have been indicated to be responsible for generating tolerance.

1.3.4 Human DCs

DCs are a heterogenous population consisting of multiple subsets with diverse functions. These cells present at a very low frequency (0.01%) in normal human blood. Based on the origin of DC progenitors and the different sets of genes they express, DCs are categorised into myeloid and plasmacytoid DCs. Both DC subsets are specialised in different functions and crucial in maintaining the balance of innate and adaptive immune responses in the host.

Blood myeloid DCs

Myeloid DCs (mDCs) also named as conventional DCs are known to differentiate from the common myeloid haematopoietic precursor and represent the classical antigen presenting cells. Phenotyping of mDCs characterised them as cells that express CD11c, HLA-DR (high expression) and lack the expression of lineage markers including CD3, CD14, CD19 and CD56 (46). They are in general short lived and could be replaced by blood borne precursors at steady state. mDCs are believed to be the most efficient APCs in priming naïve T cells and in generating antigen specific CTLs polarised towards Th1. Furthermore, they possess higher allo-stimulatory capacity than other DC subsets (47). Mature mDCs have been reported to produce pro-inflammatory cytokines and chemokines such as IL-12, TNF-α, CCL3, CCL4 and CXCL8 when achieving the maturation stage (48). However, in different environments, mDCs also appear to be tolerogenic and to exert immunosuppression within the host.

In human, mDCs exist in at least three compartments as circulating blood DCs, peripheral tissue DCs and secondary lymphoid organ-resident DCs. The circulating human mDCs consist of two major subsets: myeloid DC1 (mDC1) and myeloid DC2 (mDC2), which express the distinct surface C-type lectin receptors BDCA1 and BDCA3, respectively (46). Distinct from mDC2, the $BDCA1^+$ mDC1 express Fc receptors including CD32, CD64, and FcεR1 as well as CD2. The lack of Fc receptor expression by mDC2 suggested functional differences from mDC1 subset in performing Ig-mediated antigen uptake (46). Ito *et al.* provided evidence that GM-CSF and IL-4 cultured mDC1 but not mDC2 have the capacity to acquire the characteristics of Langerhans cells, a subtype of DCs that resides in the epidermis and expresses the Lag antigen, E-cadherin, langerin and CD1a (49). Studies on the morphology, endocytic capacity and the maturation requirement unveil similarity between both mDC subsets (46). Moreover, Lindstedt *et al.* reported a significant overlap in gene expression between the two blood DC cell subsets (50), suggesting that mDC2 may either represent a distinct DC subset or actually the same cell type as mDC1 but at different maturation stage.

Monocytes-derived DCs

Large amounts of DCs can be generated *in vitro* from $CD14^+$ monocytes isolated from the peripheral blood (51). The generation of monocyte-derived DCs (moDCs) depends on the presence of GM-CSF and IL-4 that drives monocytes to differentiate into moDCs and to lose CD14 but acquire CD1a expression (52). Several reports have shown that moDCs acquire distinct maturation features such as high migratory and IL-12p70-producing capacity under the influence of distinct cytokine cocktails comprised of IL-1β, TNF-α IL-6 together with either IFN-α and IFN-γ or PGE_2 (52). Moreover, moDCs that are stimulated with IL-15 become more efficient in inducing antigen specific CTL differentiation (53).

1.3.5 mDC and NK interaction

Although mDCs are best known as professional APCs, recent evidences have revealed their crucial function in regulating NK cell activation. The interaction of DCs and NK cells has been clearly shown to induce the cytolytic activity of NK cells against tumors (54). Furthermore, cytokines provided by mature mDCs, such as IL-12, IL-15 and IL-18 in turn promote optimal IFN-γ production by NK cells and enhance NK cell proliferation (55). Interestingly, reciprocal interaction of DCs and NK cells has been documented, in which NK cells mediate DC editing by selective elimination of immature DCs, but not mature DCs, through the NKp30 receptor (56), to ensure optimal antigen presentation and T cell priming. On the other hand, TNF-α and IFN-γ secreted by activated NK cells together with cell-cell contacts facilitate DC maturation.

1.3.6 Plasmacytoid DCs

Plasmacytoid DCs (pDCs) are a unique population of DCs that exhibits plasmacytoid morphology. They were first described by pathologists as plasmacytoid T cells or plasmacytoid monocytes in the 1950s based on their plasma-cell morphology and expression of the T-cell marker CD4 or the myeloid-cell markers MHC class II, CD36 and CD68 (57). In humans, pDCs comprise < 1% of total peripheral blood mononuclear cells (PBMCs) and are now identified as $Lin^-HLA\text{-}DR^+$ cells expressing BDCA2 and BDCA4 (50). Moreover, pDCs displayed high expression of CD123 (IL-3R), CD4 but

not CD11c, which is expressed on mDC, and distinct TLRs. BDCA2 is a marker that is uniquely expressed by pDCs but not by other DC subsets. However, it was also the first receptor found to serve as negative regulator of pDC function by suppressing their ability to secrete type I IFN in response to TLR activation (58). Under steady state conditions, pDCs have been shown to migrate from the blood into T-cell-rich areas of lymphoid organs (59). Following activation with unmethylated deoxycytidyl-deoxyguanosin dinucleotide type A (CpG A) or pathogens, pDCs produce a diverse array of cytokines and chemokines like TNF-α, IL-1, IL-6, CCL3 (MIP-1α), CCL4 (MIP-1β), CCL5 (RANTES), CXCL8 (IL-8) and CXCL10 (IP-10) in addition to type I IFN (59, 60, 61). Human pDCs do express co-stimulatory molecules and MHC II but at a lower level than mDCs and thus, are believed to be less efficient in antigen presentation as well as in eliciting proliferation of naïve T cells (62).

pDCs exhibit great functional plasticity and have also been described to be involved in the induction of immunological tolerance both in human and mice. They are circulating in peripheral tissues and spleen, which are considered to be essential for maintaining peripheral immune tolerance against self-antigens. Several studies have shown that pDCs can induce the generation of $CD8^+$ T regulatory cells upon CD40L activation (63). These $CD8^+$ Treg cells are anergic, non-cytolytic and capable of producing IL-10, which inhibits primary T cells responses (66). In addition, pDCs matured by IL-3 together with CD40L are able to prime naïve $CD4^+$ T cells into Treg cells secreting IL-10 but not IL-4, IL-5 and IL-13 (64, 36). The IL-10-producing Treg can suppress bystander T cell activation in an IL-10 dependent manner. Recent evidence suggests that up-regulation of ICOS-L by pDCs upon activation with herpes simplex virus mediates the differentiation of allogeneic $CD4^+$ T cells into cytotoxic Treg (65). A study on HIV-activated human pDCs indicates an indoleamine 2,3-dioxygenase (IDO) dependent pathway in inducing the development of $CD4^+$ Treg (66). Likewise, pDCs activated by CpG oligo DNA nucloetides (ODN) induce $CD4^+CD25^+$ Treg that produce IFN-γ, TGF-β, IL-6 and IL-10 but little of IL-2 (67).

The pDC as professional type I IFN producer

The biological distinction of pDCs from other DC subtypes is based on their capability to sense nucleic acids. Furthermore, they are professional type I IFN-producing cells, generating over 95% of type I IFN in response to viruses. Within 6 hours of activation by a virus, pDCs initiate a complex intracellular signaling that delegates 60% of the transcriptome to type I IFN genes leading to the production of 3–10 pg IFN per cell within 24 hours (61). pDCs selectively express TLR7 and TLR9, which allows them to sense viral nucleic acids or synthetic oligo DNA nucloetides (ODN) containing unmethylated CpG motifs (CpG DNA) (61, 68). It has been shown that pDCs respond to a broad range of both enveloped and non-enveloped DNA and RNA viruses, with the majority of these viruses being enveloped such as HSV and sendai virus, by inducing type I IFN production (69, 70).

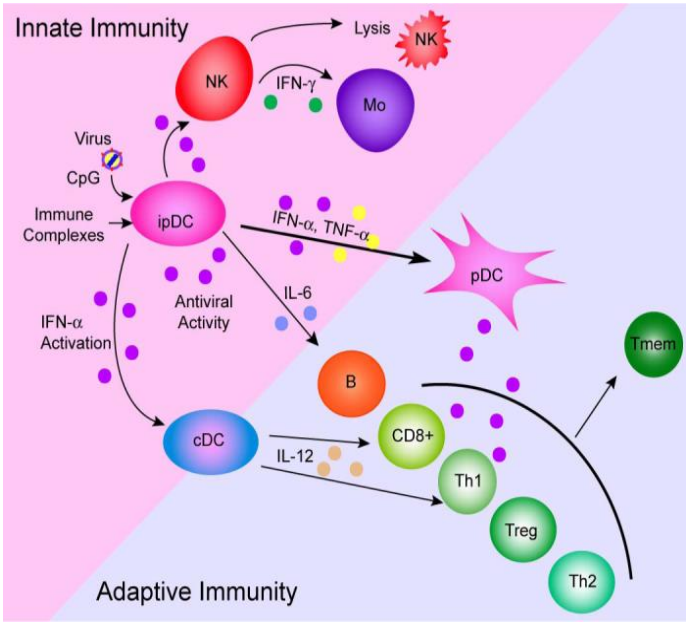

Figure 1. The role of pDCs in linking innate and adaptive immunity. pDCs produce IFN-α, IFN-λ and various pro-inflammatory cytokines upon exposure to viruses, CpG and DNA or RNA-containing immune complexes. pDCs then activate NK cells, monocytes and mDCs, which mediate innate immune responses either in a cell-cell contact dependent manner or via soluble factors. Activated pDCs undergo maturation and migrate to the lymph node and activate adaptive immune response by presenting (or cross-presenting) antigens to $CD8^+$, $CD4^+$ T cells or Treg. pDCs elicit either Th1 responses (typically in response to viruses), Th2 responses (under non-IFN-α stimulating conditions) or induce tolerance depending on the stimulus. pDCs also participate in inducing B cell maturation and differentiation to antibody-secreting plasma cells, which play vital roles in humoral immunity. *Adapted from Fitzgerald-Bocarsly P, Cytokine Growth Factor Rev. 2008*

The unique feature of pDCs to act as major producers for type I IFN and various pro-inflammatory cytokines and chemokines upon activation is crucial for linking innate and adaptive immunity (Figure 1). For instance, pDC-mediated proliferation and cytotolytic activity of NK cells *in vitro* and *in vivo* (71) appear to be mostly type I IFN dependent although IFN-independent mechanism have been identified in some cases of virus-induced NK cell activation. In parallel, pDCs participate in maximising NK cell cytokine production through cell-cell contact and in facilitating their recruitment through secretion of CXCL10, CCL3, CCL4 and CCL5, which occurs either in the lymph node or at the site of infection (59, 72).

On the other hand, it was noted that HIV-1 activated human pDCs induced the maturation of mDCs in a type I IFN and TNF-α dependent manner (73). In other studies, IFN-α either exerts direct effect or cooperates with resting NK cells to induce maturation of human mDCs through CD40, CD86 and CD80 up-regulation (52, 74). Likewise, pDC-derived IFNs together with CD40 ligand potentially induce maturation of bystander mDCs (75). Moreover, recent evidences suggested that pDCs synergise with mDCs in shaping anti-bacterial and anti-tumour immune responses in both mouse and human via cytokine and cell-cell contact dependent mechanisms (76).

Interestingly, pDCs can increase the ability of mDCs to cross-present exogenous antigens to $CD8^+$ T cells and promote their clonal expansion (77, 78). pDC-derived IFN-α is not only essential for maintaining innate immunity, but more importantly for generating potent adaptive immunity. It was established that pDCs are able to induce the differentiation of naive T cells into Th1 or Th2 cells depending on the stimulus (36, 67, 79). Recent studies revealed that pDCs possess the ability to cross-present viral antigens and to generate HIV-peptide specific $CD8^+$ T cells independent of TLR pathways (80).

Furthermore, a study by Le Bon *et al.* described the role of type I IFN in the enhancement of antibody responses and the development of immunological memory (77). pDCs have been reported to induce secretion of virus-specific antibodies by promoting the differentiation of B cells into plasma cells through the combinatory effect of IL-6 and

IFN-α (81). IFN-α secreted by pDCs also facilitates the generation of non-Ig-secreting plasma blast (82).

1.3.7 DCs in cancer

During the formation and progression of tumours, impairment of immune responses is mostly associated with deficient immunological function of DCs, NK cells and T cells. Several studies performed in different tumor entities such as breast, head and neck, lung, colorectal and pancreatic cancer (83-86), revealed numerical defects of circulating DCs with reduced numbers of myeloid DCs detected in the peripheral blood. DCs from cancer patients have been demonstrated to possess impaired APC function with low T cell stimulatory capacity (87) despite exhibiting normal endocytic ability (88). Furthermore, DCs often infiltrate into tumours that produce chemokines like MIP-3α, which selectively attract MIP-3α receptor (CCR6) expressing immature DCs (89). In an immunosuppressive milieu generated by tumours, functional defects of DCs contributed substantially to the deficiency in mounting efficient immune responses. For instance, vascular endothelial growth factor (VEGF) has been shown to be associated with inhibition of phagocytosis and differentiation of DCs in tumour (90-92). Besides, of 32 breast carcinoma tissues being analysed, more than 90% have been shown to be infiltrated by immature $CD1a^+$ mDCs while $CD83^+$DC-$Lamp^+$ mature DCs were detected in peri-tumoral areas of ≤ 60% samples (89). These tumour-infiltrating mDCs were polarized by the tumour to elicit Th2 instead of Th1 immune responses and favour differentiation of naïve $CD4^+$ T cells into IL-13 secreting cells (93). In several mouse models, Th2 T cells and IL-13 have been demonstrated to play a vital role in facilitating tumor metastases by mediating macrophages activation and the secretion of TGF-β by myeloid cells (94, 95). Meanwhile, in multiple myeloma, several studies have suggested a direct interaction of mDCs with tumour cells in promoting the survival and clonogenicity of tumour cells (96, 97). In mice, tolerogenic $CD4^-8^-$ DCs were shown to be present in progressive P815 tumors and were capable of stimulating the differentiation of IL-10-secreting $CD4^+$ Tr1 cells (98).

Numerous studies also indicate that tumours shift the functional properties of pDCs and their roles in eliciting anti-tumour immune response are depending on the secreted cytokines. For instance, approximately 10% of breast tumours were detected with infiltrated pDCs and their presence correlated with poor prognosis (99). It has been reported for breast cancer patients that the presence of IL-12 and IFN-γ producing pDCs in draining lymph nodes was correlated with good prognosis whereas, poor clinical prognosis was associated with pDCs that released higher amounts of IL-10 and IL-4 (100). In head and neck cancer, the functional properties of pDCs were shown to be altered in a way that they lack the capability in producing type I IFN upon TLR activation (101). Likewise, it is noted that pDCs infiltrating melanoma cooperate with other immunosuppressive cells in suppressing $CD8^+$ CTL activation in tumour tissues. Gerlini and colleagues reported that tolerogenic pDCs from draining lymph nodes of melanoma patients exhibited incomplete activation and an impaired IFN-α production *in-situ* (102).

1.4 NK cells and their subsets

NK cells are large granular cells of lymphoid origin and comprise about 15% of total lymphocytes. They are equipped with a unique ability to recognise and kill pathogenic cells especially viruses-infected cells and tumour cells. Unlike T cells, the cytotoxic feature of NK cells requires no prior immune sensitization of the host. Thus, NK cells can respond rapidly to abnormal cells. They have been shown to play a crucial role in the defence against cytomegalovirus, Epstein-Barr virus (EBV) and herpes simplex virus infections by resolving and controlling pathogens spread. Upon activation, NK cells produce a range of soluble factors such as chemokines to recruit other adaptive immune cells for amplifying the immune response.

NK cells are phenotypically categorized as cells expressing CD56 but lacking CD3 molecules (103). Based on the surface density of the CD56 molecule, NK cells can be divided into two sub-populations: approximately 90% of the NK cell population express CD56 at a lower density ($CD56^{dim}$) while 10% of the cells are highly positive for CD56 ($CD56^{bright}$). The $CD56^{dim}$ cells also express FcγRIII (CD16) at high density on their cell surface and are therefore termed $CD56^{dim}CD16^+$ NK cells, whereas $CD56^{bright}$ NK cells

lack CD16 or express it at a very low level ($CD56^{bright}CD16^{dim/-}$)(104). In mice, the counterpart of human $CD56^+$ NK cells is still lacking. Though murine NK cells do not express CD56 they have been demonstrated to possess the capability, similar to human NK cells, to lyse tumour cells.

Several studies revealed that there are a number of cell surface molecules that serve as unique markers and confer distinct functional properties to the human $CD56^{dim}$ and $CD56^{bright}$ NK subsets. Early functional studies proposed that $CD56^{dim}CD16^+$ NK cells can produce cytokines but are more potent as cytotoxic effectors with a capability in mediating antibody dependent cell cytotoxicity (ADCC) (105). In contrast, the $CD56^{bright}$NK cells appear to be poorly cytotoxic but exert regulatory functions by producing various immunoregulatory cytokines among them, IFN-γ, TNF-α/β, IL-10 and GM-CSF (106). Furthermore, the two NK subsets display unique repertoires of chemokine receptors in such a way that $CD56^{bright}CD16^-$ NK cells show high levels of functional CCR7 and CXCR3 receptors. (107). The CCR7 expressing $CD56^{bright}$ NK cells are found to accumulate in lymph nodes in some pathological conditions. On the other hand, $CD56^{dim}CD16^+$ NK cells that typically circulate in the blood stream express CXCR1 and CX3CR1 and respond to IL-8 (107).

1.4.1 NK cell receptors

NK cells serve as the first line of defence by recognizing altered "self". Early studies proposed recognition of target cells by a 'missing self' mechanism in such a way that cells with low expression or complete loss of MHC I alleles are killed by NK cells (Figure 2) (108, 109). Conversely, healthy cells expressing normal level of MHC I molecules are protected from NK cells recognition (110). Meanwhile, several studies demonstrated that NK cell activity is fine tuned by the balance of activating and inhibitory signals received via different receptors (110, 111). Different from TCRs and BCRs, none of the activating and inhibitory NK cell receptor genes undergo rearrangement. Each NK cell expresses several activating or inhibitory receptors that sense the expression level of their various ligands expressed on target cells (110, 111). Depending on the balance of signal, the engagement of ligands for NK cell activating

receptors has also been shown to overcome inhibitory signals delivered by MHC class I molecules and thus leads to target cell lysis (109). Normal cells express MHC I molecules but poorly express activating ligands (110, 111). In case both activating and inhibitory molecules are expressed but when inhibitory signal are stronger than stimulatory signals, cells are eventually protected from lysis.

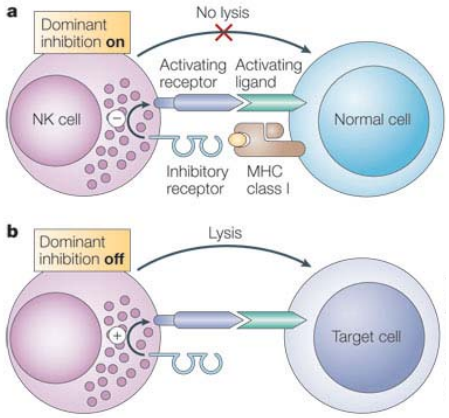

Figure 2. NK cell recognition of tumour cells. NK cell activity is regulated by a balance of signals received via activating or inhibitory receptors. Virus-infected or tumour cells often reduce or lose expression of MHC I molecules that bind to NK cell inhibitory receptors, but up-regulate ligands for NK cell activating receptors. The engagement of ligands for NK cell activating receptors can overcome inhibitory signals and lead to NK cell activation and cytolytic events. *Adapted from Fauci et al., Nat Rev Immunol. 2005.*

NKG2D and its ligands

The activating receptor NKG2D and the natural cytotoxicity receptor (NCR) family are expressed on NK cells and mediate their cytotoxicity activity. NKG2D is one of the most well studied NK cell activating receptors and its expression is not restricted to NK cells but also detectable on $CD8^+$ T cells, NKT, γδ T and under certain condition on $CD4^+$ T cells (112, 113). NKG2D is a lectin-like type II transmembrane homodimer that is associated with two different signalling subunits and provides co-stimulation signals through the YxxM-containing DAP10 and activation signals via ITAM-containing DAP12 (114). In line with this, activation of NK cells through NKG2D provides a strong signal that could overcome the inhibitory signal from MHC class I molecules and augment target cell killing. Conversely, NKG2D-ligand ligation confers T cell co-

stimulation thereby enhancing and sustaining signals from the TCR while protecting naïve T cells from activation-induced cell death (115).

Numerous NKG2D ligands have been described, which are structurally similar to MHC class I molecules and typically not expressed at substantial levels in normal cells but up-regulated in cancerous or stressed cells. So far, seven NKG2D ligands have been identified in human namely, MICA, MICB, ULBP1-4 and RAET1G (116). Several studies showed the expression of NKG2D ligands on melanoma cells, glioblastoma cells and ovarian carcinoma (117-119). In addition, accumulating evidence reveals a pivotal role of NKG2D in tumour surveillance (117, 120). Both *in vivo* and *in vitro,* elimination of NKG2D ligand expressing tumour cells by NKG2D expressing NK cells has been documented in skin cancer and ovarian carcinoma (118, 119). In the transgenic mouse prostate adenocarcinoma model (TRAMP), it was demonstrated that the incidence of highly aggressive prostate adenocarcinoma was markedly increased in mice deficient of NKG2D (121).

The NCR family

NK cells express another family of activating receptors, which are collectively termed natural cytotoxicity receptors (NCRs). Four of such receptors have been characterised in human; NKp30, NKp44, NKp46 and NKp80, however only one of them, NKp46 has been identified in mice (122). NKp30, NKp46 and NKp80 are constitutively expressed on resting and activated peripheral blood NK cells in human whereas, NKp44 is only expressed by NK cells upon activation as demonstrated for IL-2 treated NK cells (123).

NCRs are type I integral proteins with one or two Ig-like extracellular domains that contain charged transmembrane residues for association with ITAM-signalling molecules. Unlike NKG2D, ligands for NCRs are rather diverse among them, viral haematoglutinins are recognised by NKp46 and NKp44 (124) while heparin sulphate proteoglycans bind to NKp30 and NKp46 (125, 126). NCRs appear to participate in NK cell recognition and blocking one or more of these NCRs prevents the recognition of tumour cells of various origins by NK cells and inhibits their lysis (127,128). In mice, the

ability to reject transplanted lymphoma cells expressing NKp46 ligands was impaired after mutation of the gene encoding NKp46 (127). High expression of NKp46 by resting NK cells increases the killing of autologous, allogeneic and xenograft target cells (128).

1.4.2 NK cell killing

The killing of tumour cells by NK cells is mediated mainly by the release of perforin and granzyme B. Perforin is a molecule that polymerizes to form ringlike transmembrane channels or pores in the target cells to increase the permeability of the cell membrane, which consequently leads to cell death (30). Meanwhile, granzymes, a set of serine proteases, migrate through the pores created by perforin and interact with the intracellular components of the target cells to induce apoptosis (30). In perforin deficient mice, cytotoxicity of NK cells is reduced compared to wild type mice (129). Activation of NK cells also leads to the secretion of large amounts of IFN-γ and TNF-α, thereby killing locally attached target cells (130). Furthermore, NK cells can employ the FAS/FASL and TRAIL pathway to induce apoptosis in tumour cells (131, 132).

1.4.3 NK cells in cancer

The function of NK cells in tumour immunosurveillance is well-established. Several studies have demonstrated that different mouse and human tumour cell lines as well as freshly isolated human tumour cells are killed by NK cells. *In vivo*, NK cells are capable of eradicating experimentally induced and spontaneously developing tumours in mice. NK cells are efficient predominantly in eliminating metastases and small tumour grafts (133). Considerable loss of MHC class I molecules has been detected in tumour sections of human head and neck squamous cell carcinoma (HNSCC) (134) and tumour cells with MHC class I loss are more susceptible to NK cells lysis (135). Moreover, injection of IL-2 activated NK cells leads to consistent regression of HNSCC xenografts. NK cells virtually infiltrate into tumours and play a crucial role in controlling the outgrowth of tumour. In gastric cancer, tumour infiltrating-NK cells have been associated with fewer metastases, less lymphactic invasion and better clinical prognosis (136). Likewise, in a breast cancer mouse model, depletion of NK cells abrogated the effect of adenoviral

transduction of IL-12, which in the presence of NK cells increased tumour regression and long-term survival of mice (137).

On the other hand, suppression of NK cell function has been described in cancer patients. For instance, NK cells derived from ovarian carcinoma patients often display reduced function as a consequence of tumour-induced immune suppression (138). In mice, tumour cells of head and neck cancer escape from NK cell recognition by secretion of large amounts of TGF-β that down-regulates NKG2D ligands (139). Groh *et al.* and Waldhauer *et al.* have shown that shedding of NKG2D ligands from the tumour cell surface mediated by tumour associated metalloproteases prevents tumour cells recognition (140, 141). Furthermore, several lines of evidence suggest that soluble NKG2D ligands, which are readily detectable in the sera of cancer patients can trigger a down-regulation of the NKG2D receptor on NK and T cells upon prolong interaction (140).

1.5 TLR family and signalling

1.5.1 TLR family

The Toll receptor was originally described to play a role in the development of *Drosophila* and was rapidly identified to have essential functions in response to fungal infection (142). Currently, it is well known that Toll-like receptors (TLRs) play a pivotal role in all vertebrates for microbial detection via recognition of conserved products unique to the microbial metabolism and absent in host cells. Many of these metabolic pathways and gene products are essential for microbial survival and are involved in housekeeping functions. The recognition of molecular signatures of microbial infections allows the initiation of inflammation and innate immunity through engagement of differential signalling pathways and activation of DCs for inducing T cells differentiation.

To date, several functional TLRs (10 in human and 12 in mice) have been identified that recognize a variety of pathogen-associated molecular pattern (PAMPs) derived from bacteria, viruses and fungi to trigger immune responses, including induction of type I IFN genes (Figure 3). Based on the sub-cellular localization, TLRs can be subdivided into two

groups. The first group includes TLR3, 7, 8 and 9, which are localized intracellularly in the endosomal compartment while the second group consists of TLR1, 2, 4, 5 and 6, which are expressed on the cell surface at the plasma membrane (143). As illustrated in Figure 3, the respective TLR ligands have been identified, for example, TLR4 recognises lipopolysaccharide (LPS) of gram-negative bacteria while viral and microbial double stranded RNA (dsRNA) are detected by TLR3 (144). Furthermore, TLR7 and TLR8 mediate the recognition of imidazoquinolines and single-stranded RNA (ssRNA) derived from vesicular stomatitis virus, influenza virus and immunodeficiency virus type I (HIV-I) (145). On the other hand, TLR9 is responsible for the recognition of bacterial and viral CpG DNA motifs (143, 145). The recognition of nucleic acids by endosomal localized TLRs requires internalisation of viral particles or bacteria followed by their degradation in the late endosomes or lysosomes. The degradation allows the release of viral or bacterial DNA and RNA. The intracellular localization of TLRs is crucial in facilitating the discrimination of viral DNA from self-DNA and in preventing destruction of host cells (37).

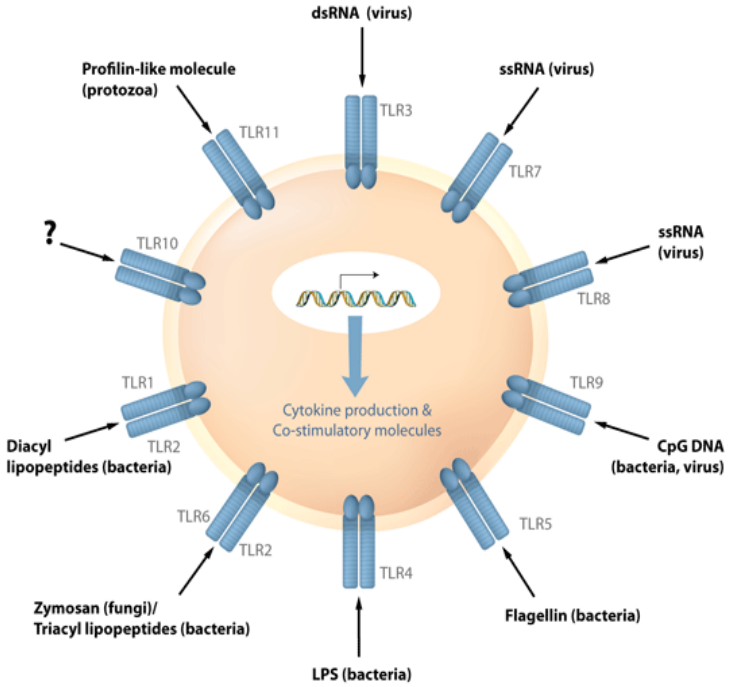

Figure 3. TLR receptors and their respective ligands. A range of TLR receptors and their ligands, the pathogen-associated molecular patterns (PAMPs) derived from bacteria, viruses and fungi have been identified. The TLR-ligand interaction activates innate immunity and protects the host from invasion by microbes. *Adapted from* research4.dfci.harvard.edu/innate/TLR

1.5.2 TLR signalling

All TLRs contain an intracellular Toll/IL-1 receptor (TIR) domain that transmits downstream signals by recruiting one or more TIR domain-containing adaptor proteins, including MyD88, TIRAP, TRIF and TRAM via TIR-TIR interaction (146). In general, two main downstream signaling pathways of TLRs have been characterized: the Myd88-dependent pathway (144) and the TRIF-dependent pathway (144). MyD88 is a universal adapter that activates inflammatory pathways and accounts for all TLRs except TLR3. The interaction of MyD88 with TLRs stimulates the recruitment of complex signaling components including the IRAK family and subsequent association of IRAK to the TRAF family that signals down respective pathways (147, 148). On the other hand, TRIF was identified as an essential adapter of the MyD88-independent pathway (148, 149) and is required for TLR3 activation. TLR4-mediated induction of pro-inflammatory cytokines such as TNF-α and IL-6 is MyD88- and TRIF-dependent. A study in MyD88-deficient mice supports the role of the TRIF-dependent pathway for IFN-β induction after TLR3 and TLR4 ligand treatment (150). Observations on the activation of NF-κB and MAP kinase (MAPK) with delayed kinetics in MyD88-deficient macrophages also support the functional role of TRIF as adaptor protein in TLR signalling (151). The recruitment of both adaptor proteins leads to the activation of at least three major downstream molecules, NF-kB, IRFs and MAPK. Furthermore, numerous studies showed that TLR7/9 activation induce the formation of complexes consisting of MyD88, IRAK-1, IRAK-4 and IRF7, which results in type I IFN production. In parallel, the NF-kB signalling pathway is also initiated, leading to the production of several pro-inflammatory cytokines and chemokines including IL-6, TNF-α, CXCL10, CCL2, CCL3, CCL5 and IL-8 (144).

1.5.3 TLRs expression on DC subsets

Different DC subsets express a unique set of TLRs that allows them to response to distinct classes of pathogens. Human pDCs selectively express TLR7 and TLR9 intracellularly, which reside in the ER (152). The expression of TLR9 is also known in B cells but not in other leukocytes such as monocytes, NK cells, γδT cells and memory CD8 T cells indicating that there is no direct effect on these cells when stimulated with

TLR9 ligands (153, 154). Conversely, human blood mDCs express a broad range of surface TLRs including TLR1, TLR2, TLR4, TLR5, TLR6 while TLR3 and TLR8 reside in the endosomal compartment (152, 155, 156). There are however evidences showing that moDCs derived from monocytes under GM-CSF and IL-4 culture express a set of TLRs distinct from freshly isolated blood mDCs. moDCs express TLR3 and TLR8 intracellularly but not TLR7 and show surface TLRs expression (TLR 1, 4, 5, and 6) similar to blood mDCs (157). The different expression pattern of TLRs between mDCs and moDCs may implicate distinct functional property between physiologically existing and *in vitro* manipulated DCs in sensing pathogens.

1.5.4 TLR9 ligands

The TLR9 receptor is unique among the TLR repertoire due to its role as the only sensor for foreign DNA. It detects the unmethylated CpG sequences in DNA molecules, which are present at high frequencies in viruses and bacteria. In the mammalian genome, most of the CpGs are methylated and this prevents the recognition of self-DNA by TLR9. The detection of viral/bacterial unmethylated CpG DNA by TLR9 requires the internalization of nucleic acids into the endolysosomal compartment before the recruitment and formation of the signaling complex consisting of MyD88, IRAK1, IRAK4 and TRAF6 can take place. This complex further interacts and activates IRF7 that can then induce type I IFN production.

In addition, synthetic oligonucleotides (ODNs) containing CpG motifs, which mimic microbial DNA have been shown to activate TLR9 expressed by pDCs and also B cells (158). The synthethic CpG ODNs differ from microbial DNA in the phosphoester backbone, which is partially or completely replaced by a phosphorothioated backbone to prevent degradation by nucleases (e.g DNase). In addition, the presence of a poly G tail at the 3' end, 5' end, or both of the synthethic CpG ODNs enhances their cellular uptake (159) and allows the formation of high molecular weight aggregates to increase the activity of the poly G sequence (160). Numerous studies have demonstrated that the distinct immunostimulatory profile induced by synthetic CpG ODNs depends on the species origin, length, DNA backbone, sequence, number and location of CpG dimers as

well as on the precise base sequences flanking the CpG dimers. For example, an optimal CpG motifs differs between mice and humans (161, 162). Three types of CpG ODN have been recently defined and described with distinct immunologic activities on both human pDCs and B cells (162).

CpG A with the prototype CpG 2216 was first described by Krug *et al.* (163). It is characterized by its unique poly G tail with phosphorothioate linkages flanking a central palindromic CpG motif-containing sequence with a phosphodiester backbone. There are five phosphorothioate modifications at the 5'- and 3'-end (polyG region) of the oligonucleotide and this structure allows spontaneous formation of CpG aggregate structures (164). The unique structure of CpG A has been demonstrated to induce specific TLR9 activation in pDCs but not B cells and serves as good stimulator for IFN-α/β induction, while possessing poor activity in inducing pDC differentiation (165).

1.6 Regulation of type I IFN production

1.6.1 Interferons

Interferons (IFNs) belong to the family of cytokines and are the most diverse of all members. The IFN family was first discovered and described for their unique characteristic in protecting cells from viral infections. This protection is conferred by preventing viral replication in surrounding cells by the expression of antiviral proteins during infections. In addition, it is now known that IFN also can induce a broad range of biological responses including anti-proliferation, regulation of apoptosis and immunoregulation of DCs and of different lymphocyte subtypes (166). The IFN family is classified into three distinct types: type I IFN with 30 subtypes (including α, β, ε, ω, μ, κ), type II IFN (γ) and type III IFN (λ).

Type I IFN

There is a large number and diversity of type I IFN genes in mammalian and all of these genes are clustered on chromosome 9 in human. IFN-α alone is subdivided into multiple subtypes such as IFN-α2a, IFN-α2b and etc, while there is only a single IFN-β gene. Most of IFN-α subtypes contain 166 amino acids and are weakly glycosylated in human

(166). Together with IFN-β, -ω, -ε and -κ, they are responsible for antiviral responses, however, IFN-α/β are known to be the key cytokines that render cells resistant to viral infection. Also, type I IFNs are general inhibitors of myelopoesis since higher numbers of circulating myeloid cells were observed in IFN α/β receptor (IFNAR)-null mice. In terms of apoptosis regulation, type I IFN are known to regulate the expression of p21/waf1, IRF1, STAT1, PKR, BCL2, TRAIL, CD95 and caspases 4/8 (167, 168). Another very important function of type I IFN is regulation of effector cell function of both the innate and adaptive immune system.

Type II and III IFNs

Type II IFN is represented by a single gene IFN-γ and produced by NK cells, NKT cells and T cells upon cytokine stimulation or activation by the antigen. IFN-γ has been shown to play an important role in adaptive immune responses to kill tumour cells and to provide protection against intracellular pathogens (169). DCs polarised by the combination of type I and II IFN are potent inducers of antigen specific T cells against chronic lymphocytic leukemia (CLL) (170). The third type of IFNs is type III IFN, which comprises three subtypes of IFN-λ : IFN-λ1, -λ2 and -λ3, also known as interleukin-29 (IL-29), IL-28A and IL-28B, respectively. These cytokines are produced in response to viral infections and the mechanisms of their induction have been suggested to be similar to those of IFN-α/β (171). The functions and the mechanisms of action of type III IFN, however, still remain largely unknown and require further investigation.

1.6.2 The regulation of IFN-α/β production

The production of type I IFN is primarily governed by the family of IFN regulatory factors (IRFs) at the transcriptional level. Activation of IRFs including IRF3, IRF5 and IRF7 can be initiated during the recognition of PAMPs (148). To sense the invasion of various types of pathogens, there are two main pathways that have been identified namely, TLR-dependent and TLR-independent pathways. The TLR-dependent pathways for IFN-α/β induction rely mainly on TLR3, 7, 8 and 9 for detecting viral or bacterial derived nucleic acids (172). Whereas, TLR-independent pathways refer to two cytosolic RNA helicases: retinoic acid-inducible gene I (RIG-I) and melanoma differentiation-

associated gene 5 (MDA5), which sense actively replicating RNA viruses (173, 174). Both TLRs and cytosolic receptors detect the presence of foreign nucleic acids in distinct cellular compartments (172, 173). Nevertheless, the two different receptor systems converge at the point of IRFs including IRF3 and IRF7, their activation then leads to type I IFN induction.

The TLR-independent signaling pathways appear to be essential in most cell types including fibroblasts, conventional DCs and macrophages during viral infections. However, RIG-I and MDA-5-mediated signaling seems to be cell type specific as it is dispensable in pDCs, which respond to a wide range of both DNA and RNA viral infection through the TLR7/8 and TLR9 pathways (148, 175, 176). During the recognition process, RIG-I senses uncapped viral ssRNA bearing 5'-triphosphate, which is absent in the cytosolic RNA of eukaryotes (177, 178). Conversely, MDA-5 recognises positive-strand ssRNA viruses by binding to poly I:C (179). The binding of viral RNA to cytosolic receptors and adaptor proteins initiates a signaling cascade that leads to NF-κB, AP-1 and IRF3/7 activation and translocation of phosphorylated IRFs into the nucleus for activating type I IFN gene transcription (180).

In contrast, the induction of IFN-α/β by TLR-dependent pathways involves TLR7 and TLR9 that are strongly expressed by pDCs in both human and mouse whereas TLR9 is expressed by conventional DCs and macrophages in mouse but not in human (181). Both of the TLRs that govern type I IFN production in pDCs are confined to the endosomal compartment in which viral particles are degraded upon endosomal acidification, thereby exposing viral nucleic acids for recognition. This compartment specifically senses viral nucleic acids and allows the recognition of microbial but not mammalian nucleic acids, which would have detrimental effects such as autoimmune diseases. The binding of ligands to TLRs is mediated via the N-terminal leucine rich repeats (LRR) and this leads to the dimerization of TLRs (172). Dimerised TLRs undergo conformational changes that lead to the formation of homotypic interactions between the C-terminal TIR domain of the TLR and the TIR domain of adaptor molecules such as MyD88 (172). In pDCs, the recruitment of MyD88 upon ligand-engagement of TLR7 or TLR9 initiates signalling

cascades that involve the formation of a complex of Myd88 with TRAF6 and IRAK-4. This complex was proven to act upstream of both NF-kB and IRF-7 as mice deficient in MyD88, IRAK-4 and TRAF6 show defects in those pathways (182-185). The deficiency of MyD88 or TLR9 expression in murine pDCs abolishes type I IFN release upon TLR7/9 ligand stimulation (186).

1.6.3 The role of transcription factors IRF3 and IRF7

The IRF family of transcription factors consists of nine members in human and mice, which have been described to play a versatile role in the development of various immune cells and in eliciting innate immune responses. IRFs were first discovered as transcriptional factors regulating type I IFNs and IFN-inducible genes. Each IRF contains a well conserved N-terminal DNA-binding domain of ~120 amino acids that possesses five conserved tryptophan repeats (187), which recognise the interferon stimulated response element (ISRE) region that is found in the promoter of genes encoding type I IFNs as well as many other genes involved in immunity and oncogenesis. Numerous studies suggest that IRFs are essential in regulating TLR-dependent and cytosolic PRRs signalling pathways that lead to the production of type I IFN. Activation of IRF3/7 is dependent on their phosphorylation, which allows their subsequent nucleus translocation and binding to the ISRE region of target genes.

IRF3, which is constitutively expressed in cells and not induced by viral infection or IFN treatment plays key role in the induction of IFN-β via a TRIF-dependent pathway but not in the activation of IFN-α genes (188,189). Phosphorylated IRF3 forms either homodimers or heterodimers with IRF7 and activates the transcription of CXCL10 and IFN-β, respectively. DCs and macrophages from $IRF3^{-/-}$ mice display a defect in the induction of genes including those encoding CXCL9 and CXCL10 (190,181) and do not release IFN-β in response to LPS.

IRF7 efficiently activates IFN-α/β genes (188,189) and virus infection induces an up-regulation of constitutively expressed IRF7 in pDCs, which correlates to the robust production of IFN-α by pDCs. Other studies revealed that the induction of type I IFN is

MyD88 dependent and that IRF7, in contrast to IRF3, directly interacts with the death domain of MyD88 in the endosomal compartment (192,193). Consistently, a severe impairment of type I IFN release is observed in mouse embryonic fibroblast (MEF) deficient in the IRF7 gene (194) and mice lacking IRF7 display a marked defect in type I IFN gene induction by splenic pDCs after exposure to CpG A or infection with HSV, a dsDNA virus (194).

The expression of IRF7 is tightly regulated at the transcriptional and translational level. Upon encountering of viral products or TLR agonist, IRF7 has been demonstrated to be rapidly up-regulated both at the mRNA and protein level for high IFN-α production in pDCs (195). Recent evidence by Colina *et al.* implicates that the IRF7 protein is rapidly generated from a pre-existing but translationally silenced mRNA pool. mRNA silencing is controlled by the 4E-BP protein, a repressor of translation initiation (195). 4E-BP has been implicated to play a crucial role in controlling cellular growth, survival and apoptosis. For example, exchange of specific threonine and serine amino acids at the 4E-BP protein, as they are detected in multiple myeloma cells, prevent the hyperphosphorylation of this protein and sensitise the cells to dexamethasone-induced apoptosis (196).

The translational repressor 4E-BP is a crucial molecule for tight regulation of eukaryotic cap-dependent mRNA translation and allows rapid production of proteins from pre-existing mRNA. Under steady state conditions, the cap binding protein eIF4E is sequestered by hypophosphorylated 4E-BP and prevented from forming the eIF4F multiprotein complex together with the scaffold protein eIF4G and the eIF4A RNA helicase (197-199). The eIF4E-4E-BP complex inhibits the ability of eIF4E to bind to the 5'cap structure or 5' UTR of mRNA for translation (198). In response to growth stimuli, hormones, cytokines, and chemokines, the 4E-BP protein undergoes phosphorylation by mTOR at position Threonine 37/46 and Threonine 70/Serine-65, which leads to the complete release of eIF4E and allows the formation of eIF4F complexes (eIF4E, eIF4G and eIF4A) (199,200). Binding of the eIF4F complex through eIF4E to the 5' capped

mRNA recruits 40S ribosomes and allows the scanning of the ribosome along the mRNA towards the translation initiation codon (197,198).

1.6.4 ISGF3 signalling pathway

Binding of IFN-α/β to IFNAR has a significant role in amplifying type I IFN response by establishing a positive feedback loop via ISGF3 signaling. IFNAR is a receptor for type I interferons expressed on the cell surface with an extracellular ligand binding domain and intracellular kinase domain (201). It possesses two chains, IFNAR1 and IFNAR2c, which are required for activating the downstream signalling cascade (202). It is now clear that binding of type I IFN to the IFNAR activates Janus kinase family members (JAK) or TYK2 and further phosphorylates STAT1 and STAT2, which dimerise and dissociate from the receptor (202, 203). STAT1/2 dimers form a heterotrimeric complex with IRF9, which is termed as IFN-stimulated gene factor 3 (ISGF3). Translocation of the ISGF3 complex to the nucleus results in the initiation of *de novo* transcription of IRF7 as well as of several interferon stimulated genes, like PKR, Mx1, OAS1a, that possess ISRE in their promoter region (204-206). It is important to note that $IFNAR^{-/-}$ mice are more susceptible to a wide range of viral infections and pDCs of IFNAR lacking mice are defective in robust type I IFN gene induction by CpG A (207-209). In addition, MEF and peritoneal macrophages lacking IFNAR exhibit severe defects in Newcastle disease virus (NDV)-induced IFN-α/β gene expression (210).

1.7 Chemokines

1.7.1 Chemokine classification

Chemokines are small, soluble molecules (8-14 kDa), structurally related to polypeptide signalling molecules, that bind to their cognate chemokine receptor. The chemokine receptors are seven transmembrane G-protein coupled receptors (GPCRs) (211) and their binding by chemokines initiates complex signalling cascades. To date 18 chemokine receptors and 47 chemokines have been identified. Many of the chemokines share common receptors and this redundancy allows initiation of distinct signaling cascades leading to different immune regulation outcome. In addition, it can compensate the deficiency of receptor-ligand interaction to fine-tune specific biological responses (212).

The chemokine families are classified into four sub-groups: CXC, CC, C and CX3C, based on the relative positioning and the presence of first two cysteine residues at the N-terminus (211). The interactions of chemokines with their receptors have been implicated in regulating leukocyte migration to inflammatory sites and maintaining immune homeostasis. Chemokines with functions in inflammation are crucial for attracting different effector leukocytes including DCs, NK cells, neutrophils, and monocytes/macrophages (213). Homoeostatic chemokines such as CXCL12, CXCL13, CCL19 and CCL20 have shown to be involved in the homing of APCs and lymphocytes to lymph nodes for eliciting immune responses (213). Furthermore, numerous studies have provided evidences for the vital role of chemokines in angiogenesis or angiostasis, tumour growth and in metastasis.

1.7.2 Chemokines in leukocytes recruitment

DCs and NK cells are two crucial innate immune cell types that are recruited by various chemokines to the site of inflammation. Both cell types can produce leukocyte recruiting chemokines such as CCL5, CCL3, CCL4, CCL2 and CXCL10 that are also the chemoattractants for DCs and NK cells. The roles of these chemokines in recruiting leukocytes are described as follow.

CCL5

CCL5 is a ligand for three distinct chemokine receptors namely, CCR1, CCR3 and CCR5. It has been demonstrated that CCL5 secreted by melanoma and breast cancers mediates a direct proliferative effect on tumor cells. In melanoma, tumour-derived CCL5 was up-regulated by TNF-α (214) and was reported to induce the apoptosis of tumour infiltrating T cells via CCR5 dependent pathways (213). On the other hand, CCL5 was shown to partially protect T cells from anti-CD3 induced apoptosis when acting alone or in combination with CCL3 and CCL4 (216-217). CCL5 is also a potential co-stimulator in activating T cells during anti-CD3 stimulation (218). Likewise, $CCL5^{-/-}$ mice showed impaired T cells activation in response to antigen or anti-CD3 stimulation (219). At higher CCL5 concentrations, T cells could be stimulated to proliferate, produce cytokine and enhance CD25 expression independent of the presence of antigens (220, 221).

Moreover, CCL5 was demonstrated to be involved in the recruitment of DCs, monocytes, T cells, NK cells and mast cells, which express CCR5 (221-224).

CCL3 and CCL4

CCL3 and CCL4 are two important inflammatory chemokines secreted by a variety of cells, among them pDCs, mDCs, macrophages, activated NK cells, $CD4^+$ T and $CD8^+$ T cells (222-226). Both chemokines are also responsible for the recruitment of $CD8^+$ T cells into the infected tissues (225). It has been noted that CCL3 and CCL4 acting alone or in combination with CCL5 partially protect T cells from anti-CD3 induce apoptosis and induces the expression of B7.1 in APCs (221).

CCL2

CCL2 is a potent monocyte chemoattractant protein with the capability to recruit NK cells, macrophages and certain T lymphocyte populations (227-231). CCL2 derived from melanoma as well as breast, ovarian and lung cancer cells has been reported to recruit monocytes/macrophages. The recruited macrophages are often polarized to M2 or tumour-associated macrophages (TAMs), which have been shown to produce the pro-angiogenic factors IL-8 and VEGF, to promote tumour angiogenesis, as well as CCL2 to amplify their recruitment to the tumour site (229, 230). In melanoma, the promotion or inhibition of tumour growth by CCL2, however, depends on the expression level of CCL2 (230, 232).

CXCL10

CXCL10, also designated IP10, is a ligand for CXCR3, a CXC chemokine receptor which is expressed especially in activated Th1 cells, B cells, NK cells, and DCs. It is categorised as an anti-angiogenic chemokine and related to the Th1-chemokine family that participates in Th1-polarized immunity (233). Moreover, it was noted that mature DCs in lymphoid tissues secrete CXCL10to mediate migration and recruitment of Th1 lymphocytes (234). Likewise, virus-activated pDCs from tonsils have shown to secrete large amounts of CXCL10 (235).

Aims of the study

Dysfunction of DCs and NK cells has been reported in patients with different type of malignancies and apparently has a critical role in promoting tumour progression. There are indications that the balance and interaction among distinct DC subsets as well as between DC and NK cells play crucial roles in inducing and shaping effective immune responses.

The objectives of this work were to investigate the absolute numbers integrity and functional properties of peripheral blood DCs and NK cells in advanced stage melanoma patients. In case of an immune dysfunction, the mechanisms behind had to be elucidated. By studying DCs and NK cells from the peripheral blood of melanoma patients in comparison to those from healthy controls, it was investigated

1) whether melanoma patients display alterations in the total and subset numbers of blood DCs and NK cells.

2) whether DCs display aberrant functions and how the functional defects potentially affect the interaction among DC subsets.

3) which mechanisms including alterations in signaling pathways and molecules are responsible for the dysfunction of DCs.

4) whether NK cells exhibit phenotypic changes and alterations in functional properties including their cytolytic machinery and interaction with DCs.

2.0 MATERIALS

2.1 Lab Equipments

BD FACSCaliburTM Flow Cytometer	Becton Dickinson, Heidelberg
Agarose electrophoresis equipment	Biorad Laboratories, Munich
BD FACSAriaTM Flow Cytometer	Becton Dickinson, Heidelberg
BD FACSCanto IITM Flow Cytometer	Becton Dickinson, Heidelberg
Biofuge® Fresco	Heraeus Instrument, Wiesloch
Bio-plex protein reader	Biorad Laboratories, Munich
Blood Cell analyser	Abbott, Wiesbaden-Delkenheim
Centrifuge	Heraeus Instrument, Wiesloch
Confocal Microscope Sp5	Leica, Wetzlar
ELISA Reader	Anthos Labtec, Krefeld
Freezer -20°C	Liebherr Premium
Freezer -80°C	Thermo Fisher Scientific, Karlsruhe
Gel Chamber for agarose gel electrophoresis	Biorad Laboratories, Munich
Gel Doc	Biorad Laboratories, Italy
Glass pipettes	Hirschmann, Eberstadt
Glassware	Schott, Mainz
Incubator HERA Cell 240	Thermo Scientific, Karlsruhe
Light microscope DMIL	Leica, Wetzlar
MACS® MultiStand	Miltenyi Biotech, Bergisch-Gladbach
Mikroskop DMLS	Leica, Wetzlar
Microwave	Bosch, Frankfurt am main
pH Meter	LMV Medizinteknik, Vetriebs GmbH
Power Pac 300	Biorad Laboratories, Munich
Quadro MACS Magnet	Miltenyi Biotec, Bergisch Gladbach
Real time PCR Mxpro 3005	Stratagene, Waldbronn
Refrigerator 4□C	Liebherr, Biberach an der Riss
Roller	Neolab, Heidelberg
SDS-PAGE electrophoresis equipment	Biorad Laboratories, Munich
Shandon Cytospin Centrifuge	Thremo Scientific, Karlsruhe
Spectrophotometer UltroSpec 3100 pro	Pharmacia Biotec, Munich
Thermocycler PTC-100	MJ Research, Inc., Watertown, Mass. (USA)
ThermoMixer 5436	Eppendorf, Hamburg
Vortex	MSI Minishaker IKA, Wilmington
Water baths	Medingen, Martinsried
Western blot equipment	Biorad Laboratories, Munich

2.2 Chemicals

Aqua ad injectabilia, sterile	Braun, Melsungen
Agarose	Sigma-Aldrich, Schnelldorf
30% Acrylamide Solution	Biorad Laboratories, Munich
Ammonium Persulfat	Serva, Heidelberg
Biorad protien assay reagent	Biorad Laboratories, Munich

Bovine Serum Albumin, BSA	Gerbu Biotechnik, Gaiberg
Bovine Serum Albumin, BSA 2mg/ml (protein assay)	Biorad Laboratories, Munich
Dimethylsulfoxid (DMSO)	Merck, Darmstadt
EDTA	Gerbu Biotechnik, Gaiberg
Ethanol, p.a.	Merck, Darmstadt
Ethidium bromide solution (10 mg/mL)	Merck, Darmstadt
Biocoll Separating Solution	Biochrom AG, Berlin
Formaldehyde	Merck, Darmstadt
GeneRuler™ 100bp DNA Ladder Plus	Fermentas, St Leon-Rot
Glycine	Carl Roth, Karlsruhe
PageRuler^{Tm} Prestained Protein Ladder	Fermentas, St Leon-Rot
Isopropanol, p.a.	Merck, Darmstadt
β-Mercaptoethanol	Merck, Darmstadt
Methanol, p.a.	Merck, Darmstadt
Milk powder	Carl Roth, Karlsruhe
Phorbol Myristate Acetate (PMA)	Sigma-Aldrich, Schnelldorf
Ionomycin	Sigma-Aldrich, Schnelldorf
Phosphate Buffered Saline, 1x, 10x PBS	PAA Laboratories, Pasching
Ortho-Phosphoric acid 85%	Merck, Darmstadt
Sodium dodecyl sulfate	Gerbu Biotechnik, Gaiberg
Sodium azide	Merck, Darmstadt
Sodium chloride	Fluka, Switzerland
Sulfuric Acid, 5N	Merck, Darmstadt
TEMED	Sigma-Aldrich, Schnelldorf
Tris-Base	Sigma-Aldrich, Schnelldorf
Tris HCl	Sigma-Aldrich, Schnelldorf
Triton-X 100	Gerbu Biotechnik, Gaiberg
Trypan blue	Fluka, Switzerland
Trypsin-EDTA solution, (10x)	Biochrom AG, Berlin
Trypsin/EDTA	Biochrom AG, Berlin
Tween20	Gerbu Biotechnik, Gaiberg

2.3 Consumables

Aluminium foil Forti	Folien, Neuruppin
Cell culture flasks (25, 75 and 125 cm2)	Renner, Dannstadt
Cell culture dishes	Renner, Dannstadt
Cell culture plates (6, 12, 24 and 48 well)	Renner, Dannstadt
Cell strainer (40 µm)	Becton Dickinson, Heidelberg
Centrifuge tubes (15 and 50 mL)	BD FalconTM, Heidelberg
Shandon filter cards	Thermo Electron Corporation, USA
Cover slips	R. Langenbrinck, Teningen
Cryovials	Costar, Cambridge
Disposable cuvette	Sarstedt, Nümbrecht
ELISA plates	Greiner, Frickenhausen
FACS tubes	Becton Dickinson, Heidelberg
FACS tubes with cell strainer (30 µm)	Becton Dickinson, Heidelberg
Laboratory gloves	Kimberly-Clark, Zaventem (Belgium)
MACS® Separation Columns LS/LD)	Miltenyi Biotec, Germany
Micro Centrifuge tubes (0.5, 1.5 – 2.0 mL)	Eppendorf, Hamburg
Neubauer cell counting chamber	Brand, Wertheim

Nitrocellulose membrane	Amersham Pharmacia, Munich
Parafilm	Pechiney. Menasha
Pasteur pipettes (Sterile)	Carl Roth, Karlsruhe
MACS® (R) Pre-Separation Filters (30µm)	Miltenyi Biotec, Bergisch Gladbach
Polypropylen tubes (15ml, 50 ml)	Falcon, BD Biosceince
Power supply for electrophoresis	Pharmacia, Freiburg
Pipette tips (1 – 1000 µL)	Eppendorf, Hamburg
Pipette filter tips (1 – 1000 µL)	Eppendorf, Hamburg
Real-time PCR plates, 96 well	Biozym, Hessisch-Oldendorf
Slides (76x26 mm)	R. Langenbrinck, Teningen
Syringes (5 – 50 mL)	Terumo, Eschborn
Syringe-driven filter units, pore size 22 µm	Renner, Dannstadt
Whatman 3MM paper	Schleicher & Schüll, Dassel
X-ray film	Amersham Biosciences, Freiburg

2.4 Enzyme/Reagents

dNTP Mix	Invitrogen, Karlsruhe
10x Buffer PCR	Bioron, Ludwigshafen
Taq polymerase	Bioron, Ludwigshafen
10X BD FACS™ lysing solution	BD Biosciences, Heidelberg
BD OptEIA TM Substrate Reagent A/B	BD Biosciences, Heidelberg

2.5 Antibodies for flow ctyometry and immunofluorescence staining

2.5.1 Primary antibody and Fc fusion proteins

BDCA1-PE/APC, Mouse IgG2a	Miltenyi Biotec, Bergisch Gladbach
BDCA2-FITC, Mouse IgG1	Miltenyi Biotec, Bergisch Gladbach
BDCA-3, Mouse IgG1	Miltenyi Biotec, Bergisch Gladbach
CD14-PE-cy5, Mouse IgG2a	Miltenyi Biotec, Bergisch Gladbach
CD19-PE-Cy5, Mouse IgG1	Miltenyi Biotec, Bergisch Gladbach
CD123-Percp 5.5, Mouse IgG1	eBiosceince, USA
CD11c-APC, Mouse IgG1	eBiosceince, USA
CD40-FITC, Mouse IgG1	BD Pharmingen, USA
CD80-PE, Mouse IgG1	BD Pharmingen, USA
CD86-PE/APC, Mouse IgG2b	BD Pharmingen, USA
CD14-FITC, Mouse IgG2a	BD Pharmingen, USA
CD3-FITC, Mouse IgG1	BD Pharmingen, USA
CD19-APC-Cy7, Mouse IgG1	BD Pharmingen, USA
TLR9-PE, Mouse IgG1	Imgenex, USA
MyD88, Rabbit polyclonal IgG	Abcam, UK
IRF7, Rabbit polyclonal IgG	Santa Cruz Biotech, Heidelberg
p4E-BP1 (Ser65/Thr70)	Santa Cruz Biotech, Heidelberg
CD45-Percp, Mouse IgG1	BD Pharmingen, USA
CD3-APC, Mouse IgG2a	Miltenyi Biotec, Bergisch Gladbach
CD56-PE, Mouse IgG1	BD Pharmingen, USA
CD16-FITC, Mouse IgG1	BD Pharmingen, USA
CD107a-PE-Cy5, Mouse IgG1	BD Pharmingen, USA
Perforin-FITC, Mouse IgG2b	BD Pharmingen, USA
IFN-γ-PE, Mouse IgG1	BD Pharmingen, USA
NKG2D-APC, Mouse IgG1	Miltenyi Biotec, Bergisch Gladbach
NKp30-PE, Mouse IgG1	Beckmann Coulter, USA

NKp46-PE, Mouse IgG1	Beckmann Coulter, USA
MICA, Mouse IgG1	R&D System, Wiesbaden
MICB, Mouse IgG?	R&D System, Wiesbaden
NKp30-Fc fusion protein	R&D System, Wiesbaden
NKp44-Fc fusion protein	R&D System, Wiesbaden
NKp46-Fc fusion protein	R&D System, Wiesbaden
GAPDH, Rabbit polyclonal IgG	Cell signaling, USA

2.5.2 Secondary antibodies

Goat anti-rabbit IgG, F(ab')2 (H+L), Alexa fluor 555-conjugated	Invitrogen, Karlsruhe
Donkey anti-rabbit IgG, F(ab')2 (H+L), PE-conjugated	Jackson Immunotech Laboratory, USA
Goat anti-rabbit IgG, HRP- conjugated	Cell signaling, USA

2.5.3. Antibodies for soluble MICA/B and ULBP2 ELISA

purified MICA/B (AMO1), Mouse anti-human monoklonal, IgG1
purified MICA/B (BAMO3), Mouse anti-human monoklonal, IgG2a
purified ULBP2 (BUMO1), Mouse anti-human monoklonal, IgG1
purified anti-ULBP2, Mouse anti-human monoklonal, IgG2a
HRP-goatanti-mouse IgG2a

2.6 Cell culture media and supplements

2.6.1 Media

RPMI 1640 with L-Glutamine,	PAA Laboratories, Pasching
IMDM with L-Glutamine,	PAA Laboratories, Pasching

2.6.2 Media supplements

Foetal Calf Serum (FCS)	Gibco Invitrogen, Karlsruhe
Penicillin/Streptomycin 100X,	PAA Laboratories, Pasching

2.7 Cells

2.7.1 Primary cells

Human PBMCs	Prepared from centrifuged human blood (buffy coat); blood was acquired from the Institute of Transfusion Medicine, Mannheim
Human mDCs	Prepared from human PBMCs of buffy coats or leukapheresis products
Human pDCs	Prepared from human PBMCs of buffy coats or leukapheresis products
Human NK cells	Prepared from human PBMCs of buffy coats or leukapheresis products

2.7.2 Human cell lines

Mel249	Melanoma; established from melanoma patients
K562	Chronic Myelogenous leukemia, provided by Prof.Dr Schadendorf, Mannheim

2.8 Oligonucleotides

2.8.1 Oligonucleotides used for standard PCR

Primer

β-Actin: 5'- CGG CTA CCA CAT CCA AGG AA -3' (Forward)
5'- GCT GGA ATT ACC GCG GCT -3' (Reverse)

2.8.2 Labelled oligonucleotides used for quantitative real-time PCR

Gene	Species	Detection chemistry
GAPDH	Human	FAM-TAMRA
IRF7	Human	FAM-TAMRA

2.8.3 Oligonucleotides used for Cell stimulation

CpG A: 5'-ggGGGACGATCGTCgggggg-3'

2.9 Kits and standards

Kits	Manufacturer
Bio-plex kit	Bio-rad, Munich
Blood Dendritic Cell Enumeration Kit (human)	Miltenyi Biotec, Bergisch Gladbach
CD1c (BDCA-1)$^+$ Dendritic Cell Isolation Kit	Miltenyi Biotec, Bergisch Gladbach
CytoFix and CytoPerm^{TM}	BD Bioscience, USA
Dead Cell Removal kit	Miltenyi Biotec, Bergisch Gladbach
ECL solution	Thermo Scientific, Karlsruhe
First strand cDNA synthesis kit (AMV)	Roche, Mannheim
IFN-α Elisa kit	Mabtech, Germany
IL-10 Elisa kit	Diaclone, Cologne
CD304 Microbead kit	Miltenyi Biotec, Bergisch Gladbach
qPCR Master Mix	Applied Biosystem, Darmstadt
Rneasy-Plus Mini Kit	Qiagen, Hilden
Taqman Gene Expresion Assay	Applied Biosystem, Darmstadt
TMB substrates for ELISA	BD Bioscience, USA
VectaShield	Vector Laboratory, Eching

2.10 Multiple protein bead array (Luminex) cytokine assay

Kits for luminex cytokine assay include 17-plex Bio-Plex human cytokine and singleplex human cytokine for CXCL10, CCl2, CCL3 and CCL5 (Bio-Rad, Munich).

2.11 Buffers

All buffers used in this study are listed in the Appendix.

2.12 Software

Software	Manufacturer
FACSDiva™	BD Bioscience, USA
CellQuest™ 3.3	BD Bioscience, USA
FlowJo™ 7.2; 8.0	TreeStar, USA
LAS AF Lite	Leica, Wetzlar
Graphprism™ 4.0	GraphPad Software Inc., San Diego, USA
Image J	Wayne Rasband, National Institutes of Health, USA
Amira	Visage Imaging, USA
WinRead	Anthos, Austria
QuantiOne	Biorad Laboratories, Italy
Bio-Plex manager	Biorad Laboratories, Munich
Mx3005 pro	Stratagene, USA

3.1 Cell biology methods

3.1.1 Sample collection

Samples were obtained from 19 female and 41 male melanoma patients (age: 26-84 years), who were diagnosed with stage IV melanoma according to the AJCC criteria and admitted to the Department of Dermato-Oncology, University Medicine Mannheim. Material was obtained from patients with or without measurable lesions and irrespective of prior treatment. Patients were either had no prior treatment or radiotherapy for at least 30 days before blood withdrawal and serum collection. Leukapherasis products were obtained from a total of 10 patients: 5 patients received no or free from prior treatment, 3 patients without treatment information and 2 patients were treated with moDC vaccination. A total of 63 age-matched normal volunteers (27 female, 34 male and 2 without information) with age range 25-69 were included as control in this study. Materials from normal donors including heparinised or EDTA treated peripheral blood, buffy product and serum were obtained from Institute of Transfusion and Immunology, Mannheim, Germany. Written informed consent as approved by the local ethical committee was obtained from all subjects included in this study.

3.1.2 Cell culture method

All cells were grown at 37 °C in an incubator with 5 % CO_2. If not mentioned otherwise all cell culture media were supplemented with 100 U/mL penicillin, 100 µg/mL streptomycin and 10% heat-inactivated FCS (at 56°C for 1 h). All media supplements

were steril-filtered (pore size: 22 µm) before addition. Adherent cells were detached from the surface of the cell culture flasks using trypsin/EDTA. Before the detachment, growth medium was removed and the cells were washed by the careful addition and subsequent removal of 5–10 mL PBS. Then 2 mL of trypsin/EDTA solution/75cm^2 were added and the cells were kept for 2-3 minutes at 37 °C in a cell incubator. After detachment, cells were washed in 10 mL fresh complete medium to inactivate the trypsin/EDTA. For culturing K562, a suspension cell line, cells were maintained by replacement with fresh complete medium. Cells were in part used for culture maintenance and for experiments.

3.1.3 Preparation of human PBMCs from buffy coats

PBMCs used in experiments were prepared from buffy coats of normal donors or from peripheral blood or leukapheresis products of melanoma patients diagnosed with disease stage IV. Buffy coats, peripheral blood and leukapheresis products were diluted with 1 x PBS at 3:1 ratio before subjected to Ficoll (Biocoll) separation solution. PBS diluted buffy coat blood was gently layered on the 15 mL pre-chilled Ficoll (Biocoll) solution in 50 ml Falcon tubes at ratio of 3:1 and subjected to centrifugation (2000 rpm no break, 20 min). The interphase layer, which represents mononuclear cells were gently harvested using a sterile pastuer pipette and washed 3 times with 1x PBS followed by centrifugation at 1200 rpm, 7 min, room temperature. The isolated PBMCs were filtered using a cell strainer and then counted using trypan blue and a hemocytometer. The single cell suspension was cryopreserved in freezing medium until used in further experiments.

3.1.4 Cryopreservation and thawing of cells

For freezing isolated PBMCs, cells were adjusted to numbers of 2-5 x 10^7 in freezing medium (see Appendix) pre-cooled on ice. The cell suspension was then transferred into 1.8 mL cryovials and immediately transferred to freezing containers containing isopropanol (MrFrosty, Nunc, Denmark) and stored at -80°C. After 24-48 h the cryo vials were transferred to liquid nitrogen containers and stored at approximately -170 °C. In order to thaw cells, cryovials were placed in a 37°C water bath for approximately 2 min followed by adding pre-warmed growth medium drop wise to the cell suspension. One washing step was performed in 10 mL complete growth medium to remove the DMSO.

After centrifugation at 1200 rpm for 7 min, cell pellets were resuspended in complete medium and seeded as indicated.

3.1.5 Dead cell removal

Prior to MACS (magnetic-activated cells sorting) cell separation, dead cells were removed using the dead cell removal kit according to the instruction of the manufacturer (Miltenyi Biotech). Briefly, 3 x 10^8 total cells were pelleted by centrifugation at 1200 rpm for 7 min at room temperature. After complete removal of the supernatant, cells were resuspended in 3 mL (100 µL/10^7 cells) of Dead Cell Removal MicroBeads. Cells were mixed well followed by incubation for 15 minutes at room temperature and separated using the MACS cell separation technology.

3.1.6 Isolation of BDCA1$^+$ mDCs and BDCA4$^+$ pDCs from cryopreserved PBMCs using MACS Separation

Cryopreserved PBMCs from leukapheresis products of melanoma patients and from buffy coats of age-matched healthy donors were used for mDC1 and pDC isolation. One day prior to DC subset purification, PBMCs were thawed and cultured as bulk PBMCs overnight in fully supplemented RPMI-1640 medium without exogenous stimuli. Dead cells were removed using the dead cell removal kit. Both DC subsets were sequentially purified by magnetic cell sorting (MACS) using a high gradient Maxi-MACS® device. Myeloid DCs (mDC1) were obtained from PBMCs by depletion of CD19$^+$ B lymphocytes prior to mDC1 purification via incubation with biotin-conjugated anti-CD1c and anti-biotin-conjugated magnetic microbeads. Additional depletion of CD3 and CD14 cells were performed prior pDC isolation using anti-CD304 (BDCA-4)-conjugated magnetic microbeads.

3.1.7 Co-culture of BDCA1$^+$ mDCs with BDCA4$^+$ pDCs

mDC1 (~1.75 x 10^4/ well) and pDCs (~5.0 x 10^3/ well) were seeded in V-bottom microwells alone or in co-culture. Cells were cultured with or without the following stimuli: CpG A oligodeoxynucleotide (ODN) at 10 µg/ml, LPS at 1 µg/ml or UV-inactivated Newcastle Disease virus (kindly provided by Prof. Zatwasky, DKFZ, Heidelberg) at a dilution of 1:100. Cells were cultured in complete RPMI-1640 medium and incubated for 18 h. The supernatants were collected and stored at -20°C until

analysis. Expression of CD40, CD80 and BDCA1 on mDC1 was analysed by direct immunofluorescence staining with anti-CD80-PE mAb, anti-CD40-FITC and APC-conjugated anti-BDCA-1 for myeloid DC (mDC1) as described in method 3.2.1, followed by flow cytometry analysis.

3.1.8 PBMC stimulation for cytokines, chemokines and growth factor analysis

PBMCs (2×10^6/200 µl) were seeded in 96-well round-bottom plates and stimulated with 10 µg/ml CpG A or left untreated for 22 h. Cell culture supernatant were collected after 22 h stimulation and kept at -20°C until use for IFN-α and IL-10 ELISA analysis (method 3.2.6) and for multiplex protein bead array analysis to detect cytokines, chemokines and growth factor (method 3.2.10).

3.1.9 Immunofluorescence staining

IRF-7 translocation was determined by stimulating PBMCs (2×10^6/200 µl/well with a total of 1-2 $\times 10^8$ cells) in 96-well round-bottom plates with 10 µg/ml CpG A for 6 h. Cells were first stained with the following monoclonal antibodies: FITC-labelled anti–BDCA-2, Percp-Cy 5.5-labelled anti-CD123, APC-labelled anti-CD11c. Subsequently, cells were fixed overnight with 1% formaldehyde. Pre-stained cells were then permeabilized with 0.25% Triton-X 100 for 5 min at room temperature. Samples were blocked with 3% BSA for 1 h and labelled with rabbit polyclonal anti–human IRF-7 (Santa Cruz Biotechnology). Anti–rabbit IgG Alexa Fluor 555 was used as secondary antibody. As a negative control, rabbit polyclonal anti–human IRF-7 was omitted and cells were stained similarly with Anti–rabbit IgG Alexa Fluor 555. Cells were subjected to cell sorting (method 3.2.4) and the sorted cells were cytospun on glass slides at speed of 700 rpm for 4 min. Mounting was performed using Vectashield mounting medium containing DAPI (Vector Laboratories).

3.1.10 Confocal microscopy and quantification of nuclear translocation

All images were acquired using a confocal fluorescence microscope and a 63×/1.4 NA objective, with the pinhole set for a section thickness of 1 Airy (95.5 µm). Scan speed of 100 Hz and 4 frames averaging was used. Sequential image acquisition using separate

laser was performed for avoiding cross-talk between different fluorophores. Translocation of IRF7 was quantified by measuring nuclear fluorescence alone that was compared to the intensity of the cytoplasmic staining to obtain relative measure of IRF7 as nuclear:cytoplasmic ratio. This prevents increased background levels of IRF7 expression or artificial differences in staining intensity. Therefore, the IRF7 translocation is represented by an increasing nuclear:cytoplasmic ratio. The median of nuclear:cytoplasmic ratio derived from 50-80 images of each sample were calculated using statistic software.

3.1.11 Analysis on NK and DC interactions

3.1.11.1 Generation of monocyte-derived DCs

Monocytes were purified from isolated PBMCs by MACS separation using anti-CD14 microbeads. Cells were then seeded and cultured in complete RPMI1640 supplemented with 10% FCS at density of $2x10^5$ cells/mL in the presence of GM-CSF (1000 IU/mL) and IL-4 (500 IU/mL). After 6 days, monocytes developed into immature moDCs that were then harvested and subjected to NK/moDC interaction studies.

3.1.11.2 Interaction of IL-2 activated NK cells with moDCs

NK cells were isolated from PBMCs obtained from healthy controls using the MACS Cell separation technology. NK cells were obtained by depleting $CD3^+$ T cells with anti-CD3 mAb coupled magnetic beads followed by positive selection using anti-CD56 mAb coupled magnetic beads. The purified NK cells were either cryopreserved until use as resting NK cells or stimulated with IL-2 (100 IU/mL) in complete RPMI1640 culture medium for 6 days. Then, IL-2 activated NK cells were harvested while resting NK cells were retrieved from cryopreservation. Both activated and resting NK cells were counted and adjusted to a concentration of 1×10^6 cells/mL. Similarly, immature moDC were harvested and washed two times with complete medium then adjusted to 1×10^6 cells/mL. Activated or resting NK cells were co-incubated with immature moDCs at a ratio of 1:1 and co-cultured for 48 h. As positive control, moDCs were stimulated with IFN-α (1000 IU/mL) for the same time period. After 48 h, cells were harvested, stained and assessed for CD40 and CD80 expression by flow cytometry.

3.1.11.3 Interaction of IL-2 activated NK cells with mDC1

Both mDC1 and NK cells were purified from PBMCs collected from age-matched healthy controls and patient by MACS cell separation using anti-$BDCA1^+$ and anti-CD56 monoclonal antibody coupled magnetic beads, respectively. $CD3^+$ T cells and $CD14^+$ monocytes were depleted during the separation procedure. Two rounds of $BDCA1^+$ and $CD56^+$ cell selection were performed during isolation. Freshly purified $BDCA1^+$ mDC1 (2×10^5 cells) were then cultured together with autologous NK cells (1×10^5 cells) in the presence of IL-2 (100 IU/mL) or LPS (1 μg/mL) or in medium alone. After 48 h, cells were harvested and stained with a FITC-conjugated anti-CD40 monoclonal antibody then evaluated by flow cytometry. Fold increase of CD40 expression on mDC1 was derived from the ratio of $MFI_{stimulated}$ to $MFI_{unstimulated}$ co-cultures. Data are shown as median from three normal donors and four patients.

3.2 Immunological methods

3.2.1 Determination of cell surface antigen expression using flow cytometry

Cell surface antigen staining was performed by staining $1\text{-}2 \times 10^6$ of thawed PBMCs with or without stimulation as indicated, or 1×10^5 cultured melanoma cells in round-bottom Falcon tubes. Cells were first washed twice with FACS buffer, then centrifuged at 1500 rpm, 5 min. The cell pellet was dispersed by gentle vortexing and 5 μL of heat inactivated pooled human sera (PHS) was added into the tubes when performing staining on PBMCs. In parallel, cells were stained with fluorochrome-conjugated or non-conjugated primary monoclonal antibody against respective cell surface antigen and shaked on ice for 20 min at about 200 rpm in the dark. After incubation, pre-stained cells were then subjected to 2 washes with FACS buffer at 1500 rpm, 5 min. For the case that non-conjugated primary antibody was used, fluorochrome-conjugated secondary antibody was added after washing and further incubated at the same condition as mentioned above. Cell surface stained cells were then fixed with 3.75% formaldehyde solution and kept at 4°C in the dark until FACS measurement. Prior measurement, cell clumps were removed by passing the cells through a cell strainer with a pore size of 30 μm to obtain single cell

suspensions. Appropriate isotype controls or staining with secondary antibody only were included in each experiment. FACS measurements were performed either with FACS Calibur or FACS Canto II and acquired using Cellquest or FACsDiva software. Forward- and side- scatter gates were used to exclude cell debris prior to analysis of expression of each phenotypic marker. The gain in the FSC and SSC channel was adjusted so that the cell populations were centralised on the dot plot. The desired cell population was included in the analysis through the gating approach. FACS data were analysed using the Flowjo software and the frequency of cells expressing the proteins of interest or the expression were presented as percentage or Median Fluorescence Intensity (MFI), respectively.

3.2.2 Whole blood enumeration of mDCs and pDCs

Blood circulating DCs were identified and enumerated by flow cytometry using the FACS Calibur. The assay was performed using the blood DC enumeration kit according to the manufacturer's instructions. Briefly, the cell count of white blood cells (WBCs) in heparinized peripheral blood samples were obtained by using a blood counter prior to labeling of whole blood cells with a cocktail of antibodies containing anti-CD14, anti-CD19, anti-BDCA1 (mDC1 marker), anti-BDCA3 (mDC2 marker) and BDCA-2 (pDC marker) or isotype antibodies. A proprietary dead cell discriminator dye was also included to exclude dead cells. Erythrocytes were then lysed using FACS lysing solution and after one time washing, cells were fixed and examined using FACS Calibur and analysed using the Flowjo software. Results are expressed as the percentage of mDCs or pDCs in WBCs or as absolute numbers per mL blood (calculated as [% positive- % negative cells] × WBCs per ml [$\times 10^6/100$]).

3.2.3 Whole blood enumeration of NK cells

The TruCOUNT™ assay was designed to determine absolute $CD56^+CD16^{-/dim}$ and $CD56^+CD16^+$ NK cells counts. 100 µL of well-mixed anti-coagulated, freshly withdrawn peripheral blood obtained from age-matched healthy donors and stage IV melanoma patients were stained within 6 h after blood collection and were added to TruCOUNT™ tubes. The directly fluorophores-conjugated mAbs as follows: CD56-PE, CD45 Percp,

CD3-APC and CD16-FITC or isotype controls were then added to the TruCOUNT™ tube, mixed well and incubated for 15 min in the dark at room temperature.

To each tube, 400 µL of FACS Lysing solution was added and incubated for 15 min in the dark at room temperature. Samples were vortexed gently just before data acquisition and analyzed within 24 h of staining on a FACS Calibur. NK cell number of whole blood samples was calculated according to the manufacturer's instruction, for example:

[Total NK cells absolute number] = [($CD56^+/CD3^-$ cell count) / (bead count)] × [total number of beads (provided by manufacturer) / 100 µL].

The same equation was used for calculating non-specific bindng cells when cells were stained with corresponding isotype controls. The corrected total NK cells absolute number was calculated by subtracting non-specific binding cell number from total NK cells number.

3.2.4 Cell sorting using flow cytometry

1-2 $x10^8$ PBMCs were stimulated as mentioned in method 3.1.9. Cells were stained for surface antigens CD123, CD11c and BDCA2 (method 3.2.1). After the last wash, cells were suspended at a concentration of 3 x 10^7 cells/ml in PBS with 10% BSA. Cell clumps were then removed using cell strainer (30 µm) to obtain single cell suspensions. PBMCs were kept on ice in the dark until cell sorting was performed using the FACSAria. Appropriate compensation controls were prepared for setting up parameters for cell sorting and dead cells were determined using Sytox-Blue, which only binds to DNA of dead cells with compromised cell membrane. pDCs were sorted into PBS containing 5% heat in-activated FCS and subjected to cytospin.

3.2.5 Detection of intracellular TLR9, MyD88, p4E-BP1 and IRF7 by flow cytometry analysis

PBMCs (1-2 x 10^6 cells) of healthy donors and patients were thawed and either stimulated with CpG A or left unstimulated for the time point described in the result section. Cells were stained with antibodies against surface markers specific to pDC (anti-BDCA2 and anti-CD123) and with markers for exclusion of unwanted cells (anti-CD14, anti-CD3 and anti-CD19 or anti-CD11c) as described in 3.2.1. PBMCs were then fixed

and permeabilized with cytofix and perm buffer according to the manufacturer's instruction. Subsequently, cells were then stained with either TLR9 or MYD88 or p4E-BP1 antibodies in the presence of PHS. The similar procedure as described in method 3.1.9 was performed for IRF7 staining. After two continuous washes, anti–rabbit IgG-PE was used as secondary antibody at a dilution of 1:50. Data were obtained using FACSCanto II. Corresponding isotype controls or fluorescence minus one (FMO) controls were included to exclude non-specific binding.

3.2.6 Enzyme-link immunosorbent sandwich assay (ELISA) for cytokine detection in cell culture supernatants

Cell culture supernatants harvested during mDC1 and pDC co-cultured were measured for the presence of IFN-α or IL-10 by ELISA kits. Both ELISA have a detection range of 4–400 pg/ml and were performed according to the manufacturer's recommendations. Briefly, a 96-well plate with flat bottom was pre-coated with a capture antibody detecting the cytokine of interest for overnight at 4°C. To remove unbound capture antibody, the plate was washed 5 times and then blocked with blocking solution for 1 h at room temperature. Each standard curve from 0-400 pg/mL of the cytokine of interest was prepared by serial dilutions using respective stock standard solutions provided by the manufacturer. The frozen cell supernatants stored at -20°C were thawed and diluted accordingly with recommended assay diluents and added at 100 µL into individual wells of the microtiter plate in duplicates. Plates were incubated with test samples and the serially diluted standard for 2 h and then washed 5 times with washing buffer prior to adding 100 µL of diluted biotinylated detection mAb. After incubation for the recommended period of time, unbound antibody was removed by washing 5 times. Then, 100 µL of diluted Streptavidin-horseradish peroxidase (HRP) conjugate solution were added and incubated as indicated by the manufacturer. Upon completion of the incubation, the plate was washed and 100 µL of TMB substrate solution were added into each well. The plate was covered with aluminium foil and incubated for 15-30 min in the dark. The reaction between HRP and TMB was stopped by adding 50 µL of stop solution and by swirling the plate gently for proper mixing. The absorbance value was then determined at 450 nm with a reference wavelength at 650 nm using a mircroplate reader

within 5-30 minutes after adding the stop solution. The concentrations of the cytokine of interest in the samples were determined based on the standard curve.

3.2.7 ELISA for soluble NKG2DL detection in sera from melanoma patients

For detecting the soluble NKG2DL including sMICA/B and sULBP2, ELISA was performed as previously described by Paschen *et al.* (236).

3.2.8 Degranulation assay

NK cell degranulation in response to co-incubation with tumour cells devoid of MHC class I molecules (K562, Mel249) was analysed with PBMCs obtained from healthy donors and patients. Cryopreserved PBMCs were thawed and rested overnight in complete IMDM medium supplemented with 10% PHS and 1 % Pen/Strep. Subsequently, 100 µL of 1 x 10^5 PBMCs in assay medium were transferred to U-bottom 96-well plate and co-incubated with 1 x 10^4 target tumour cells. The PE/Cy5 conjugated anti-CD107a mAb or an isotype control was added and incubated at 37°C and 5% CO_2 for 1 h. After 1 h incubation, the protein transport inhibitor GolgiStop was added to the co-culture, followed by further 3 h co-incubation. To monitor the spontaneous degranulation of NK cells, control samples were incubated without target cells. Prior to flow cytometric analysis, cells were stained on ice with anti-CD3, -CD56 and -CD16 mAbs and washed as described in section 3.2.1.

3.2.9 Detection of intracellular IFN-γ and perforin by flow cytometry

To determine the intracellular perforin expressing NK cells during steady-state and IFN-γ production of NK cells upon PMA/ionomycin activation, PBMCs were thawed and rested overnight as described in (section 3.2.8). 2 x 10^6 of untreated PBMCs were used for perforin staining. For IFN-γ staining,2 x 10^5 cells were incubated in a final volume of 200 µL in the assay medium in the presence or absence of PMA (2.5 µg/mL) and Ionomycin (0.5 µg/mL) for 4 h at 37°C in a humidified 5% CO_2 incubator. Brefeldin A, a secretion inhibitor (10 µg/mL) was added after the first hour of stimulation. Thereafter, cells were harvested, washed twice with FACS staining buffer and stained with mAb against CD3 and CD56 for NK cells identification for 30 min on ice in the dark. Cells were then washed and followed by fixation and permeabilization using CytoFix and

CytoPerm buffer as recommended by the manufacturer. Intracellular staining was performed with anti- IFN-γ or anti-perforin mAbs for 30 min on ice in the dark. Cells were washed twice prior to flow cytometric acquisition.

3.2.10 Multiplex protein bead array assays for cytokines, chemokines and growth factors detection

Blood samples were drawn for serum collection by using vacutainers containing no anticoagulant. All collected blood samples were allowed to coagulate for 30 min at room temperature. For sera separation, samples were centrifuged at 3000 rpm for 10 min. All specimens were aliquoted immediately and stored at –20°C before being assayed in a Luminex bioassay. Only sera with no more than two freeze-thaw cycles were analysed. A variety of different human cytokines and chemokines were investigated following the manufacturer's instructions using the multiplex bead array assays. This technology allows the simultaneous analysis of different cytokines, chemokines and growth factors in a small sample of serum (50 µL) in a single microplate well. Using this technology, it allows the quantitation of a panel of cytokines and chemokines (IL-1β, IL-10, IL-6, IL-8, IL-12(p70), CXCL10, IFN-γ, TNF-α, CCL2, CCL3, CCL4 and CCL5). The assay was performed by first incubating colour-coded polystyrene beads conjugated to a capture antibody for the cytokine, chemokine or growth factor of interest with cell culture supernatants or sera and corresponding standards for 30 min on a shaker. After incubation, a biotinylated antibody was added and incubation was again carried out for another 30 min on a shaker. The biotinylated antibody was then bound by streptavidin-conjugated with PE and analyzed using the Bio-plex protein array reader. During data acquisition, the beads are interrogated by a red laser (to identify the bead type) and by a green laser, which determines the amount of bound analytes. Data were analyzed using the Bio-Plex manager software with 5PL curve fitting.

3.3 Molecular biological method

3.3.1 RNA isolation from PBMCs

PBMCs from stimulation experiments (method 3.2.5) were pelleted by centrifugation after washing with PBS, frozen in liquid nitrogen and either stored at -80 °C or used immediately for total mRNA extraction with the RNeasy Plus Mini-Kit according to the

manufacturers instructions. Isolated RNA was kept at -80°C in RNAse-free water. RNA concentration was determined using the spectrophotometer (method 3.3.2).

3.3.2 Quantitation of nucleic acids concentration using the spectrophotometer

The DNA/RNA concentration in a sample was determined using a spectrophotometer via the absorbance at 260 nm (A_{260}) using the following formula:

Nucleic acid [µg/mL] = ε x A_{260} x dilution factor, with $\varepsilon_{DNA} = 50$ and $\varepsilon_{RNA} = 40$.

The ratio A_{260}/A_{280} was taken as a measure of the purity of a DNA/RNA sample.

3.3.3. cDNA synthesis from total RNA

Total RNA was reversely transcribed into cDNA using the First Strand cDNA synthesis kit with AMV Reverse Transcriptase according to the manufacturers instructions. In general, about 300-400ng total RNA per sample were reverse transcribed using oligo$(dT)_{12-18}$ primers and the generated cDNA was used in subsequent PCR reactions.

Condition for cDNA synthesis:
1. 25°C 10 min
2 .42°C 60 min
3. 99°C 5 min
4. 4°C 5 min

3.3.4 Polymerase chain reaction (PCR)

Standard PCR using primers specific for the housekeeping gene beta-actin was performed to assess the quality of cDNA product after reverse transcription. The PCR were amplified according to the condition described as following:

1. 95°C- 3 min
2. 95°C- 30 sec
3. 57°C- 30 sec
4. 72°C- 45 sec
5. Step 2 3X
6. 95°C- 30 sec
7. 56°C- 30 sec
8. 72°C- 45 sec
9. Step 6 29X
10. 72°C- 3 min
11. 4°C forever

After PCR amplification, PCR products were loaded onto 1% agarose gels followed by electrophoresis, ran at a constant voltage of 100 V and visualized with ethidium bromide staining.

3.3.5 Quantitative real-time RT-PCR

Reverse transcription quantitative real-time PCR is a method that can be used for determining gene expression by combining amplification and simultaneous quantification on the relative mRNA amount of a gene. This method allows accurate relative quantification as the amplified cDNA amount is measured after each cycle during the PCR and not only after the last cycle as in traditional standard PCR. Highly accuracy of real-time PCR is achieved by normalizing the target gene expression to an endogenous control in a given sample. Real-time PCR was performed using cDNA reverse transcribed from RNA extracted from PBMCs treated or non- treated with CpG A for 6 h. The analysis was performed on a Stratagene sequence detector system. Data were analysed with the Mx3005pro software using primers and Taqman probes specific for the target gene IRF7 [FAM-labeled probe (Assay ID: HS00242190_g1)], with GAPDH as endogenous control (RefSeq: NM_002046.3). Singleplex PCR reactions for amplification of target or endogenous control cDNA were performed in 96-well plates. Amplification was conducted as follow: 95°C, 10 min, 50 cycles of 95°C, 15s and 60°C, 1 min. In every experiment, a negative control was included consisting of a reaction mixture that did not contain a cDNA template. For each sample, the threshold cycle (CT) value for IRF7 was normalized to the CT value of the endogenous control, using the equation $\Delta c_T = c_T$ (target gene) – c_T (reference gene). Fold increase of relative quantity of the target genes after stimulation with CpG A was calculated by the formula $2^{-\Delta\Delta cT}$, with $\Delta\Delta c_T = \Delta c_T$ (stim) – Δc_T (unstim), where Δc_T (unstim) and Δc_T (stim) refer to threshold cycle values obtained prior stimulation and after CpG A treatment, respectively. For each sample, CT values were determined from triplicate of target and housekeeping gene amplifications that were performed and set as the mean of these measurements ± the standard deviation.

3.4 Protein chemical methods

3.4.1 Generation of cell lysates

Cells were harvested, washed once in PBS (1200 rpm, 7 min.) and counted using trypan blue. Second wash with PBS was removed by centrifugation (3000 rpm, 3 min.) and 100 µL RIPA lysis buffer (containing 4 µL Protease Inhibitor Cocktail) was added per 1x 10^6 cells. The cells were homogenised in the buffer by pipetting up and down and then

incubated for 15 minutes on ice. After centrifugation in a table centrifuge (13,000 rpm, 15 min), the protein containing supernatant was transferred to a pre-cooled eppendorf tube and stored at -80 °C until use.

3.4.2 Bradford protein assay

The Bradford protein assay is commonly used to determine the total protein concentration of a sample. The assay is based on a shift of absorbance from 465 to 595nm for an acidic solution of Coomassie Brilliant Blue G-250 when binding of the dye to proteins occurs. Both hydrophobic and ionic interactions stabilise the anionic form of the dye, causing a visible colour change. Within the linear range of the assay, it can be assumed that the more protein is present, the more Coomassie dye binds to proteins. BSA stock solution was diluted accordingly (2.0 – 12.0 mg/mL) with 1x PBS and used to generate a standard curve. 1 µL of the standardised and the test samples were transferred into a disposable cuvette containing 800 µL PBS. Then, 200 µL of Coomassie Brilliant Blue was added to each cuvette and the absorbance at 595 nm was read out by a spectrophotometer within 5 minutes.

3.4.3 SDS poly-acrylamide gel electrophoresis and western blot

SDS poly-acrylamide gel electrophoresis (SDS-PAGE) is a method used to separate proteins based on their molecular weight. During the process, the detergent SDS is used to denature proteins to the same linear shape and to coat them with many negative-charged SDS molecules. During poly-acrylamide electrophoresis, proteins migrate towards the positive pole and the migration speed depends on the size of the protein. The proteins migrate through two gels of different pore size. The stacking gel enhances the sharpness of the protein bands whereas the separation of proteins begins in the separating gel. Both stacking and separating gels were prepared as described (Laemmli method) and cast with gel cassette. After polymerization of both separating and stacking gels, the cassette with the complete gels was fixed in the electrophoresis chamber, which was then filled with electrophoresis buffer. 10 µg of protein lysate per sample was denatured in 5x sample buffer by heating for 3 minutes at 95 °C and then resolved by SDS-PAGE gel electrophoresis. The test samples and molecular weight marker were loaded into separate wells. The electrophoresis was run at a constant voltage of 100V. After electrophoresis

was stopped, the separated proteins were transferred to a nitrocellulose membrane using a wet transfer system. A sandwich was formed by using 2 pre-wet blotting sponges, a total of 6 sheets of pre-wet Whatman paper in transfer buffer with the SDS-PAGE gel and a nitrocellulose membrane in between the sponges and Whatman papers. The mini sandwich was prepared on a blotting cassette without the inclusion of air bubbles. Blotting was performed for 60 minutes at constant voltage. Complete transfer of the protein onto the nitrocellulose membrane was indicated by the pre-stained molecular weight marker. After blotting, the nitrocellulose membrane was blocked with 5% BSA (w/v) in PBS-T solution for 1 h at room temperature on a roller. The primary antibody binding to the protein of interest was diluted with 5 % blocking buffer and added to the membranes and incubated for overnight at 4 °C. Membranes were washed thrice for 5 minutes in PBS-T solution followed by adding the HRP-conjugated secondary antibody, which was diluted in 1.0 % milk solution and incubated for one hour at room temperature. Next, washing was performed thrice on membranes for 5 minutes in PBS-T solution and once in 1x PBS. Antibody binding was then visualized using the ECL detection system. The detection solutions were mixed at equal volume and evenly distributed onto the membranes followed by 3 min incubation. The membranes were then placed in a film cassette and the chemiluminescence on the membranes was detected with x-ray films. The time for development varied depending on the intensity of the chemiluminescence. GAPDH antibody was used as loading control. Each film of a blot was first scanned and stored as TIF format. The signal intensities on the films were then determined using the Image J software. Relative fold increase of signal intensity of a target protein e.g p4E-BP1 from stimulated sample is calculated by setting the normalised signal intensity of p4E-BP1 from unstimulated sample as 1.

3.5 Statistical analysis

All the statistical analyses were performed with the GraphPad Prism software version 4. The correlation between two qualitative variables was assessed by the Spearman's rank test. The Mann-Whitney rank sum test was performed to compare two groups of values for evaluating the significance of difference in the median values between healthy donors and melanoma patients. For all statistical analysis, $p<0.05$ was considered as significant.

4.1 Results

4.2 Absolute number and balance of circulating DC subsets in advanced melanoma patients

4.1.1 Reduction of pDC and mDC2 but not mDC1 numbers in melanoma patients

We characterized and enumerated three subsets of circulating DCs in age-matched healthy controls (n = 18) and stage IV melanoma patients (n = 23), who are free from previous treatment for at least 30 days.

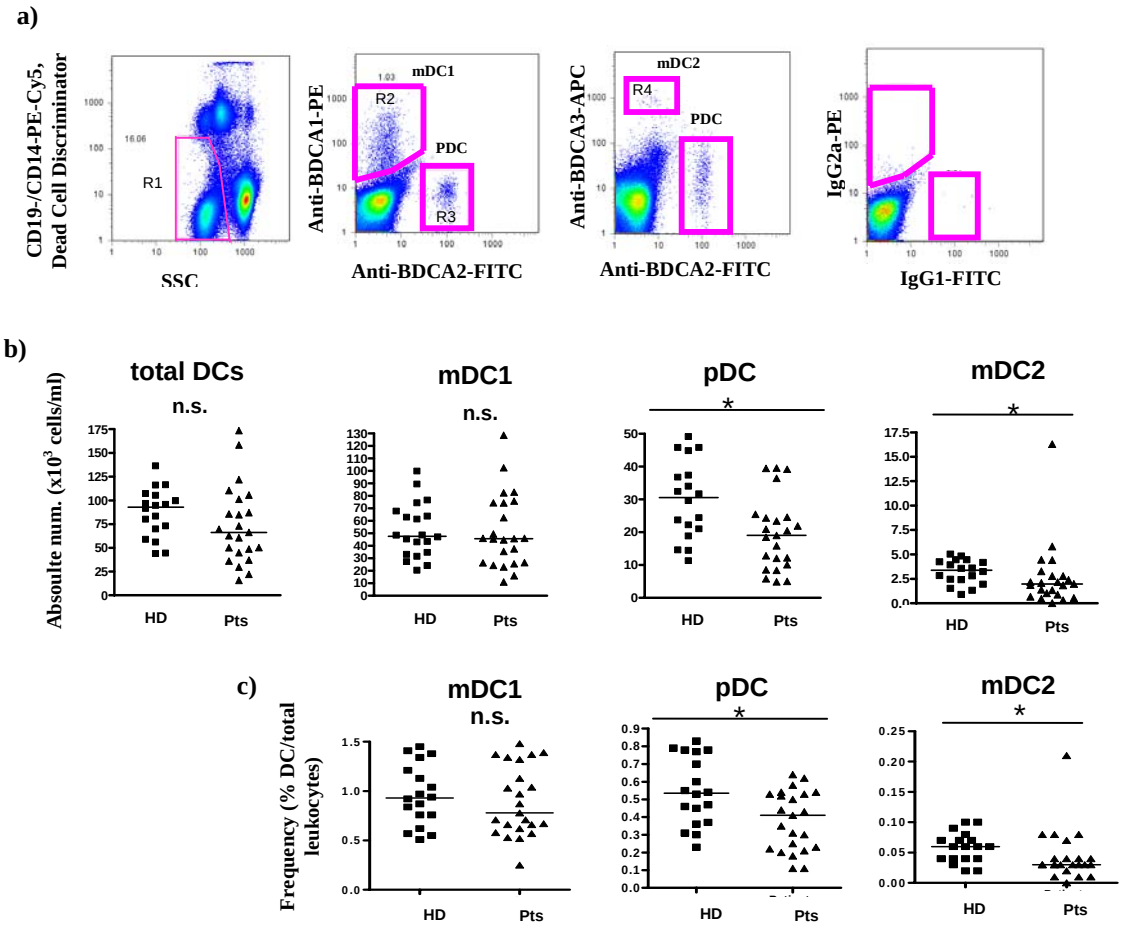

Figure 4: Enumeration of circulating DC subsets in whole blood from stage IV melanoma patients and healthy controls. (a) Gating strategy that was used to define absolute DC numbers, which represented all viable cells within total leukocytes using regions (solid boxes) to exclude dead cells, $CD19^+$ and $CD14^+$ cells (R1) and to define DC subpopulations by expression of $BDCA1^+$ myeloid DC subpopulation 1 (mDC1) (R2), $BDCA2^+$ plasmacytoid DC (pDC) (R3) and $BDCA3^+$ myeloid DC subpopulation 2 (mDC2) (R4). (b) Absolute numbers of DC populations in peripheral blood samples obtained from age-matched healthy donors (HD) (n=18) and stage IV melanoma patients (Pts) (n=23). (c) Frequency of each DC subset in peripheral blood of healthy controls and melanoma patients. Data are shown as median. *$p<0.05$; n.s., not significant.

The three subsets of blood DCs were identified and quantified based on the expression of BDCA1 (mDC1), BDCA2 (pDCs) and BDCA3 (mDC2) as depicted in Figure 4a by multiparametric flow cytometry on freshly collected whole blood. The absolute numbers of distinct DC subpopulations and total DC count are shown as scatter plots in Figure 4b.

As depicted in Figure 4b, the median (range) absolute numbers of total blood DCs among total leukocytes were 66.3 (22.10-173.5) x 10^3 cells/mL in melanoma patients and 92.85 (44.13-136.0) x 10^3 cells/mL in healthy individuals, respectively. There was no significant difference in the total circulating DC count between patients and normal controls. The absolute number of the mDC1 population in patients (median (range): 45.67 (11.03-128.5) x 10^3 cells/mL) was similar to that observed in healthy subjects (47.66 (23.93-99.62) x 10^3 cells/mL). In contrast, mDC2, a minute population of circulating DCs was found to be significantly reduced in patients as compared with healthy controls with median absolute numbers of 1.97 (0.0-16.3) x 10^3 cells/mL and 3.38 (0.87-4.99) x 10^3 cells/mL, respectively. Interestingly, the pDC count was also significantly decreased in stage IV melanoma patients (19.01 (4.85-39.58) x 10^3 cells/mL) compared to normal individuals (30.6 (11.2-49.0) x 10^3 cells/mL) (Figure 4b). The frequency of each DC subset displayed the same trend as absolute numbers with significantly reduced percentages of pDCs and mDC2 in melanoma patients (Figure 4c).

4.1.2 Imbalance in blood DC compartments of melanoma patients

The homeostatic balance of DC compartments has been previously demonstrated to be associated with the successful withdrawal of immunosuppression in liver or heart transplanted recipients (237, 238). It was suggested that the mDC/pDC ratio might serve as an index for monitoring the immune reconstitution in patients who received transplants. Moreover, the balance of the DC compartment has been shown to correlate with a shift towards a Th2 immune response in patients with atopic dermatitis (239). Thus, the reduction in pDC and mDC2 counts that we observed in melanoma patients may implicate an imbalance in circulating DC compartments. To investigate if this is indeed the case, we determined the ratio of mDC subsets to pDCs in our sample group (Figure 5a).

As expected, the mDC1:pDC ratio was significantly higher ($p<0.05$), while the mDC2:mDC1 ratio was significantly reduced ($p< 0.03$) in patients compared with healthy subjects. The ratio of mDC2:pDC in patients, however, remain unchanged. The high mDC1:pDC and low mDC2:mDC1 ratios that we observed in melanoma patients were associated with a reduction in the number of pDCs and mDC2 in the peripheral blood. Notably, the reduced pDC numbers significantly correlated with decreased numbers of mDC2 in melanoma patients ($p<0.0001$, $r=0.7441$) (Figure 5b). This observation implicates an imbalance of DC compartments among melanoma patients which might impact the generation of efficient anti-tumour immune responses.

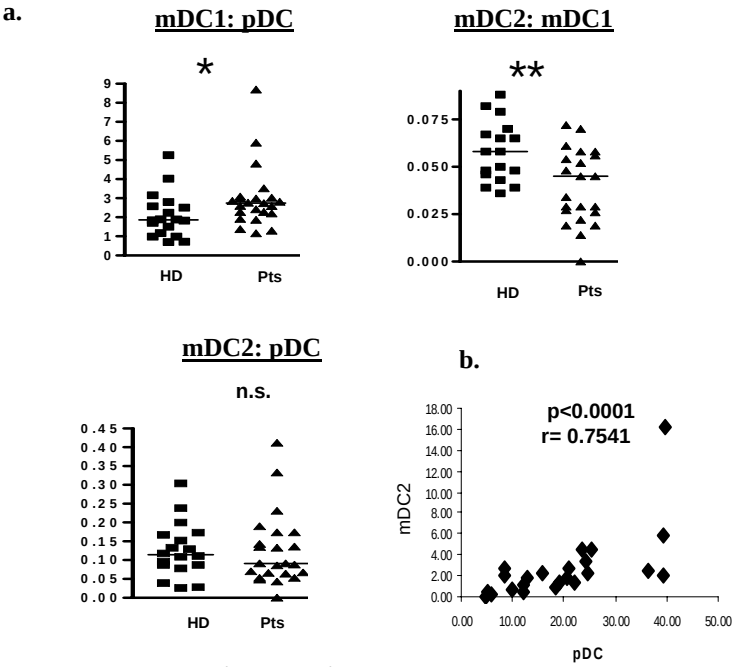

Figure 5: Imbalance in blood DC compartments of melanoma patients. (a) Ratio of different blood DC subsets in healthy donors (HD) and melanoma patients (Pts). (b) Correlation between mDC2 and pDC subpopulations in the peripheral blood of melanoma patients ($p<0.0001$, $r=0.7541$, Spearman's rank test). Data are shown as median. *$p<0.05$; ** $p<0.03$; n.s., not significant.

4.2.1 mDC1/pDC interaction upon TLR9 engagement in stage IV melanoma patients

4.2.2 TLR9 triggering on pDCs leads to an up-regulation of CD40 on co-cultured mDC1 from healthy donors but not from melanoma patients

The cross-talk between mDCs and pDCs has been recently demonstrated to be important for anti-bacterial and anti-tumour immune responses, both *in vivo* (240) and *in vitro* (76)). Phosphorothioate ODNs with specific CpG A motifs, shortly termed CpG A, activate human pDCs that in turn can induce partial maturation of mDCs upon interaction, detectable as an up-regulation of co-stimulatory surface molecules on mDCs.

To examine if the interplay of pDCs and mDC1 was disturbed in melanoma patients, mDC1 and pDCs were purified from PBMCs of buffy coats from healthy subjects and of leukapheresis products from melanoma patients. The isolation of mDC1 and pDCs was based on the specific expression of BDCA1 (mDC1) and BDCA4 (pDCs). Due to the very high amount of total blood cells needed in order to obtain sufficient numbers of pDCs for analysis, the isolation procedure could only be performed on PBMCs from a small set of patient and healthy donor (n = 4).

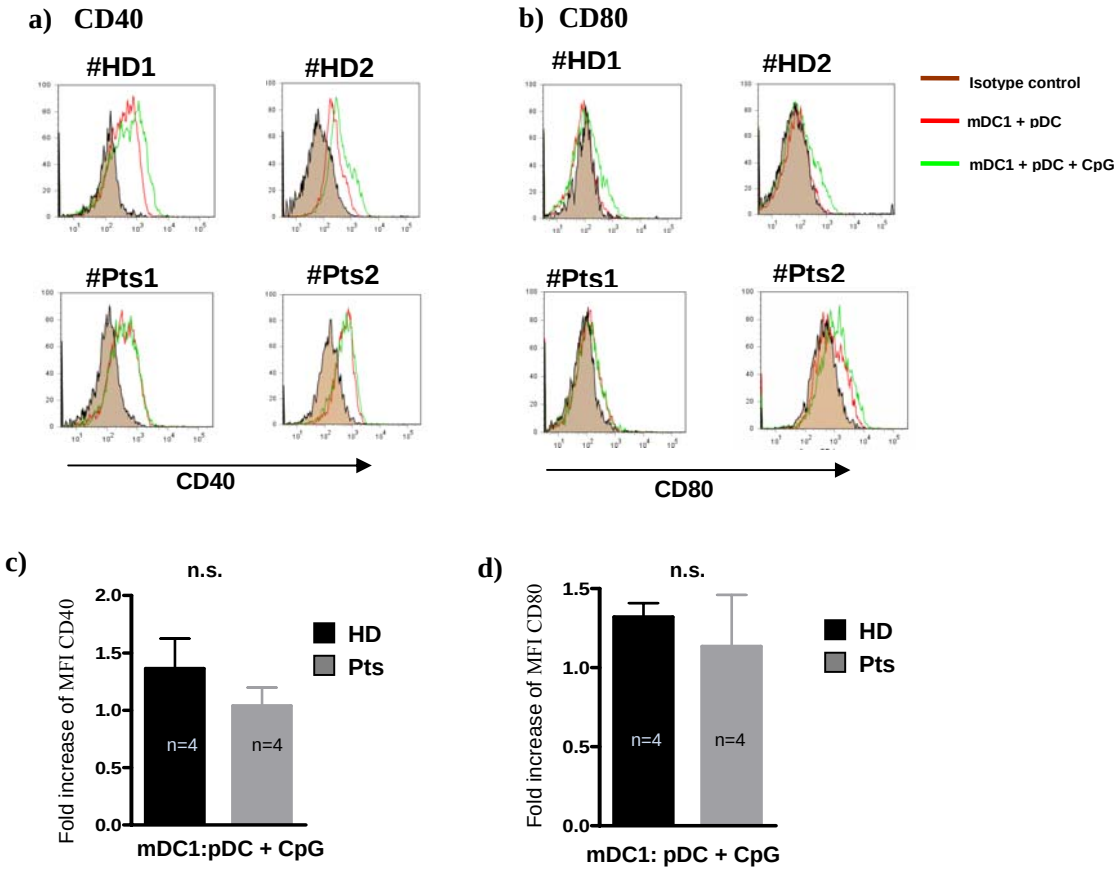

Figure 6: Aberrant mDC1/pDC interaction in melanoma patients (Pts). (a) mDC1 and pDCs were purified from isolated PBMCs by positive selection with anti-BDCA1 and anti-BDCA4 coated magnetic beads, respectively. Purified mDC1 and pDCs were either cultured alone or together at ratio of 3.5:1, which reflects a close to physiological ratio in circulating blood cells. Cells were incubated with CpG A (10 µg/mL) or without stimulus (medium) for 18 h and harvested for assessing the expression of co-stimulatory molecules by flow cytometry. (a, b) Representative histograms from 2 experiments depict the effect of CpG A stimulation on CD40 and CD80 expression by mDC1 in mDC1/pDC co-cultures from healthy donors and patients. The background staining using isotype control antibodies in the different co-culture systems was similar and representative histograms are depicted. (c, d) The medians of four healthy donors and patients are shown and the results are reported as fold increase of MFI on mDC1 (MFI of CD40 and CD80 on MDC1 in CpG A stimulated relative to non-stimulated cocultures). n.s., not significant.

Since responsiveness to TLR4 and TLR9 ligands is restricted to human mDCs and pDCs, respectively, the capability of pDCs in inducing mDC1 maturation upon TLR9 ligand stimulation was analysed. Histograms in Figure 6a and 6b show the expression of CD40 and CD80 on mDC1. Compared to unstimulated co-cultures, which provided the basal expression of CD40 and CD80 on mDC1 in contact with pDCs, there was a moderate up-regulation of CD40 and CD80 expression on mDC1 purified from healthy donors after 18 h of CpG A incubation. However, under the same conditions, mDC1 from melanoma patients showed a slightly impaired CD40 and CD80 upregulation. The accumulated data on the increase of CD40 expression in melanoma patients in comparison to control subjects tested in parallel are depicted in Figure 6c and 6d. Expression of CD40 and CD80 plays a crucial role in facilitating the priming of T cells by DCs. Hence, defective mDC1/pDC interactions upon TLR9 activation may perturb T cells priming in melanoma patients.

4.2.3 Aberrant IFN-α production by pDCs from melanoma patients

pDCs are major producers of IFN-α among all cell types upon sensing of bacteria and virus nucleic acids (68-70). The large amount of IFN-α produced during innate defence plays a critical role not only in exerting direct protection to host cells, but also in priming and activating mDC1 (52, 74). Recently, Piccioli and colleagues provided evidence that the TLR mediated mDC/pDC interaction is partially IFN-α dependent (76). Since there were reduced peripheral blood pDC numbers and impaired mDC1/pDC interactions in melanoma patients, this may suggest a dysfunction in IFN-α production. Thus, we examined the secretion of IFN-α by pDCs in response to CpG A, which triggers TLR9 signaling and induces a strong production of IFN-α rather than the up-regulation of co-stimulatory molecules on pDCs.

To prove our hypothesis, the purified peripheral blood BDCA4$^+$ pDCs from healthy donors and melanoma patients were co-cultured with BDCA1$^+$ mDCs in the presence or absence of TLR9 stimulation. As expected, neither LPS nor CpG A stimulation led to detectable IFN-α release by mDC1 (Figure 7a). In contrast, we detected substantial levels of IFN-α in pDCs cultures (Figure 7b) and in mDC/pDC co-cultures (Figure 7c) from

healthy donors after CpG A stimulation. Under the same conditions, no or only minimal IFN-α was detected in mDC/pDC co-cultures from melanoma patients.

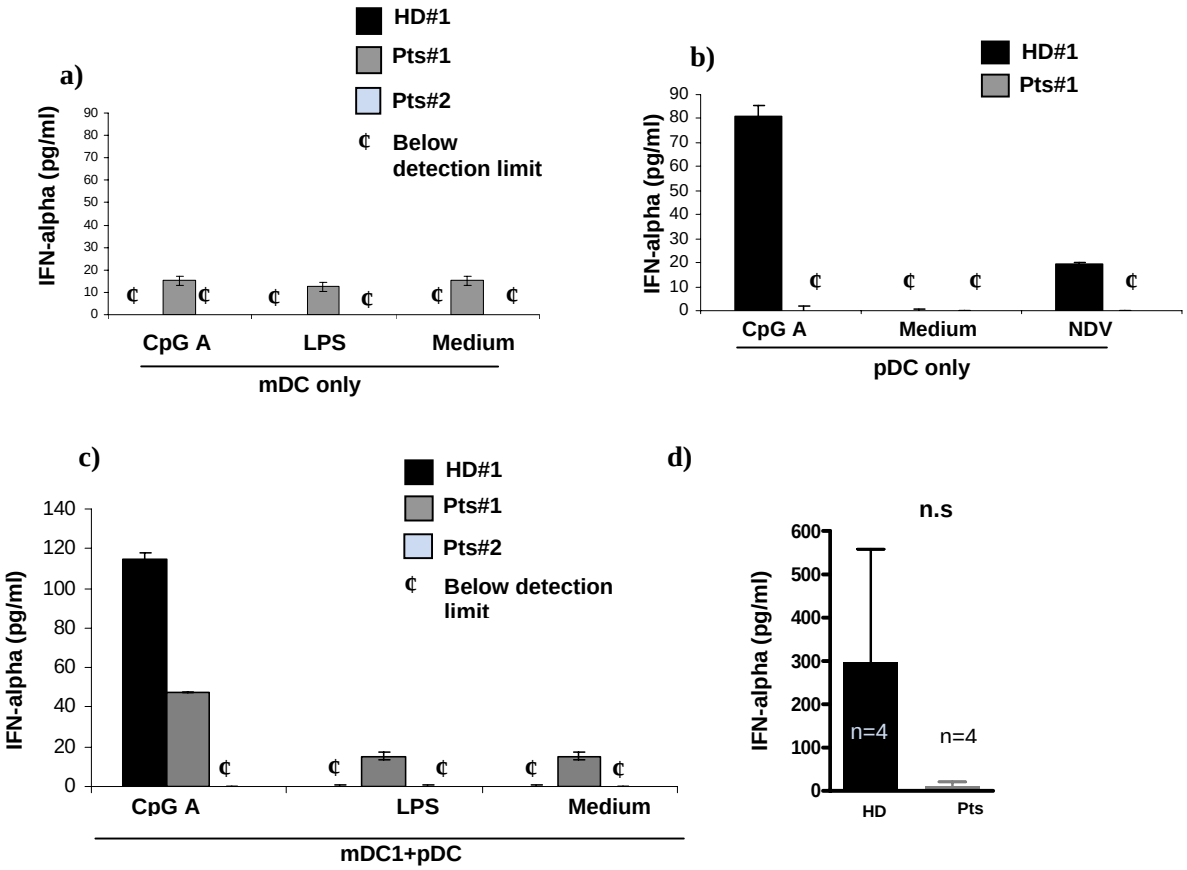

Figure 7: IFN-α production by pDCs during mDC1/pDC interaction upon TLR9 activation. Purified mDC1 were co-cultured with BDCA4$^+$ pDCs at a ratio of 3.5:1 and stimulated with CpG A (10 μg/mL), LPS (1 μg/mL) or left without stimuli (medium) for 18 h. Supernatants were collected and tested for IFN-α levels. (a) mDC1, (*b*) pDCs and (c) mDC1/pDCs were cultured in medium alone or in the presence of CpG A or LPS. (b) The purified pDCs from healthy donors (HD) (n=2) and melanoma patients (Pts) (n=2) were treated with NDV at a dilution of 1:100. (a,c) Representative data (mean of duplicates) from one out of four healthy donors (HD#) and 2 out of 4 melanoma patients (Pts#) are depicted. (d) Accumulative data on IFN-α levels determined in mDC/pDC co-cultures upon TLR9 triggering by CpG A are presented. n.s., not significant.

Accumulative data (Figure 7d) point to an impaired IFN-α production by CpG A stimulated mDC/pDC cultures from patients (n = 4) with a median concentration of 9.7 pg/mL versus 297.6 pg/mL in healthy controls, although the levels of IFN-α was proved not statiscally different due to the low number of patients. Treatment of pDCs with NDV that can trigger TLR7 signaling also revealed an aberrant function of pDCs from

melanoma patients in secretion of IFN-α (n=2). Only pDCs purified from normal donors produced IFN-α in response to NDV (n=2).

4.2.3 TLR4 engagement up-regulates CD40 and CD80 on mDC1 from patients and healthy donors

The unresponsiveness of pDCs from melanoma patients prompted us to determine whether mDC1 from patients also displayed dysfunctional properties. Since mDC1 but not pDCs express the TLR4 receptor, mDC1 can respond to LPS stimulation and undergo maturation. To analyse this, we stimulated mDC1/pDC cultures with LPS and compared the expression levels of CD40 and CD80 on mDC1 from stimulated and non-stimulated control cultures. As expected, purified BDCA1$^+$ mDC1 from healthy controls that were cultured together with autologous pDCs augmented the expression of CD40 and CD80 after LPS activation for 18 h (Figure 8a, b).

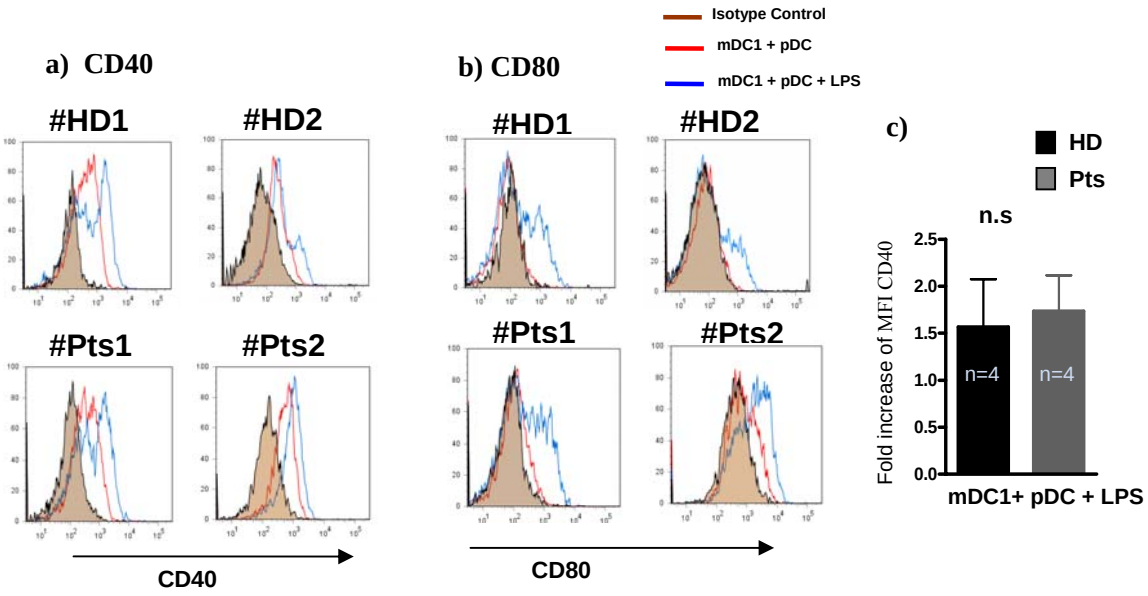

Figure 8: Similar up-regulation of CD40 and CD80 on mDC1 from patients (Pts) and healthy donors (HD)upon TLR4 engagement. mDC1 and pDCs were isolated from PBMCs of healthy subjects and melanoma patients, co-cultured at ratio of 3.5:1 and stimulated with LPS (1 µg/mL) or without stimulus (medium) for 18 h. Cells were harvested for assessing the expression of co-stimulatory molecules by flow cytometry. Representative histograms of two healthy donors and two patients depict the effect of LPS stimulation on (a) CD40 and (b) CD80 expression by mDC1 in mDC/pDC co-cultures. The background staining using isotype control antibodies in the presence or absence of stimulus was similar and representative histograms are presented. (c) Medians of CD40 expression on mDC1 from four donors and four patients are shown and the results are reported as fold increase of MFI on mDC1 (MFI of CD40 on MDC1 in CpG A stimulated relative to non-stimulated cocultures n.s., not significant.

Similarly, upon TLR4 engagement, expression of both co-stimulatory molecules was also up-regulated on mDC1 purified from melanoma patients. As illustrated in Figure 8c, statistical analysis revealed no significant increased of MFI fold change on CD40 expression on mDC1/pDC from patients and healthy controls in response to LPS.

4.2.4 TLR4 activation by LPS triggers IL-10 production by blood mDC1

IL-10, an anti-inflammatory cytokine, has been frequently detected in higher amounts in sera of cancer patients and demonstrated to induce tolerogenic feature in DCs. Therefore, we examined whether blood mDC1 produced IL-10 and if these cells from melanoma patients produced more IL-10 than healthy controls. Interestingly, we found that LPS stimulation triggered production of IL-10 by mDC1 from both healthy controls and patients when cultured alone as shown by one representative experiment (Figure 9a).

The mDC1 isolated from melanoma patients produced similar levels of IL-10 compared to healthy controls after LPS activation. Co-culture of mDC1 together with pDCs without stimulus or in the presence of CpG A did not lead to substantial secretion of IL-10 (Figure 9a). As shown in Figure 9b, there was no significant difference in IL-10 levels detected in mDC/pDC co-cultures from healthy donors and patients upon LPS stimulation. The interaction of mDC1 with autologous pDCs from patients do not enhanced the secretion of IL-10 upon TLR4 activation. These data suggest that unlike tumour induced tolerogenic DCs, blood circulating mDC1 from melanoma patients are not polarised to produce more IL-10 than healthy donor mDC1 in the presence of LPS.

To further underline that mDC1 are the major producers of IL-10 in response to LPS treatment during the mDC/pDC interaction, different mDC1:pDC ratios were tested by increasing the amount of mDC1 and keeping the number of pDCs constant. We found that co-culture of mDC1 and pDCs without exogenous stimulus produced little to low IL-10 (~50 pg/mL) (Figure 9c). An increased mDC1 number led to the production of greater amounts of IL-10 after LPS stimulation, suggesting that mDC1 are the major IL-10 producers.

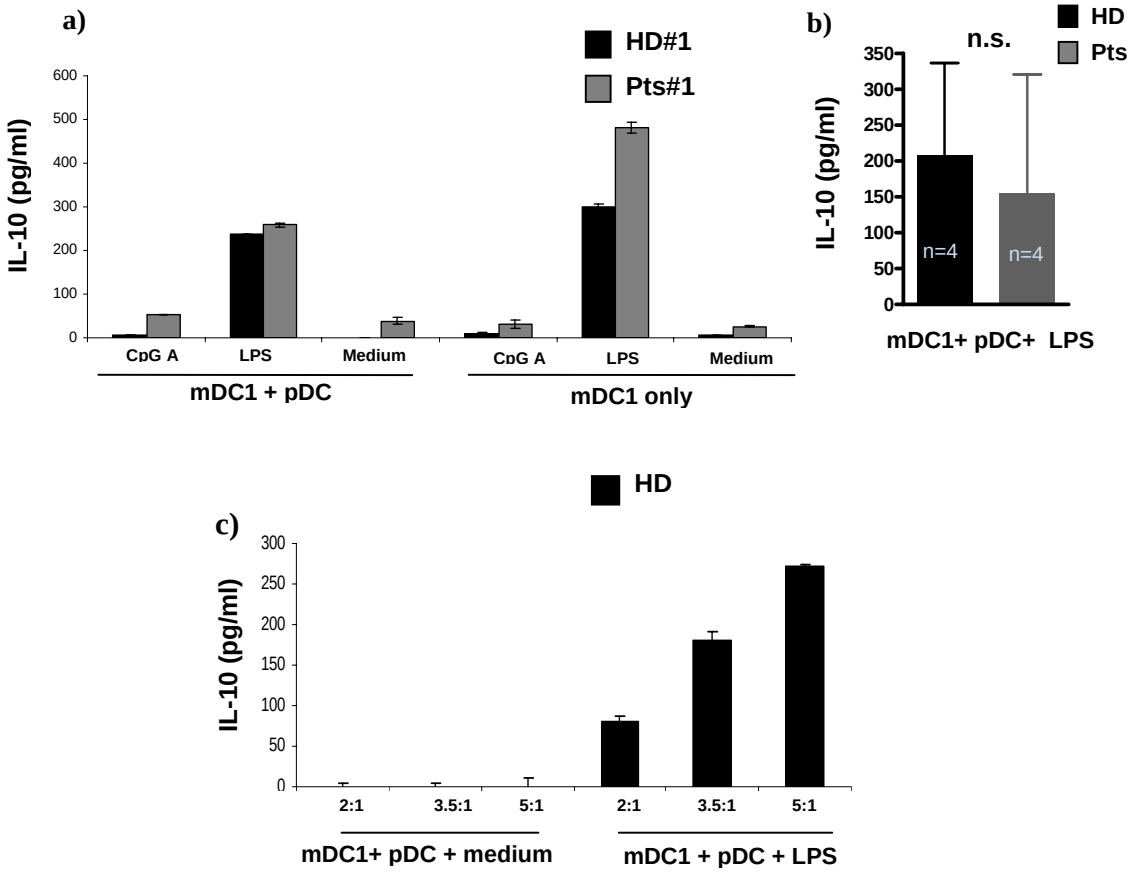

Figure 9: IL-10 production by mDC1 upon TLR4 engagement. mDC1 were isolated and co-cultured with or without purified pDCs at a 3.5:1 ratio. Cells were exposed to LPS (1 μg/mL) or left without stimulus (medium) for 18 h. Supernatants were collected and tested for the IL-10 levels by ELISA. (a) Representative data (mean of duplicates) on IL-10 secretion in response to LPS stimulation in mDC1/pDC or mDC1 cultures purified from one healthy donor (HD#) and one melanoma patient (Pts#).(total n = 4) (b) Accumulative data are shown as median of IL-10 levels in cell culture supernatants after LPS stimulation. n.s., not significant (c) Representative IL-10 secretion (mean value for duplicates) by mDC1/pDCs from one healthy donor (n = 2) cultured at different ratios either with or without LPS.

4.3 Cytokine and chemokine levels in PBMCs and in sera of stage IV melanoma patients

4.3.1 Aberrant IFN-α secretion by PBMCs from melanoma patients

Due to the limited samples available to perform co-culture experiments with purified pDCs, we extended our study by examining the functional properties of pDCs in whole PBMCs. This is possible since the production of IFN-α in response to TLR9 ligation by CpG A is restricted to pDCs. Hence, we examined whether a similar impairment of IFN-

α production by pDCs was detectable in PBMCs from melanoma patients compared to healthy controls.

The bars depicted in the Figure 10 show accumulative data of IFN-α production by PBMCs from 8 patients in comparison to 6 healthy controls. By stimulating PBMCs from melanoma patients with CpG A for 22 h, a very low level of IFN-α was detected at a range of 1.67-1200 pg/mL. Conversely, PBMCs of all healthy subjects being tested

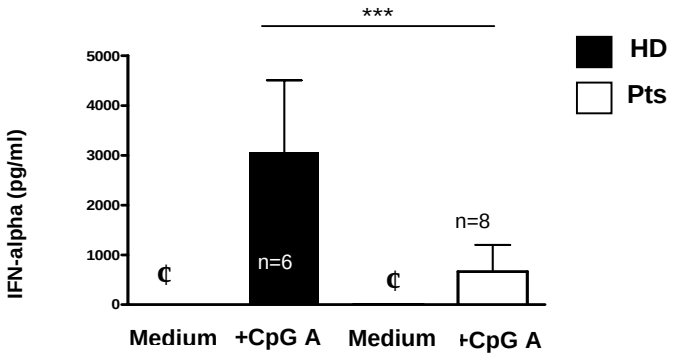

Figure 10: IFN-α production by PBMCs stimulated with CpG A. Cryopreserved PBMCs isolated from healthy donors (HD) or melanoma patients (Pts) were thawed and stimulated with CpG A (10 μg/mL) or left without stimulus (medium) for 22 h. Supernatants were collected and tested the IFN-α content by ELISA. Note: *** p=0.0007; ¢, below detection limit.

strongly secreted IFN-α with a range of 2155-4505 pg/mL. There was an approximately 5-6 fold higher IFN-α production in PBMCs from healthy controls compared to melanoma patients. The significantly lower amounts (p = 0.0007) of IFN-α secreted by PBMCs from melanoma patients than healthy controls in response to TLR9 activation was in agreement with lower level of IFN-α released in mDC/pDC co-cultures from patients (Fig.7). This further suggested that an aberrant IFN-α production by PBMCs from patients may be associated with a lower responsiveness to TLR9 activation.

4.3.2 Reduced cytokine and chemokine production by PBMCs from stage IV melanoma patients

There is increasing evidence that pDCs are critical in bridging innate and adaptive immune responses in the context of systemic viral or bacterial infections. This is known to be mediated via a complex cytokine and chemokine network released by pDCs upon

activation. Taking advantage of the beads based multianalyte profiling technology (MAP) from Luminex, we analysed a panel of pro-inflammatory cytokines and chemokines secreted or induced by pDCs upon TLR9-ligand engagement.

4.3.2.1 TLR-9 engagement by CpG A results in TNF-α, IL-1β and IL-6 production in PBMCs

TLR9-receptor binding by its ligand CpG A not only induces the production of IFN-α in pDCs but also stimulates the MyD88-TRAF6 pathway that activates multiple signalling cascades for example NF-κB signaling. Activated NF-κB subsequently translocates into the nucleus, which allows its binding to the promoter of multiple genes such as TNF-α, IL-6 and IL-1β genes that leads to tremendous production of these cytokines. These cytokines play crucial roles in inflammation and have been implicated to contribute to tumour development and progression. Since there was significant lower production of IFN-α by pDCs from patients, which suggested dysregulation of TLR9-MyD88-IRF7 signaling, we thus asked if there is defect in the production and induction of inflammatory cytokines and chemokines by pDCs in PBMCs upon CpG A treatment.

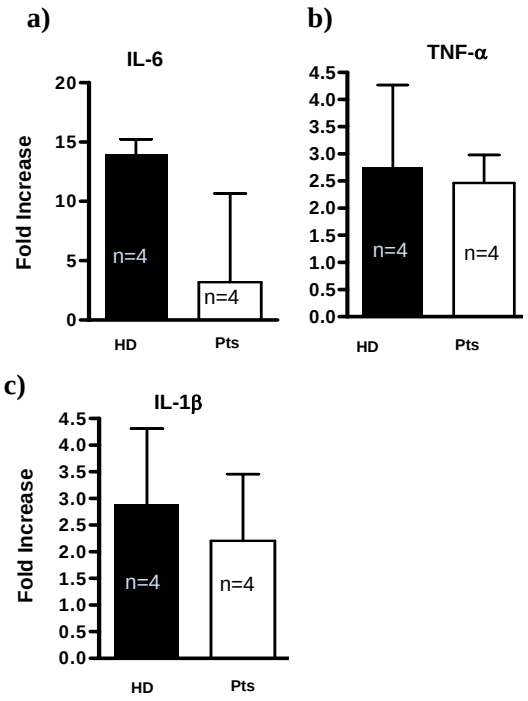

Figure 11: Cytokine secretion by PBMCs activated with CpG A. PBMCs from melanoma patients and healthy donors were stimulated with CpG A for 22 h and the supernatant were harvested and analysed for the production of (a) IL-6, (b) TNF-α and (c) IL-1β. Black bars indicate median value of cytokine expression in healthy donors (HD) and white bars represent melanoma patients (Pts). Results are reported as fold increase of cytokine release in CpG A stimulated relative to non-stimulated PBMCs.

To address this possibility, we analysed cytokine levels in the supernatant of PBMCs from healthy donors and patients after incubation with CpG A for 22 h using the beads based multiplex cytokine assay from Luminex. After CpG A exposure, increased levels of IL-6, TNF-α and IL-1β were released by PBMCs treated with CpG A compared to non-treated cells. (Figure 11a-c) The increase in IL-6 levels secreted by PBMCs from healthy controls upon stimulation was stronger compared to that observed for PBMCs from patients, however, this did not achieve statistical significance (Figure 11a). The IL-1β and TNF-α production by PBMCs from healthy controls and patients during TLR9 activation were not significantly different (Figure 11b, 11c).

4.3.2.2 Reduced CCL3 and CCL5 secretion by CpG A treated PBMCs

In addition, pDCs have been demonstrated to produce Th1 chemokines including CCL3, CCL4, and CCL5 after CpG A stimulation (60, 61). These chemokines particularly promote the recruitment of DCs, NK cells and activated memory T cells to the site of inflammation by the expression of CCR5, the receptor for CCL3, CCL4 and CCL5. Other studies have also shown that IFN-α could serve as stimulus for Th1 cytokine production by cells other than pDCs in PBMCs, in particular NK cell, $CD4^+$ T and APCs, leading to IFN-γ and IL-12p70 secretion (241, 242). Thus, we first assessed the levels of CCL3, CCL4 and CCL5 in PBMCs treated with CpG A using the beads based multiplex chemokine assay. The analysis revealed a low basal level of CCL3 but moderate levels of CCL5 in PBMCs from normal conrols and patients when cultured in the absence of TLR9 ligands. The stimulatory effect of CpG A on pDCs led to dramatic increase of CCL5 in the healthy controls while a less profound effect was observed for PBMCs from patients. The overall fold changes of CCL5 after CpG A stimulation were 3.1 and 1.6 for healthy donors and patients, respectively ($p < 0.05$) (Figure 12a). The secretion of CCL3 by PBMCs in healthy controls and patients followed a trend similar to CCL5, which showed a strong tendency of reduced overall fold change in PBMCs from patients after CpG treatment ($p=0.0571$) (Figure 12b). Similarly, the fold change of CCL4 levels in patients also showed tendency of reduction as compared to healthy controls (Figure 12c).

Assessing cytokine secretion in PBMCs allowed us to examine other Th1 cytokines, which are not produced but induced by activated pDCs. Thus, we also determined the IFN-γ and IL-12p70 levels (Figure 12d, e) in PBMCs after TLR9 activation. Both Th1

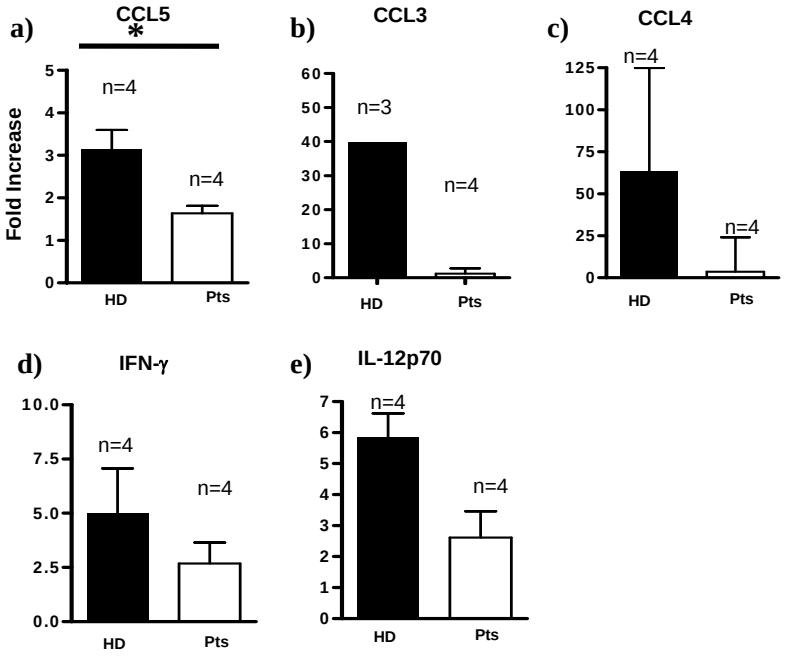

Figure 12: Secretion of Th1 cytokines and chemokines by PBMCs activated with CpG A. PBMCs from melanoma patients (Pts) and healthy donors (HD) were stimulated with CpG A for 22 h and the supernatant were harvested and analysed for the production of Th1 cytokines and chemokines (a) CCL5, (b) CCL3, (c) CCL4, (d) IFN-γ and (e) IL-12p70. Black bars indicate median value of fold increase in the release of cytokines after CpG A stimulation in PBMCs from healthy donors and white bars represent melanoma patients . *p<0.05.

cytokines, that in principle can be secreted or induced by NK and $CD4^+$ T cells, were found to be produced at a low level in PBMCs from patients and healthy control prior CpG A stimulation. CpG A treatment resulted in a lower extent of IFN-γ secretion in PBMCs from patients compared to healthy donors, however the overall fold change between both was not significantly different. On the other hand, statistical analysis revealed a strong tendency of reduced IL-12p70 levels ($p = 0.057$) in PBMCs from patients as compared to healthy donors upon CpG A exposure. Our observation suggested a defect in the cytokine and chemokine production by PBMCs from melanoma patients, pointing to an impairment of pDCs since CpG A is designed to stimulate this subset of

cells. These factors play a crucial role in initiating and maintaining Th1 immune responses via recruitment of DCs, NK and T cells to the site of inflammation.

4.3.2.3 Production of CXCL10 and CCL2 by PBMCs after TLR9 activation

Furthermore, pDCs have been included as one of the cell types besides monocytes, endothelial cells and fibroblast that could secrete IFN-γ inducible protein-10 (CXCL10) (243, 244). The impaired production of IFN-α and other chemokines by pDCs from melanoma patients prompted us to analyse the ability of PBMCs to secret CXCL10 following CpG A stimulation. Assessment of CXCL10 level using Luminex multiplex protein assay revealed a dramatic increase of CXCL10 production in all investigated PBMCs from healthy controls (Figure 13a), while PBMCs from patients displayed increased production albeit to a lower extent than the healthy donors.

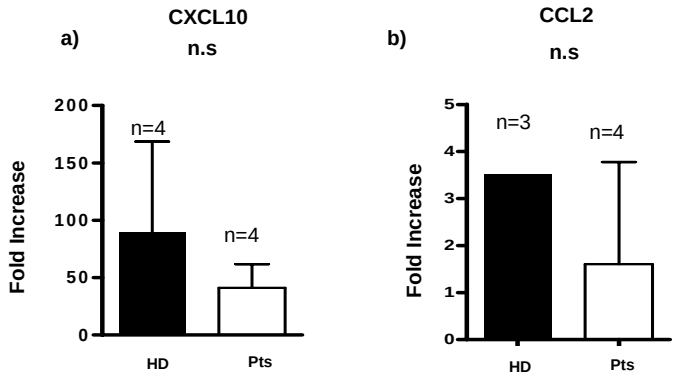

Figure 13: Secretion of CXCL10 by PBMCs activated with CpG A. PBMCs from melanoma patients and healthy donors were stimulated with CpG A for 22 h and the supernatants were harvested and analysed for the production of (a) CXCL10 and (b) CCL2. Black bars and white bars indicate median values of fold increase in the release of chemokines after CpG A stimulation by healthy donors (HD) and melanoma patients (Pts), resepctively. n.s., not significant.

Several studies have suggested CCL2 can be produced by monocytes (61) and it is also produced or induced upon the activation of TLR9 signalling in pDCs (37, 59, 61). Here, we measured the secretion of CCL2 and found a consistent increase of the CCL2 level in PBMCs from healthy donors after CpG A activation (Figure 13b). Also, PBMCs from patients released CCL2 upon CpG A stimulation but showed a tendency to lower production than PBMCs from healthy donors with medians of 1.6 and 3.5, respectively.

The tendency to lower CXLC10 and CCL2 secretion by PBMCs from patients that tested in this study suggested altered pDCs functions in patients.

4.3.3 Dysregulated cytokine and chemokine profiles in the sera of melanoma patients

Multiple cytokines, chemokines and pro-angiogenic factors appear to be involved in the progression of melanoma as they are secreted by malignant cells as well as stromal cells and leukocytes of the tumour microenvironment. The defective pDC activation in melanoma patients and the diminished secretion of multiple cytokines and chemokines in response to TLR9 engagement suggested dysregulated immunity in these patients.

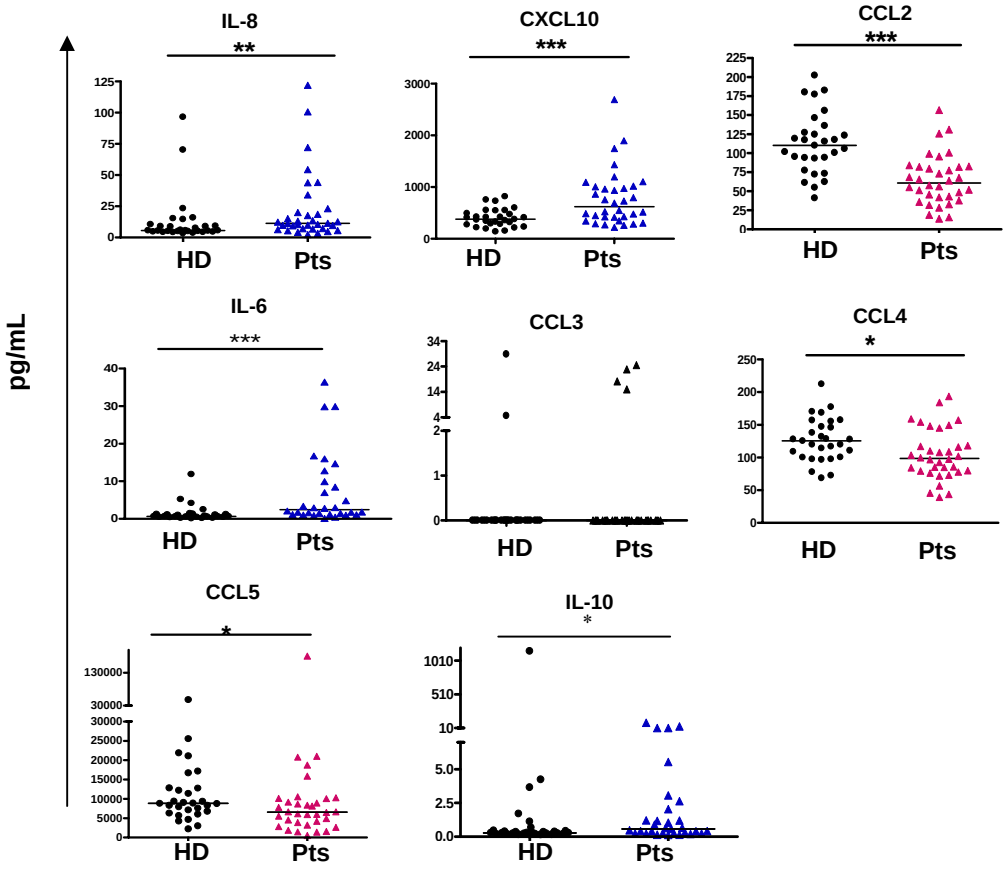

Figure 14: Sera cytokine and chemokine profiles of melanoma patients. Sera from 29 age-matched healthy individuals (HD) and 34 melanoma patients (Pts) at disease stage IV were collected and kept at -20°C until use. Multiple cytokines and chemokines within the sera including IL8, CXCL10, CCL2, IL-6, CCL3, CCL4, CCL5 and IL-10 were analysed using the xMAP multiplex protein bead array assay technology. Scatter plots and bars indicate median value of respective cytokine and chemokine concentration (pg/mL). Note: ($p < 0.001$ (***); $0.001 < p < 0.01$ (**); $0.01 < p < 0.05$ (*)).

Dysregulation of cytokine and chemokine profiles in the circulation could have substantial impact on the functional properties of immune cells as well as on the recruitment of the cells to inflammation sites. We performed a multiple protein bead array assay to define the cytokine and chemokine profiles of melanoma patients and healthy subjects. Sera collected from patients for this analysis were obtained from those who received no previous systemic treatment for at least 30 days.

The multiplex protein bead array assay revealed that serum concentrations of IL-6 and IL-8 ($p<0.005$) were found to be significantly higher in stage IV melanoma (Figure 14). Also the CXCL10 level with a median concentration of 620.1 pg/mL in patients was significantly higher than in healthy subjects (393.3 pg/mL) ($p<0.001$). As depicted in Figure 14, CCL2 (108.0 pg/mL vs 60.79 pg/mL), CCL4 (126.6 pg/mL vs 98.61 pg/mL) and CCL5 (8866 pg/mL vs 6555 pg/mL) were released in lower amounts into the sera from melanoma patients than from healthy subjects. Furthermore, the level of CCL3 was largely undetectable in both groups. For IL-10, only very low but significantly elevated amounts were detected in the sera from patient group ($p<0.05$) (Figure 14). This analysis highlights a significant difference in serum cytokine and chemokine profiles between controls and melanoma patients.

4.4 The role of TLR9 signalling in the aberrant immune function of pDCs in stage IV melanoma patients

4.4.1 BDCA2 expression by pDCs from melanoma patients

BDCA2, a pDC specific marker was described to be crucial as negative regulator of IFN-α signalling upon BDCA2 ligation. To define if BDCA2 was differentially expressed in pDCs from melanoma patients, we assessed the expression level of BDCA2 on freshly collected whole blood from both healthy controls and melanoma patients. We found no significant differences in the expression of BDCA2 on pDCs in whole blood from patients compared to healthy controls. However, BDCA2 was expressed to a lower extent on healthy pDCs after CpG A activation than on non-stimulated pDCs (Figure 15a). This was in agreement with the finding (245) that pDCs down-regulated BDCA2 upon

encountering maturation signals. Conversely, this effect was not seen in the case of patients (Figure 15b).

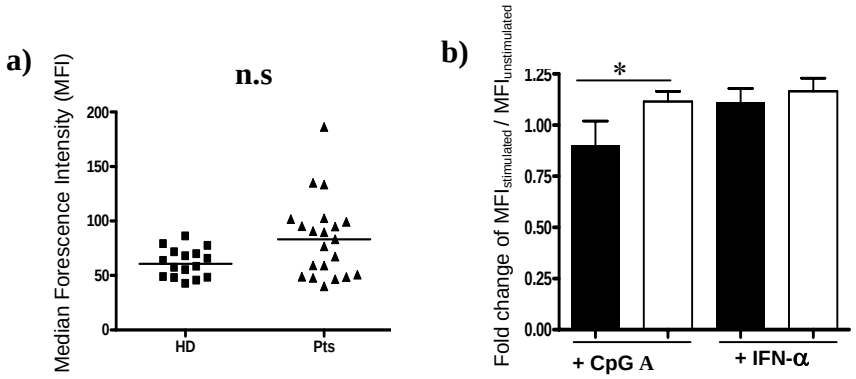

Figure 15: BDCA2 expression by pDCs from melanoma patients. (a) Whole blood cell samples were collected from age-matched healthy donors (n=16) and stage IV melanoma patients (n=21). Cells were stained with the BDCA2 antibody and measured by flow cytometry. The scatter plot represents median fluorescence intensity (MFI) values of BDCA2 expression on pDCs from (■) healthy donors (HD) and (▲) melanoma patients (Pts). (b) PBMCs ($2x10^6$) from healthy donors and patients were either cultured in the presence of CpG A (10 μg/mL) or IFN-α (10,000 IU/mL) or in medium only for 6 h. The data represent the median of fold change of BDCA2 expression on stimulated to unstimulated pDCs in PBMCs from 7 donors (black bars) and 10 patients (white bars). *$p<0.05$; n.s. not significant.

4.4.2 Conserved intracellular TLR9 expression in pDCs from melanoma patients

Engagement of the TLR9 receptor by its ligands followed by recruitment of the TLR adapter protein MyD88 is crucial for activating TLR9 downstream pathways. This process leads to pDC activation, maturation, and to the production of large amounts of type I IFN (144). As TLR9 is primarily found in the endosomal compartment, the detection of CpG A ligands by TLR9 only occurs as these compounds become internalized into the endosomal compartment. To investigate whether a defect in TLR9 signalling could be the potential mechanism that leads to aberrant IFN-α production by pDCs from melanoma patients, we first analysed the intracellular expression of TLR9 in pDCs. The intracellular TLR9 expression in $BDCA2^+$ pDCs was assessed by flow cyotmetry and determined as median fluorescence intensity (MFI). Histograms (Figure 16a) show intracellular TLR9 expression in pDCs from two representative patients in comparison to two healthy controls. As illustrated here, pDCs from normal controls expressed abundant TLR9. Similarly, TLR9 was constitutively expressed in $BDCA2^+$ pDCs from melanoma patients. Figure 16b depicts accumulative data on TLR9

expression by pDCs from nine melanoma subjects in comparison to pDCs from nine control subjects tested at the same time.

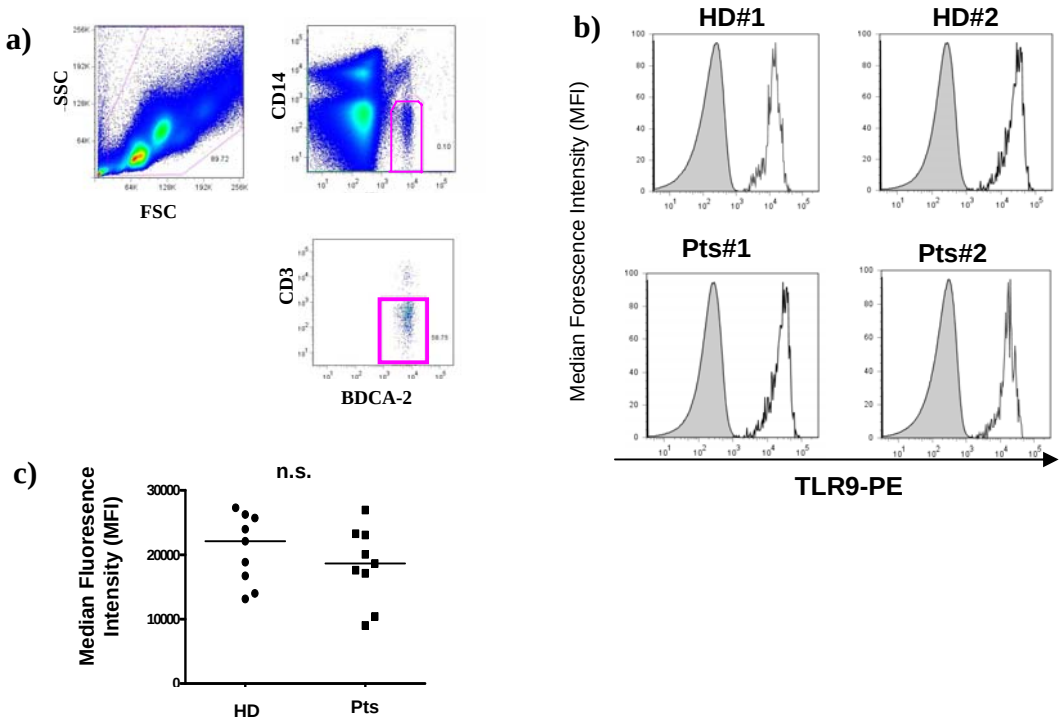

Figure 16: TLR9 expression in pDCs from melanoma patients. PBMCs isolated from melanoma patients (Pts) (n=9) and healthy donors (HD) (n=9) were stained with anti-TLR9 mAb. (a) Gating strategy for pDC identification is shown. (b) Intracellular expression levels of TLR9 on BDCA2$^+$ pDCs are shown in representative histograms from 2 out of 9 (n=9) per each group. Grey histograms represent the background staining using isotype control antibodies. (c) Scatter plots show the MFI of TLR9 expression and bars indicate median value of expression in healthy donors (HD) and melanoma patients (Pts). n.s., not significant.

Statistical analysis revealed no substantial difference in TLR9 expression between melanoma patients and healthy controls based on MFI values. This suggests that pDCs may be intrinsically impaired in TLR9 signalling that leads to poor responsiveness of pDCs to CpG A stimulation and subsequent impaired IFN-α production in melanoma patients.

4.4.3 Impaired MyD88 up-regulation in pDCs from melanoma patients upon CpG A ligand stimulation

Binding of CpG A ligands by TLR9 has been shown to lead to the recruitment of MyD88, which plays a crucial role in activating the downstream complexes including

TRAF6, IRAK1 and IRAK4 (182-184). Therefore, we studied if the expression of MyD88 was modulated in response to CpG A and IFN-α. Due to the reduced amount of circulating pDCs and the lack of adequate patient materials for cell purification and stimulation, we performed subsequent experiments investigating downstream molecules of TLR9 signalling on BDCA2^{+}CD123^{+}CD11c^{-} pDC from whole PBMCs instead of purified pDCs.

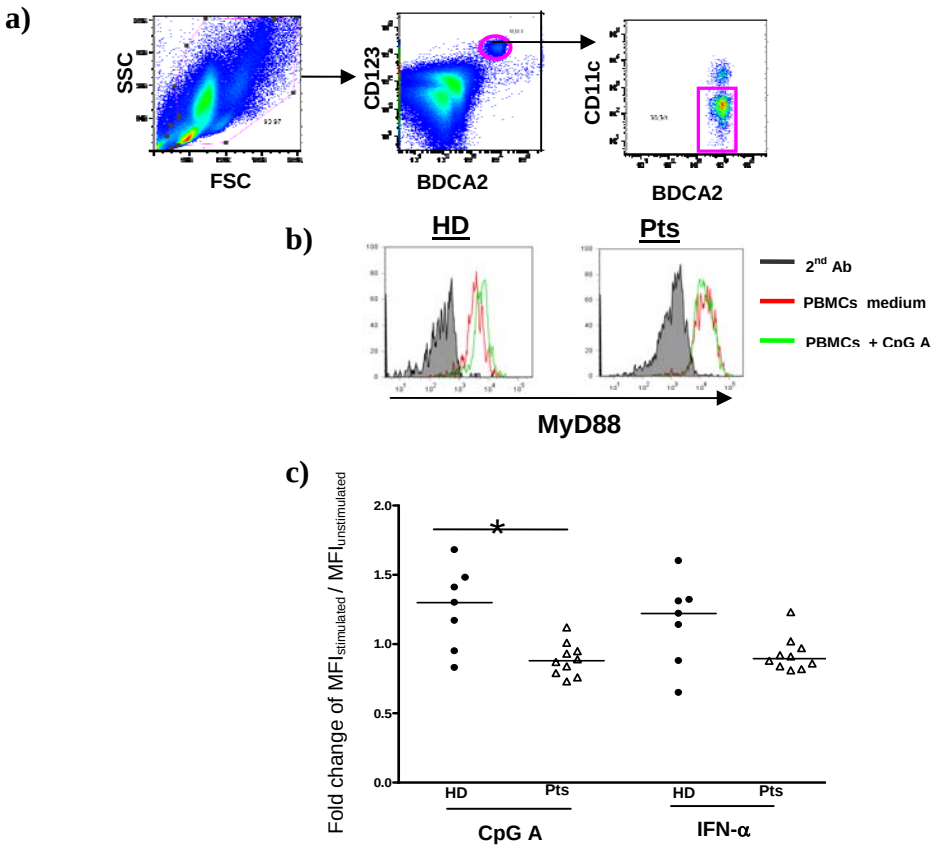

Figure 17: MyD88 expression in pDCs from melanoma patients. PBMCs from melanoma patients (Pts, n=10) and healthy donors (HD, n=7) were incubated with either CpG A, IFN-α or in medium for 6 h. The cells were then harvested and stained with antibodies against surface antigens CD123, CD11c and BDCA-2 followed by intracellular staining of MyD88. (a) Gating strategy for pDC identification is shown. (b, c) The expression level of MyD88 on CD123^{+}BDCA2^{+}CD11c^{-} pDCs are shown in histograms and as median fluorescence intensities (MFI). (b) Representative histograms are from one healthy donor and one patient. The background staining using only secondary antibody on cells that were cultured in the presence or absence of stimulus was similar and representative histograms are presented in the figure. (c) The fold changes of MyD88 expression ($MFI_{stimulated}$ / $MFI_{unstimulated}$) are presented in scatter plots, bars indicate median value of expression. *p<0.05.

Dot plots show the gating strategy on BDCA2^{+}CD123^{+}CD11c^{-} pDCs from PBMCs (Figure 17a) while histograms (Figure 17b) depict intracellular MyD88 expression in

pDCs from one representative patient in comparison to pDCs from one healthy subject. The scatter plot indicates the fold changes ($MFI_{stimulated}/MFI_{unstimulated}$) that were calculated for comparing MyD88 expression. PBMCs exposed to CpG A treatment significantly up-regulated MyD88 expression in $CD123^{+}BDCA2^{+}$ pDCs from healthy donors. However, as illustrated in both histogram and scatter plot (Figure17b, c), pDCs from patients were insensitive to the same stimulation and contained similar amounts of MyD88 prior and after CpG A treatment. When we stimulated PBMCs with UV-inactivated NDV, a tendency of lower fold changes ($MFI_{stimulated}/MFI_{unstimulated}$) of MyD88 expression was noted in $CD123^{+}BDCA2^{+}$ pDCs from patients (Appendix 8.2, Figure 30). Furthermore, there was no change in MyD88 expression in pDCs from patients in response to IFN-α treatment whereas MyD88 expression was increased in pDCs from healthy donors though the difference between both groups did not reach statistical significance (Figure17c). Taken together, the lack of MyD88 up-regulation upon TLR9 activation points to a defective TLR9 signalling pathway in pDCs from melanoma patients.

4.4.4 Regulation of IRF7 expression at the mRNA level

The aberrant IFN-α production in parallel to a lack of up-regulation of MyD88 expression upon TLR9 ligand stimulation among melanoma patients prompted us to further examine the signal transduction downstream of TLR9. One of the key players of the TLR9 downstream pathway is IRF7, a transcription factor which is responsible for TLR9-mediated production of type I IFN. During TLR9 activation, recruitment and direct interaction of MyD88 with IRF7 is a pre-requisite for IRF7 phosphorylation and activation (182, 192). Thus, the influence of TLR9 triggering on IRF7 expression in pDCs of melanoma patients was investigated. Since the responsiveness of TLR9 ligand activation and IRF7 up-regulation is restricted to pDCs in PBMCs within 6 h of CpG A stimulation, this allows the analysis to be performed on mRNA isolated from PBMCs obtained from healthy controls and melanoma patients.

Figure 18a depicts the fold increase of IRF7 mRNA expression in CpG A stimulated PBMCs after normalization to endogenous GAPDH from one representative healthy

donor in comparison to PBMCs from one patient (Figure 18b). PBMCs of healthy controls were found to augment IRF7 expression to a greater extent in response to CpG A activation (median = 9) compared to PBMCs from 6 melanoma patients (median = 2) (Figure 18c).

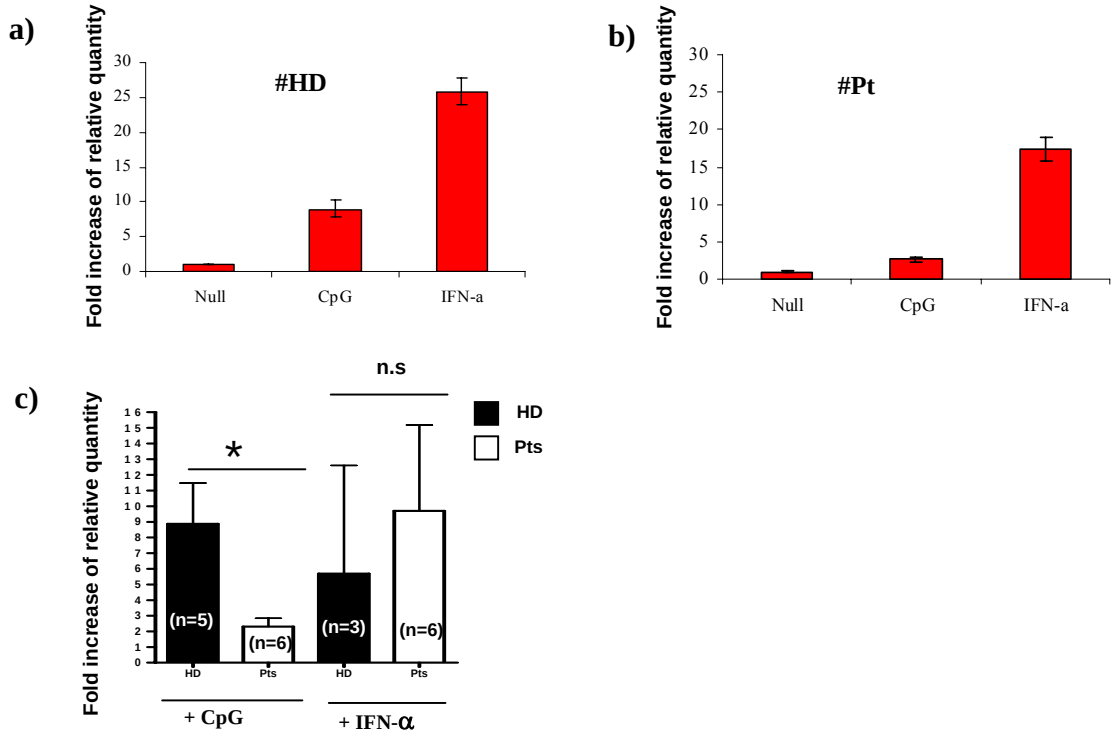

Figure 18: Real-time quantitative RT-PCR analysis of IRF7 expression in pDCs from melanoma patients and healthy controls. Cryopreserved PBMCs ($2x10^6$) from healthy donors (HD) and patients (Pts) were thawed and either left untreated or stimulated with CpG A (10 µg/mL), or IFN-α (10,000 IU/mL). Cells were harvested after 6 h and lysed for mRNA isolation. IRF7 expression levels determined by quantitative real time RT-PCR in PBMCs upon CpG A and IFN-α stimulation from one representative (a) HD and (b) Pts are depicted. IRF7 levels were normalized to endogenous GAPDH mRNA levels. Relative IRF7 expression was quantified using the comparative $2^{-\Delta\Delta Ct}$ method. (c) The mRNA expression of IRF7 was measured in unstimulated and CpG A or IFN-α stimulated PBMCs from melanoma patients (white bar) and age-matched healthy controls (black bar) by quantitative real-time RT-PCR. The results are represented as median of fold increase of relative expression. The expression level of IRF7 is shown relative to the basic level of untreated PBMC. *P<0.05, n.s. not significant.

Statistical analysis revealed significantly higher fold increase of IRF7 mRNA levels in PBMCs from the control group compared to PBMCs from melanoma patients. As a positive control, the up-regulation of IRF7 mRNA level was determined by stimulating PBMCs with a high dose of IFN-α (10,000 IU/mL). Interestingly, the IRF7 mRNA level was strongly enhanced when both PBMCs from healthy controls and patients were

activated with a high dose of IFN-α. The induction of the IRF7 mRNA level in PBMCs from patients after treatment with high doses of IFN-α was greater than stimulation with CpG A (8 fold versus 2 fold).

4.4.5 Hyporesponsiveness of pDCs to TLR-9-CpG A activation leads to impaired IRF7 up-regulation

In order to define if the IRF7 protein expression corresponded to the mRNA level in PBMCs, we further analysed the IRF7 expression in pDCs by flow cytometry. To assess the IRF7 protein expression in pDCs, we analysed the expression level on $CD123^{+}BDCA2^{+}CD11c^{-}$ gated pDCs in PBMCs (Figure 19a). Histograms (Figure 19b) depict intracellular IRF7 expression in pDCs from one representative patient in comparison to pDCs from one healthy control in response to CpG A and IFN-α simulation. Before CpG A exposure, we found constitutively high expression of IRF7 in $CD123^{+}BDCA2^{+}$ pDCs from both healthy donors and patients. The basal expression level of IRF7 was not significantly different between the control and patient group regardless of disease burden.

Of note, CpG A stimulation for 6 h strongly up-regulated IRF7 level in $CD123^{+}BDCA2^{+}$ pDCs from the healthy donors with a median of 1.45 fold increase (Figure 19c). The effect of CpG A in up-regulating IRF7 expression was abrogated in pDCs from melanoma patients (median fold increase = 1.0) (Figure 19c). Incubation of PBMCs obtained from healthy donors with high concentrations of exogenous IFN-α led to a median fold increase of 1.8 on IRF7 expression. pDCs from melanoma patients responded to IFN-α in a similar pattern as healthy controls. A tendency of lower fold change of IRF7 expression was observed in $CD123^{+}BDCA2^{+}$ gated pDCs from patients after UV-inactivated NDV treatment (Appendix 8.2, Figure 30). Taken together, these data suggested that pDCs from melanoma patients analysed in this study exhibited an impaired TLR9-MyD88-IRF7 signalling but retained an intact IFN-α feedback response that activates ISGF3-IRF7 signalling.

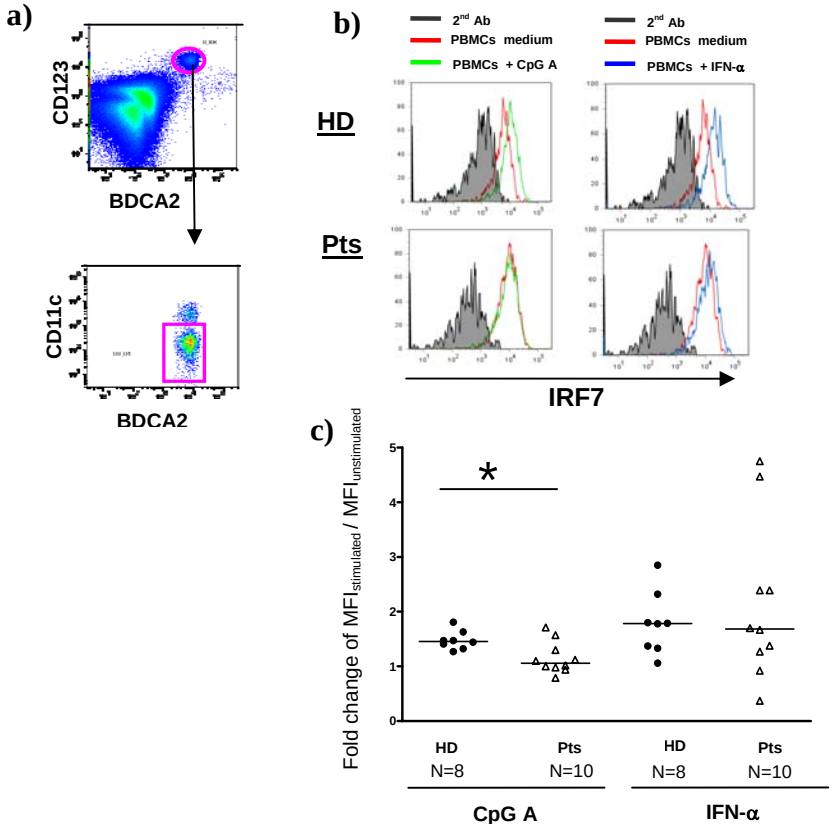

Figure 19: IRF7 expression in pDCs from melanoma patients.PBMCs (1 x 10^7) from melanoma patients (Pts) and healthy donors (HD) were and incubated with either CpG A, IFN-α or in medium for 6 h. The cells were then harvested and stained with antibodies against surface antigens CD123, CD11c and BDCA-2 followed by intracellular staining of IRF7. (a) Gating strategy for pDC identification is shown. (b) The expression levels of IRF7 on $CD123^+BDCA2^+CD11c^-$ pDC are shown in histograms, the fluorescence intensity is determined as median fluorescence intensity (MFI). Representative histograms from one healthy donor and patient are shown. The background stainings using only secondary antibody on cells that were cultured in the presence or absence of stimulus was similar and representative histograms are presented in the figure. (c) The fold change of IRF7 expression in $MFI_{stimulated}$ / $MFI_{unstimulated}$ pDCs are presented in scatter plot and bars indicate median value of expression. *$p<0.05$.

4.4.6 Low levels of 4E-BP1 phosphorylation in PBMCs from melanoma patients after CpG A stimulation

4E-BP1, a 5'UTR dependent translational repressor acts as inhibitory protein that suppresses translation via binding to eIF4E. This inhibition is relieved when 4E-BP1 undergoes sequential phosphorylation first at Threonine-37/46 sites followed by phosphorylation of Serine-65 and Threonine-70. The phosphorylation of Ser65/Thr70 have been shown to play a crucial role in the release of eIF4E and increased eIF4E availability leads to translation initiation of a subset of mRNAs with substantial

secondary structures in the 5'-UTR (196). The deletion of 4E-BP1 genes increased the translation of IRF7 mRNA in fibroblast (195). The discrepancy between the fold changes for IRF7 RNA and protein in pDCs after CpG A or IFN-α stimulation prompted us to assess the regulation of IRF7 translation in pDCs from melanoma patients in response to TLR9 activation. In this regard, we measured the level of p4E-BP1 since the increased level of this protein may promote the translation of IRF7 mRNA.

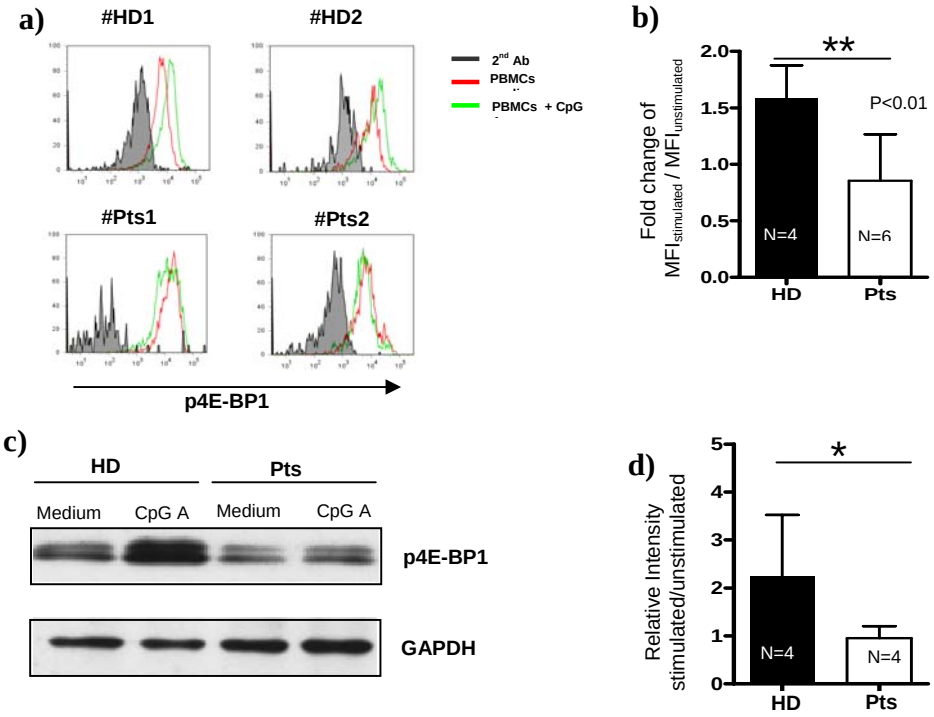

Figure 20: PBMCs (1 x 10^7) were activated with either CpG A (10 µg/mL) for 6 h or left untreated. (a) Cells were stained with surface markers for pDCs and gated on $CD11c^-CD123^+BDCA2^+$ cells followed by intracellular staining with anti-p4E-BP1. (b) Fluorescence intensity of stained cells was measured by flow cytometry. The background stainings using only secondary antibody on cells that were cultured in the presence or absence of stimulus was similar and representative histograms are presented in the figure. Relative fold increase of $MFI_{stimulated}$ / $MFI_{unstimulated}$ is shown for PBMCs from patients (white bars) and healthy controls (black bars). (c) CpG A-treated cells and control cells were harvested and total cell lysates were resolved by SDS-PAGE followed by immunoblotting with an anti-p4E-BP1 (Ser65/Thr70) antibody. (d) Blots were reprobed with anti-GAPDH antibody as a loading control. The intensity of p4E-BP1 was normalized to the intensity of GAPDH and the relative fold increase of 4E-BP1 phosphorylation is shown as normalized signal intensity of stimulated/unstimulated samples. Data are shown as median. * $p<0.05$; ** $p<0.01$

Figure 20a shows histograms on p4E-BP1 (Ser65/Thr70) expression determined as MFI in pDCs from two representative patients and healthy controls in response to CpG A treatment. Exposure of PBMCs from healthy controls to CpG A induced rapid

phosphorylation of 4E-BP1 at Ser65/Thr70 in BDCA2$^+$ pDCs already 15 min after stimulation onset (Figure 20a, 20b). PBMCs of all control subjects tested contained higher amounts of p4E-BP1 (Ser65/Thr70) compared with non-stimulated cells (Figure 20b). The increased of p4E-BP1 level in BDCA2$^+$ pDCs after CpG A stimulation correlated with up-reuglation of IRF7 proteins, suggesting an enhancement of the IRF7 mRNA translation.

In contrast, p4E-BP1 was not significantly augmented in pDCs from melanoma patients in the presence of CpG A (Figure 20b). An increased p4E-BP1 level was also detectable in PBMCs from healthy controls after incubation with CpG A as analysed by immnunoblotting (Figure 20c & 20d). The relative fold increase of 4E-BP1 phosphorylation was determined as signal intensity over loading control and compared to untreated sample. In controls, the median relative fold increase of 4E-BP1 phosphorylation assessed by immunoblotting was 2.75 fold whereas the p4E-BP1 level remained unchanged in PBMCs from melanoma patients (median relative fold increase = 1.0) (Figure 20c). Collectively, both flow cytometry and immunoblotting analysis revealed low p4E-BP1 levels in pDCs and PBMCs from melanoma patients in comparison to healthy subjects upon TLR9 activation.

4.4.7 Hyporesponsiveness of pDCs to TLR-9-CpG A activation is associated with an impaired IRF7 nuclear translocation

As previously shown, activated IRF7 regulates IFN-α production in pDCs by translocation to the nucleus and lead to type I IFN gene transcription (192). The up-regulation of IFN-α then promotes the transcription of downstream genes such as cytokines and chemokines responsible for inflammation and migration. Although no up-regulation of IRF7 expression was observed in patients' pDCs after CpG A treatment, constitutively expressed IRF7 may remain capable to undergo phorphorylation and to migrate to nucleus. Hence, we investigated if the deficiency of IFN-α production in pDCs from patients could be a consequence of the reduced capability of IRF7 translocation to the nucleus.

After we activated PBMCs using CpG A for 6 h, the cells were further sorted by flow cytometer as $CD123^{+}BDCA2^{+}$ pDC for visualisation using confocal microscopy. In pDCs from healthy controls, majority of the IRF-7 translocated to the nucleus, as assessed by the localization of IRF-7 (red) and DAPI (blue) stainings (Figure 21a), while the pDCs from melanoma patients did not show similar localization of IRF7 in the nucleus after TLR9 ligand activation. An accumulation of IRF7 in the nucleus was also not found in the pDCs of both healthy donors and patients without CpG A stimulation.

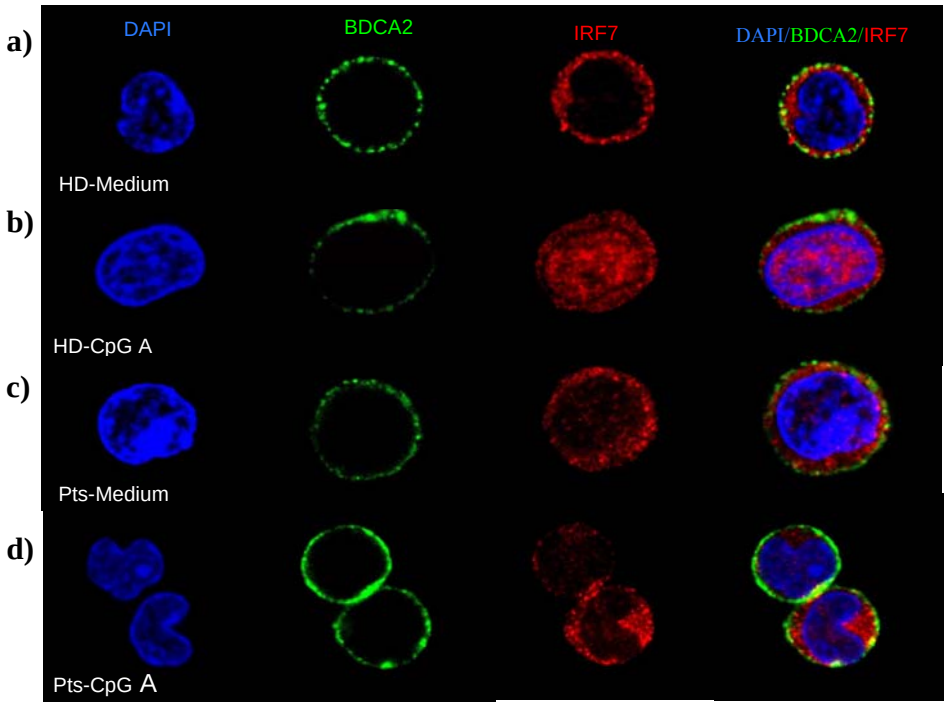

Figure 21: Impaired IRF7 nucleus translocation in pDCs from melanoma patients. PBMCs (1-2 x 10^{8}) were stimulated with CpG A (10 µg/mL) or cultured in the absence of stimulus for 6 h. Cells were then harvested and stained with antibodies against the surface antigens CD123, CD11c and BDCA-2 followed by intracellular staining of IRF7. $CD123^{+}BDCA2^{+}CD11c^{-}$ pDCs were sorted prior visualisation by confocal microscope. The sorted cells were cytospun and mounted with Vectashield containing DAPI. pDCs were visualized by cell surface staining of BDCA2 (FITC), whereas the nucleus was identified using DAPI (blue). IRF7 antibody labelled with Alexa fluor 555 (red) was used to analyse nucleus translocation of the transcription factor. Representative data from a healthy donor (HD) (n = 6) and a melanoma patient (Pts) (n = 5) are shown in (a) HD in medium; (b) HD stimulated with CpG A; (c) Pts in medium; (d) Pts stimulated with CpG A.

The localization of IRF7 in the nucleus was further confirmed by 3-dimensional reconstruction, which allowed the visualisation of the molecule in 3-dimensional images versus images acquired as single plane (Figure 22). IRF7 was found to localise in the nuclear compartment in both single plane and 3D-reconstructed images.

Figure 22: Visualisation of IRF7 localisation in the cell nucleus via 3-dimensional reconstruction of pDC stacking images. Stacking images for visualizing of IRF7 translocation in pDC were acquired using confocal microscopy and subsequently reconstructed using image processing software.

In addition, to avoid staining variation, IRF7 translocation was measured as ratio of nuclear to cytoplasmic IRF7. Assessment of nuclear:cytoplasmic ratio revealed a strong reduction of detectable IRF7 in the nuclear compartment in pDCs from the patient group (Figure 23a). There was a similar trend of low nuclear:cytoplamic IRF7 in pDCs sorted from patients after CpG A activation, suggesting aberrant IFN-α production is associated with impair of IRF7 translocation in pDCs from melanoma patients.

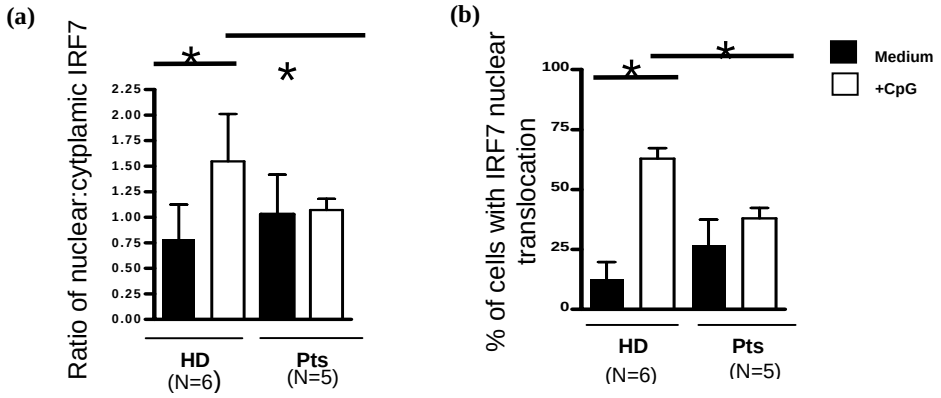

Figure 23: Quantitative evaluation on IRF7 translocation. (a) IRF7 translocation was determined by the ratio of IRF7 fluorescence intensity in the nucleus and cytoplasmic using Image J. (b) Frequency of pDCs with clear IRF7 translocation in the nucleus. Quantitative analysis was performed on at least 50 cells from six different healthy donors and five different patients. Bar plots indicate the median values of the ratio of nulear: ctyoplasmic fluorescence. *P<0.05, statistical significance when compared with the respective controls.

Quantitative analysis revealed that a median of 63% sorted pDCs in healthy controls showed a clear nucleus translocation of IRF7 upon CpG A stimulation (Figure 23b). In contrast, a significant reduced frequency of IRF7 translocated in pDCs from patients (median of 38%). Based on both qualitative and quantitative analysis illustrated here,

pDCs from melanoma patients displayed impaired TLR9 signal transduction that led to reduced IRF7 translocation.

4.5 Absolute number and phenotype analysis of NK cells in melanoma patients

4.5.1 Altered absolute numbers of NK cells in peripheral blood of melanoma patients

NK cells are lymphocytes of the innate immunity that play a crucial role in tumour recognition. The interplay of DCs and NK cells is of great importance in maintaining efficient immune response. To assess the integrity of NK cells in the peripheral blood of melanoma patients, we first enumerated absolute NK cell numbers by combining FACS staining with Trucount beads, a 7–9 μm mean diameter beads that serve as an internal counting standard for precise cellular quantification. The assay was performed on whole

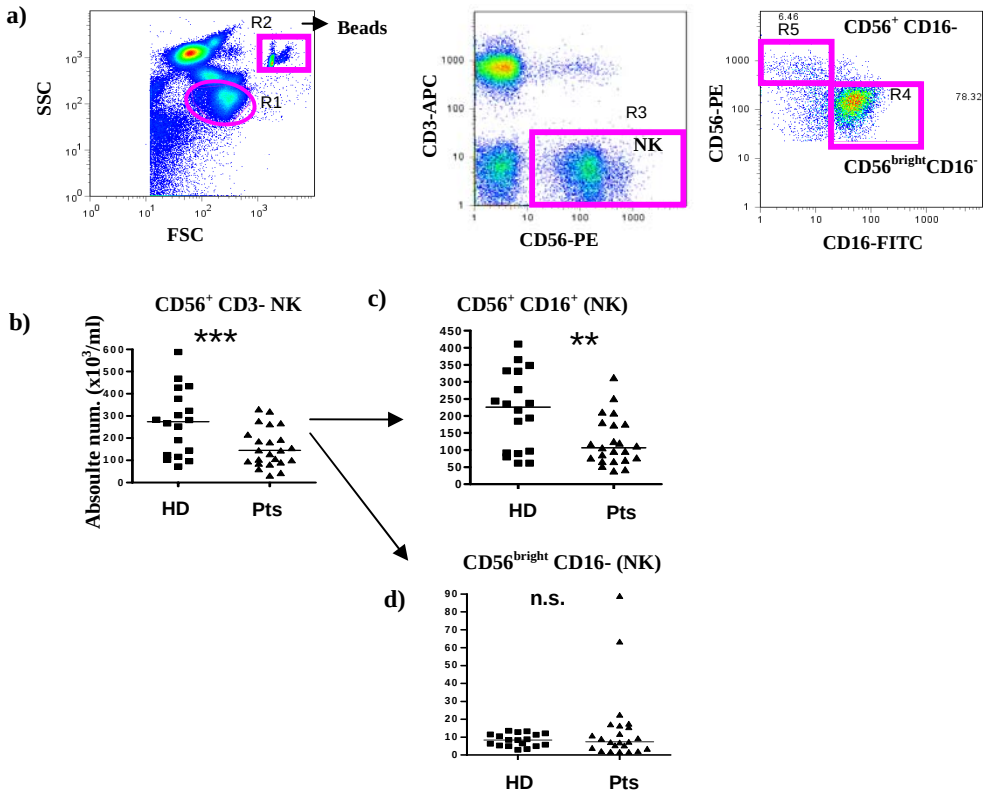

Figure 24: Absolute count of NK cell subsets in whole blood of stage IV melanoma patients and healthy controls. (a) Gating strategy used to define absolute NK cell numbers by TruCOUNT assay. Total lymphocytes and TruCount beads were included in regions (solid boxes) R1 and R2, respectively. R3 was created to define $CD56^{+}CD3^{-}$ NK cells. NK subpopulations were defined as $CD56^{+}CD16^{+}$ (R4), or $CD56^{bright}CD16^{-}$ (R5). (b-d) Scatter plots represent absolute numbers of total NK cells, $CD56^{+}CD16^{+}$ and $CD56^{bright}CD16^{-}$NK cells of age-matched healthy donors (n=18) and stage IV melanoma patients (n=23). Data are shown as median. ***$p<0.005$, ** $p<0.02$ and n.s., not significant.

blood samples without cell isolation to eliminate potential cell loss. Figure 24a shows the gating strategy for defining absolute NK cell numbers from one representative patient. Assessment by FACS revealed a significantly decreased proportion of total $CD56^+$ NK cells in the peripheral blood of stage IV melanoma patients (n=23) compared with age-matched healthy controls (n=18).

In order to understand the contribution of different NK cell subsets to the total numbers of NK cells, co-staining for CD16 and CD56 was performed, which allowed further definition of the two major NK subsets, the $CD56^+CD16^+$ and $CD56^{bright}CD16^-$ NK cells (Figure 24b-24d). The absolute $CD56^+CD16^+$ NK cells count (cells/µL) was significantly reduced in melanoma patients (median (range): 106.8 (38.90-312.42)) compared to healthy controls (226.1 (61.75-410.9)). However, there was no significant difference in the $CD56^{bright}CD16^-$ NK cell number in patients (8.377 (1.74-88.9)) versus healthy controls (7.410 (1.74-88.9)). This suggested that the decrease in the $CD56^+CD16^+$ NK cell subset strongly contributes to the reduction of total circulating NK cell numbers in patients.

4.5.2 Melanoma cell line expresses ligands for NK cell-activating receptors and sheds sMICA and sULBP2 in the sera of melanoma patients

Ligands for NK cell-activating receptors including NKG2D, NKp30, NKp44 and NKp46 are expressed on virus infected or transformed cells. The expression of these receptor-ligands has been detected on several tumour types such as ovarian cancer and glioblastoma, both on tumour cell line and primary tumours (119, 120). This implicates the capability of NK cells to recognise tumour cells. Thus, we analysed the expression of ligands for NK cell-activating receptors on the melanoma cell line Mel 249 that was established from an advanced stage melanoma patient. By assessing the surface expression of these ligands, we found a constitutive expression of different ligands for the NKG2D receptor including MICA, MICB and ULBP2 (Figure 25a). Interestingly, NKp30L and NKp46L, the ligands for NCRs were also substantially expressed by Mel-249.

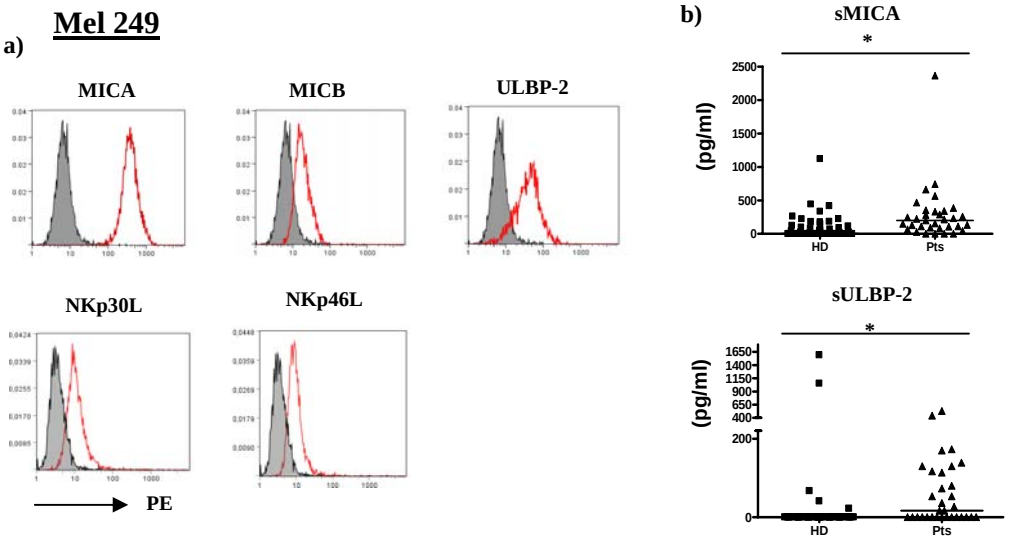

Figure 25: Detection of expression of ligands for NK cell-activating receptors on melanoma cell line Mel 249 and detection of soluble NKG2D ligands in the sera of melanoma patients. (a) Human melanoma cell line, Mel 249 was established from a patient with metastatic melanoma lesion and stained for the surface expression of ligands for NK cell-activating receptors including MICA, MICB, ULBP2, NKp30L-Ig and NKP46L-Ig fusion proteins. Cells were washed and further stained with either PE-conjugated goat-anti-mouse or PE-anti-human-Fc secondary antibody. Grey histograms represent the background staining using only PE-conjugated secondary antibody (b) Soluble forms of MICA (sMICA) and ULBP2 (sULBP2) in sera of stage IV melanoma patients (Pts) (n=33) and healthy donors (HD) (n=50) were determined by ELISA. *p<0.05.

Shedding of these ligands has been implicated to facilitate tumour evasion as prolong interaction of MIC molecules with the NKG2D receptor could impair NKG2D expression (140). The down-regulation of NKG2D receptor has been shown due to the endocytosis of the receptor and subsequent degradation upon prolong interaction of NKG2D receptor with its ligand (140). Thus, we assessed whether soluble forms of MICA and ULBP2 could be detected in the sera of stage IV melanoma patients in this study using ELISA. Analysis of sera from 33 melanoma patients revealed that MICA was present in most of the sera (29/33) while ULBP2 was found in 18 patients (Figure 25b). The levels of sMICA ($p < 0.0001$) and sULBP2 ($p=0.0006$) were significantly higher in the sera of melanoma patients than in healthy controls (n=50). Taken together, melanoma cells not only expressed ligands to NK cell-activating receptors but also the soluble forms of these ligands are readily detectable in the sera of melanoma patients with advanced disease stage.

4.5.3 Circulating NK cells from melanoma patients displayed increased NCR expression but no aberrant expression of NKG2D

The substantial difference in the NK cell count in melanoma patients compared with healthy controls and the detection of soluble ligands for NK cell-activating receptors in the sera of melanoma patients prompted us to explore the expression of their cognate receptors namely, NKG2D and NCRs (NKp30 and NKp46) (Figure 26a, b). We first found that the proportion of $CD56^{+}CD3^{-}$ NK cells expressing the NKG2D receptor was comparable between healthy donors and patients.

Surprisingly, analysis of the same population revealed 69.7 % (median) of total NK cells expressed NKp30 in healthy controls whereas 81.67% (median) of $NKp30^{+}$ NK cells were detected in melanoma patients. Similarly, fewer $NKp46^{+}CD56^{+}$ NK cells were detected in the control group than in patients with a median of 63.6% versus 78.75% (Figure 26b). Parallel analysis of the surface expression levels of NKG2D on $CD56^{+}$ NK cells from melanoma patients and healthy donors demonstrated no difference. In contrast,

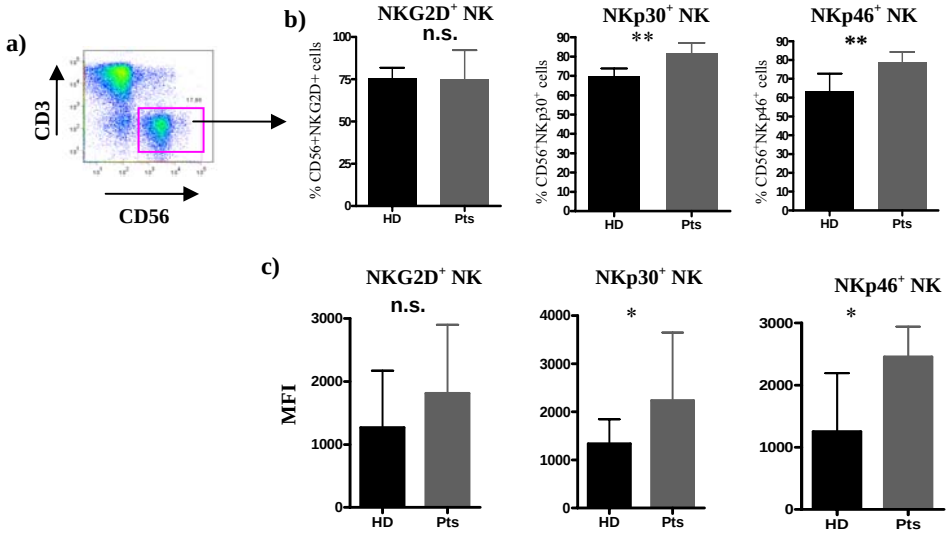

Figure 26: Detection of NK cell-activating receptors expression in PBMCs from healthy controls (HD) and melanoma patients (Pts). PBMCs ($2x10^{6}$ cells) from healthy subjects (n=6) and melanoma patients (n=6) were stained with antibodies against cell surface NK cell-activating receptors including NKG2D, NKp30 and NKp46. (a) Dot plot represents the gating used to define the region of $CD56^{+}$ NK cells for further analysis. (b) Bar plots indicate median percentage of $CD56^{+}CD3^{-}$ NK cells expressing NKG2D, NKp30 and NKp46 (c) Expression of NK cell-activating receptors on $CD56^{+}CD3^{-}$ NK cells is given as MFI. All data are presented as median value.*$p<0.05$, **$p<0.01$, n.s not significant.

circulating NK cells from patients displayed significantly increased surface NKp30 and NKp46 expression ($P<0.05$) (Figure 26c). Our data reveal higher frequencies of NKp30 and NKp46 expressing NK cells and expression level of both receptors in melanoma patients compared to healthy donors, but no differences in NKG2D.

4.6 Functional properties of NK cells from stage IV melanoma patients

4.6.1 Conserved NK cell degranulation, perforin content and IFN-γ secretion in melanoma patients

We next evaluated the integrity of the functional responsiveness of NK cells in melanoma patients. In this analysis, we compared the capability of resting NK cells to produce IFN-γ in response to PMA/ionomycin stimulation, which bypasses upstream receptor signalling. Stimulation with PMA substantially elicits production of IFN-γ by NK cells in healthy controls whereas the IFN-γ secretion by NK cells from melanoma patients seems to be reduced (Figure 27a, b). However, this did not reach statistical significance.

Apart from IFN-γ production, the perforin content, which is responsible for pore formation during cytolysis could also provide hints on the functional status of NK cells. FACS analysis revealed that similar percentage of NK cells from melanoma patients and healthy donors were positive for perforin (Figure 27c). We further analysed the function of NK cells by co-incubation with Mel249 and K562, which are both HLA-class I deficient cells (Figure 27d). In this assay, we monitored the expression of CD107a, a lysosomal associated membrane protein (LAMP-1), which residing in cytolytic granules membranes. Upon activation of NK cells, CD107a is mobilized to the cell surface following activation-induced granule exocytosis and serve as surrogate markers for degranulation (246, 247). Degranulation of NK cells from patients was not significantly impaired, despite of reduced $CD56^{+}CD16^{+}$ NK cell count (Figure 27d). These data suggest augmentation of NKp30 and NKp46 expression together with increased frequency of $NKp30^{+}$ and $NKp46^{+}$ NK cells that we observed may play a role in conferring similar cytolytic property of NK cells in peripheral blood from melanoma patients to NK cells from healthy donors.

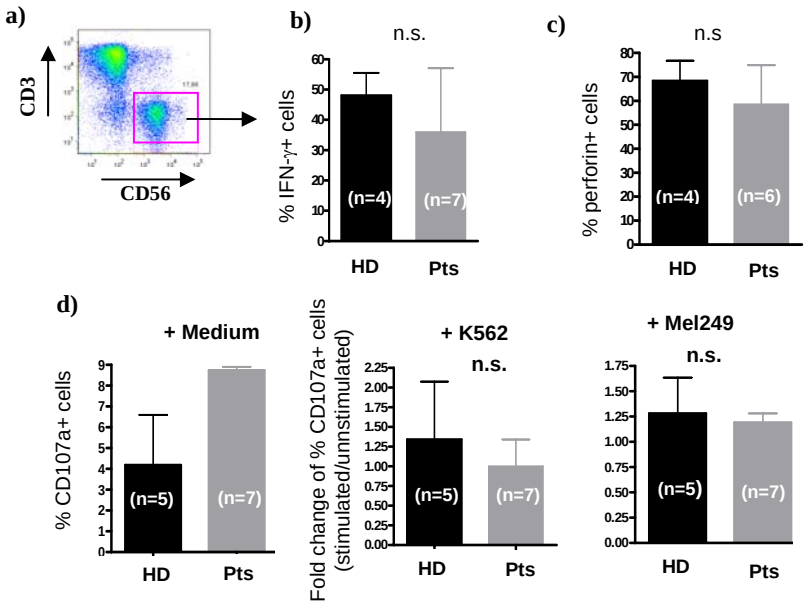

Figure 27: Detection of IFN-γ production, perforin content and degranulation in NK cells from melanoma patients. PBMCs (2-5X 10^7 cells) from healthy subjects (HD) and melanoma patients (Pts) were incubated in culture medium containing 10% PHS in IMDM for overnight. 2x10^6 PBMCs were then either cultured alone in complete cell culture medium or stimulated with PMA (2.5 μg/mL) and Ionomycin (0.5 μg/mL) for 4 h. After 4 h stimulation, cells were surface stained with antibodies against NK cell markers and fixed and permeabilised for intracellular staining. PMA/iono stimulated PBMCs were stained intracellulary with anti- IFN-γ and measured by flow cytometry. (a) Dot plot depicts the gating of NK cells. (b) Bars indicated the median value of IFN-γ producing cells in healthy donors and melanoma patients. For detecting the perforin content, cells after rested in cell cultured medium were harvested and subjected to intracellular perforin staining without stimulation. (c) Accumulative data from 4 healthy subjects and 6 patients are shown for percentage of perforin positive NK cells. (d) Degranulation capacity of NK cells was examined by culturing PBMCs either alone in medium or together with target cells (K562 or Mel 249) at a ratio 10:1 for 4 h in the presence of CD107a antibody. The cells were then harvested and subjected to surface staining and measured by flow cytometry. The percentage of CD107a NK cells was determined. Results are reported as fold change of percentage of CD107a+CD56+ NK cells in stimulated relative to unstimulated PBMCs. All data were presented as median value. n.s. not significance when compared with the respective controls.

4.6.2 IL-2 activated NK cells induced up-regulation of CD40 and CD80 expression on moDCs

To further address the functional role of NK cells in inducing autologous mDC activation in melanoma patients, we first determined whether IL-2 activated NK cells could induce activation of moDCs in healthy controls. This analysis was performed by co-incubating moDCs generated from monocytes with a GM-CSF and IL-4 cocktail together with autologous resting or IL-2 activated NK cells at a ratio of 1:1. After 48 h co-culture, the expression of co- stimulatory molecules on moDCs was measured by flow cytometry.

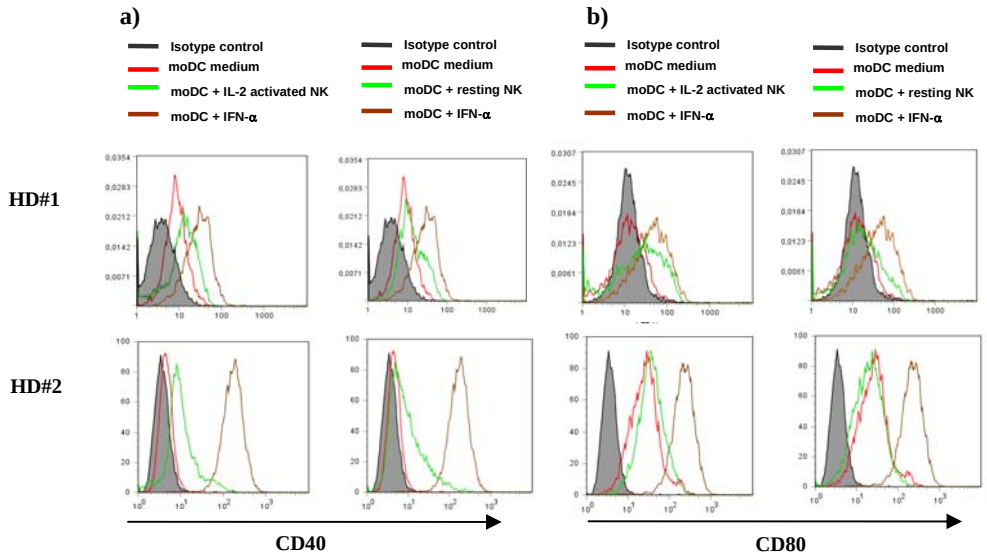

Figure 28: IL-2 activated NK cells induced up-regulation of CD40 and CD80 expression on monocyte-derived DCs (moDCs). IL-2 activated (100 IU/mL for 6 days) or resting NK cells from different healthy donors were co-incubated with autologous immature moDCs at the NK cell to DC ratio of 1:1. As positive control, moDCs were stimulated with IFN-α (1,000 IU/mL). After 48 h, cells were harvested and assessed for (a) CD40 and (b) CD80 expression by flow cytometry. Representative results from two healthy controls were shown for CD40 and CD80 expression. The background stainings using isotyope control antibodies on cells cultured in the presence or absence of stimulus was similar and representative histograms are presented in the figure.

As positive control to assess the expression of CD40 and CD80 on maturated moDC, 6 days cultured immature moDC were stimulated with IFN-α at 1000 IU/mL. IL-2 activated NK cells increased the expression of CD40 and CD80 on moDC although to a lesser extent than IFN-α. However, CD40 and CD80 were only slightly augmented upon co-culture of resting NK cells together with moDCs (Figure 28a & 28b). This indicates that IL-2 activated NK cells are more efficient than resting NK cells in promoting maturation of DCs by up-regulating expression of CD40 and CD80. The expression of these two co-stimulatory molecules is essential for the role of DCs in priming T cells.

4.6.3 IL-2 activated NK cells induced up-regulation of CD40 expression on mDC1 in both healthy donors and melanoma patients

Previous evidence shown by Gerosa *et al*. (71) and our results demonstrated the ability of IL-2 activated NK cells to induce moDC maturation. We then assessed whether mDC1 from melanoma patients could be activated by NK cells in the presence of IL-2 stimulation.We evaluated the up-regulation of co-stimulatory molecules on freshly

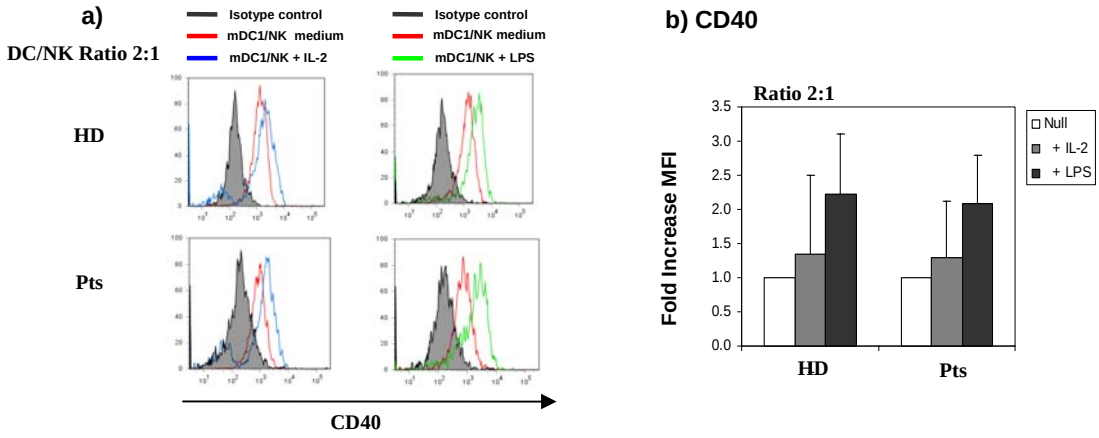

Figure 29: Activation of NK cells by IL-2 induces CD40 expression on mDC1 during NK/DC interaction from healthy controls (HD) and patients (Pts). (a) Freshly purified BDCA1$^+$ myeloid DC (mDC1) were cultured together with autologous NK cells in the presence of IL-2 (100 IU/mL) or LPS (1 µg/mL) or in medium alone at the indicated DC: NK cells ratio. After 48 h, cells were harvested and evaluated for expression of CD40 on BDCA1$^+$ gated mDC1by flow cytometry. (a) Representative histograms of one experiment from each group of healthy donors and patients depict the effect of IL-2 *(left panel)* and LPS *(right panel)* stimulation on CD40 expression by mDC1 after mDC1/NK co-culture. The background stainings using isotyope control antibodies on cells cultured in the presence or absence of stimulus was similar and representative histograms are presented in the figure (b) The bars indicate fold increase of CD40 MFI (MFI of stimulated/unstimulated) after stimulation with either IL-2 or LPS at the indicated mDC1/NK ratio and data are shown as median from the healthy donor (n=3) and the patient (n=4) group.

purified BDCA1$^+$ mDC1 that were co-cultured with autologous NK cells at mDC1/NK ratio of 2:1 in the presence or absence of IL-2 for 48 h. Histograms depict the expression of CD40 on mDC1 obtained from one representative control and patient. Upon co-culture of mDC1/NK cells together with IL-2, there was up-regulation of CD40 expression in mDC1 from healthy donors. This increased expression was also found on mDC1 purified from melanoma patients when cultured under the same condition (Figure 29a & 29b). As positive control, mDC1/NK cells were treated with LPS, which predominantly activates mDC1 by up-regulating CD40 expression. Both mDC1 from healthy donors and melanoma patients showed a similar increase of CD40 expression in response to LPS stimulation (Figure 29a & 29b), suggesting no differences in activation of NK cells.

5.0 Discussion

Immune dysfunction is an early event in cancer development and exaggerates during tumour progression. It is of importance to define the potential mechanisms that are involved in immune dysfunction for improving and tailoring new cancer therapy. To understand the mechanisms of immune dysfunction, the current study aimed at investigating the integrity of peripheral blood DCs and NK cells in melanoma patients from the aspect of the absolute numbers and functional properties. It also aimed to identify the decisive signalling pathway and molecules that are responsible for the functional alteration observed in both immune subsets. Our analyses were performed on materials collected from stage IV melanoma patients and age-matched healthy donors. This excludes the possibility of aging-related deficiencies in the immune system between healthy donors and patients. Besides, a similar defect was observed among all the patients included in the analysis and excludes the possibility of therapy-related effect on immune deficiency in melanoma patients.

5.1 Reduced DC numbers in the peripheral blood of melanoma patients

DCs are considered as the most potent antigen presenting cells, responsible for initiating and regulating immune responses (33, 34). Circulating blood DCs are essential for conferring adequate immunity to the host. Thus, in response to various inflammatory stimuli, a substantial increase of DC numbers appears to be important to replenish the pool of tissues-resident DCs. Three main DC subsets including mDC1, mDC2 and pDCs are found in human peripheral blood and equipped with distinct immunological functions. Human mDC1 are believed to be more efficient in presenting antigens and in eliciting proliferation of naïve T cells than mDC2 and pDCs. So far, the function of mDC2 is largely unknown while pDCs are known to be responsible for robust production of type I IFN.

During tumour initiation and progression, DCs are frequently targets of tumour immune escape mechanisms. Altered circulating DC numbers have been reported for breast cancer, lung cancer, head and neck squamous cell carcinoma and hepatocellular carcinoma (248-252). Thus, enumeration and functional characterisation of the DC subsets in cancer patients are crucial to understand their immunological role, also in melanoma. Of specific importance are studies related to distribution of DC subsets in fresh peripheral blood and tumour tissues from melanoma patients. The current study focuses on DC subsets in peripheral blood from stage IV melanoma patients. The lack of tumour tissues in this cohort of patients precluded the possibility to analyse tumour-infiltrating DCs in the patients.

Based on the application of novel markers for blood DCs (46), the present study analysed the numbers of mDC1, mDC2 and pDCs in the peripheral blood of stage IV melanoma patients in comparison to age-matched healthy controls. It was observed that numbers of circulating human blood pDCs and mDC2 were significantly lower in stage IV melanoma patients than in age-matched healthy controls. In contrast, Gerlini *et al.* reported that the frequency of DC subsets in the peripheral blood from melanoma patients with clinically evident lymph node metastasis were not statistically different from healthy donors (102). The discrepancy between the two analyses might be attributable to the methods used for DC subset identification. In the current study, circulating human DC subsets were enumerated in freshly collected whole blood in the presence of appropriate anti-coagulant, whereas Gerlini *et al.* examined isolated PBMCs. DC subset identification in whole blood allows high accuracy and provides reproducible DC subset enumeration as it circumvents substantial cell loss and formation of unwanted cell aggregates that occur during PBMC isolation, which could lead to inaccuracy in DC count determination. In this study, whole blood samples were processed within 6 hours after blood withdrawal and the acquisition of antibody stained fixed samples was performed within 24 h after blood collection. This reduces the variability related to the method of DC enumeration. Moreover, both BDCA1 and BDCA3 low expressing B cells and monocytes as well as dead cells, which could non-specifically bind the antibodies, were also excluded from analysis within the present study, demonstrating the superiority of this method. As

already mentioned, our analyses were performed on materials collected from patients and age-matched healthy donors. This excludes aging-related deficiency in the immune system between healthy donors and patients. The reduced numbers that we observed in our study are unlikely due to prior treatment since materials used to perform this analysis were collected according to approved clinical protocol from patients who either had not received any treatments or were free from systemic treatment and radiotherapy for at least 30 days and had recovered from all toxicities associated with prior regimen. Furthermore, similar defects were observed among all patients included in this analysis.

So far, it is unclear whether the reduction of pDC counts observed in melanoma patients, is due to poor pDC survival or to the migration of pDCs to lymphoid organs or tumours. It has been reported that a high proportion of pDCs is present within metastatic lymph nodes and forms aggregates in close vicinity to melanoma nests (102). In particular, pDCs have been frequently detected between high endothelial venules and melanoma cells (102). This supports the possibility that pDCs migrate from the circulation towards the tumour area (102), which potentially leads to reduced pDC numbers in the blood. Besides melanoma, tumor-infiltrating pDCs have been detected also in the solid malignant tissue of patients with head and neck squamous cell carcinoma and breast cancer (99, 101). Furthermore, accumulation of pDCs in the lesions of patients with psoriasis and systemic lupus erythematosus has been found to be associated with reduced circulating blood pDCs (253, 254).

The migration capability of pDCs is related to the expression of CXCR3, the receptor for CXCL10 (255). In this study, substantially elevated CXCL10 was found in sera from melanoma patients, which implicates a potential association of decreased pDC numbers with their migration. Unfortunately, due to the lack of tissue from patients enrolled in the present study, tumor homing of pDCs could not be verified.

Besides migration, the decline of blood DC numbers might be attributed also to cell death presumably induced by tumour-derived factors. Increased spontaneous apoptosis of blood DCs has been previously described in patients with breast cancer implicating that the

inhibitory influence of tumours could extend far beyond the tumour microenvironment (256). It has been suggested that IL-10 and TNF-α reduce the viability of pDCs and induce apoptosis (257) and both of these cytokines could be produced by tumours for example melanomas (258, 259). Moreover, tumour derived TGF-β could induce apoptosis of DCs (260). Systemic DC cell death may thus impose chronic stress on the immune system of cancer patients and result in progressive paucity of DCs in the circulation (261). Alternatively, the reduced DCs numbers in peripheral blood might be related to a disturbed DC differentiation. However, the inhibition of pDCs and mDC2 development from $CD34^+$ progenitors has so far not been well studied.

5.2 Altered balance of the peripheral blood DC compartment in melanoma patients

There are increasing numbers of studies exploring the balance of the DC compartment as an indicator of the immune status of patients with autoimmune disease and patients who underwent transplantation. These studies suggest that the mDC/pDC ratio potentially serves as an index of the immune balance and allows monitoring of the patients immune reconstitution. Thus, a lower mDC/pDC ratio has been associated with successful withdrawal of immunosuppression in liver or heart transplanted recipients (235-237). Furthermore, it has been shown that anti-bacterial and anti-tumour immune responses rely on the cross-talk of mDCs and pDCs (76, 262) and that the balance of the DC compartment potentially influences the distribution of Th1 and Th2 cells in the peripheral blood (239). A study on patients with atopic dermatitis revealed a low mDC/pDC ratio that was associated with a shift towards Th2 immune responses and disease severity (239). In contrast, a higher mDC/pDC ratio has been detected in the synovial fluid compared to the peripheral blood of patients with rheumatoid arthritis and has been suggested to be involved in the initiation, maintenance and/or regulation of inflammatory responses (263). In diabetes, IFN-α production correlates inversely with the mDCs/pDCs ratio (264). Thus, the mDCs/pDCs ratio was determined in this study. A profound increase of the mDC/pDC ratio was detected in melanoma patients compared to age-matched healthy controls. The increased mDC/pDC ratio was not related to changes in

the IFN-α level in the sera of melanoma patients as IFN-α was not detectable in most of the samples being analysed (data not shown).

Interestingly, a positive correlation between pDCs and mDC2 numbers was demonstrated in the present study. mDC2 are a minor and rare myeloid DC subset, their numbers declined in melanoma patients. So far, there are only a few observations on the behaviour of mDC2 in different pathological states (265-267). A recent study revealed an association of pDC and mDC2 numbers in Sjoren syndrome, a chronic inflammatory disease (268). However, the functional properties of mDC2 are poorly understood due to the extreme rarity of this cell type in the blood especially in pathological situation. Therefore, it remains unclear how the association between pDCs and mDC2 and the low mDC2/mDC1 ratio contribute to the immune status of melanoma patients. A better understanding on the significance and function of mDC2, including their role in development and/or maintenance of the immune system during various pathological situations remains to be established. Besides, it remains unclear if mDC1 and mDC2 are two distinct population or the same cell type at different maturation stages. Thus, the current study can not rule out if the low mDC2/mDC1 ratio in melanoma patients is due to a disturbed differentiation of mDC2 to mDC1 or vice versa.

5.3 Impaired interaction between mDCs and pDCs from melanoma patients

The role of the mDC and pDC interplay, in which pDCs promote mDC differentiation and activation, has been previously established in systemic lupus erythematosus patients (269) and during the development of antiviral immunity (270). The synergy of mDCs and pDCs has so far not been investigated in cancer patients. The lack of this information is mainly attributable to the limited patient material, which does not allow an isolation of sufficient pDC numbers especially when pDC numbers are decreased during disease. By taking advantage of the availability of leukapheresis products from some melanoma patients, the mDC1/pDC cross-talk was analysed in the current study, though only on a small number of patients. We are aware of the fact that the enormous amount of blood cells needed for purification of minor cell populations such as pDCs is provided only by a few advanced-staged melanoma patients. Since alternative systems to perform such study are

not available due to the lack of animal models with similar pDCs biology as human and *in vitro* systems that mimic the immune dysfunction of melanoma patients, this is the only way to gain insight on the pDCs functions between tumor patients and healthy individuals. The small numbers of patients with sufficient blood materials is due to the poor survival rate of stage IV melanoma patients and the challenge encountered in patient recruitment and follow up process. This can be, at least in part, overcome by improving patient recruitment for clinical studies. Furthermore, the application of new technologies with increased sensitivity and specificity that allows single cell preparation for multiple parameters analysis may overcome the need to obtain large quantity of samples.

When mDC1 and pDCs from healthy controls were co-cultured and stimulated with TLR9 ligands, a modest but clear CD40 and CD80 up-regulation on mDC1 was observed. In agreement with this observation, the synergy between murine pDCs with mDCs in response to CpG has been shown to lead to an increased CD40 and CD86 expression by mDCs (262). Likewise, a very recent report from Piciolli *et al.* suggested that TLR9 ligand stimulated human pDCs activate mDCs and induce a significant up-regulation of CD40 and CD80 on mDCs during co-culture (76).

Upon mDC1/pDC interaction, little or no up-regulation of CD40 and CD80 occurred on mDC1 from melanoma patients and accumulative data showed the up-regulation is to a lesser extent than on cells from controls. This finding suggested that the impaired CD40 up-regulation might be due to a certain unresponsiveness of pDCs to CpG A treatment, alternatively mDC1 from melanoma patients might be dysfunctional. mDCs from different cancer patients have been often described to be dysfunctional and to express low co-stimulatory molecules (271). However, stimulation of mDC/pDC co-cultures with LPS induced comparable up-regulation of CD40 and CD80 on cells from patients and healthy controls. Moreover, IL-2 activated autologous NK cells from melanoma patients were capable of inducing CD40 up-regulation on mDC1 to the same extent as in healthy controls.

Several studies have demonstrated the crucial role of pDC-derived type I IFN in inducing maturation of mDCs, which can be partially blocked by neutralising antibodies against the type I IFN receptor (73, 76). In agreement to these studies, the impaired mDC1/pDC interaction in melanoma could be attributed, at least in part, to the inability of pDCs to produce normal amounts of IFN-α in response to TLR9 stimulation. Indeed, much lower amounts of IFN-α were released in mDC1/pDC co-cultures from melanoma patients than from healthy controls though it did not reach statistical sigificance. The lack of statistical significance can be due to the low number of patients and the intrinsic variations among individuals. The defect in IFN-α production by pDCs in mDC/pDC co-culture is supported by a similar and significantly lower IFN-α level in PBMCs from melanoma patients than from controls upon CpG A stimulation.

Although mDC1 from melanoma patients undergo maturation following LPS stimulation, it is very likely that they also secrete IL-10, since IL-10-secreting tolerogenic DC do expressed B7 molecules (272). In fact, purified mDC1 from healthy controls secreted IL-10 in response to LPS activation and the rise in IL-10 corresponded to the increase of the mDC/pDC ratio, pointing to the mDC1 as the major source of IL-10 production. Palucka *et al.* reported that IL-10 suppresses IFN-α production by pDCs in a dose-dependent manner (256). However, under LPS simulation, similar levels of IL-10 were measured in mDC/pDC co-cultures from healthy controls and patients. This excludes the possibility that the altered IFN-α production by patients' pDCs was due to suppression by higher IL-10 levels.

Interestingly, *in vitro* generated moDCs secrete IL-12p70 in response to LPS. However, stimulation of blood mDC1 from patients or healthy controls with LPS alone did not result in IL-12p70 production (data not shown). Similar finding were reported by Picciolli *et al.* (76) further emphasizing the physiological difference between blood mDC1 and *in vitro* generated human moDC. Taken together, this study demonstrates a defect of pDCs from melanoma patients to respond to CpG A stimulation and to mediate mDC1 maturation. Since the mDC/pDC cross-talk enhances the ability of mDCs to present antigen to T cells (262), the defect of the mDCs/pDCs interaction in melanoma

patients might have impact on the capacity of DCs from patients to elicit and amplify efficient anti-tumour T cell responses.

5.4 Altered cytokine and chemokine profile released by PBMC after CpG A stimulation and in sera of melanoma patients

Increased production of pro-inflammatory mediators including cytokines and chemokines upon TLR activation is one of the major functions of DCs (273). In this study, we observed a reduction of IFN-α release by PBMCs and mDC/pDC co-cultures from melanoma patients after CpG A stimulation. Consistent with this data, dysfunction of pDCs lacking the ability to produce type I IFN upon TLR exposure have been shown in patients with head and neck cancer (101). A low or moderate production of type I IFN by pDCs has also been reported for pDCs infiltrating sentinel lymph nodes or tumours from melanoma patients (102). In breast cancer, type I IFN production by pDCs was described to be completely absent (99). Type I IFN seems to influence tumor development and progression via different mechanisms. The cytokine has been shown to inhibit proliferation of certain tumours, to protect $CD8^+$ T cells from activation-induced cell death (274) and to promote terminal differentiation of mDCs (275).

Human pDCs are not only responsible for robust production of type I IFNs (276, 277) they also produce substantial amounts of other inflammatory molecules upon TLR9 activation. Several studies defined that pDC stimulation leads to the production of cytokines like TNF-α, IL-1β and IL-6, as well as chemokines such as CCL3, CCL4, CCL5 and CXCL10 (278-280). Expression of some of these cytokines and chemokines, secreted by pDCs after TLR ligation, is enhanced by autocrine type I IFN. Furthermore, pDC-derived IFN-α could also induce cytokine and chemokine production by other cell types. In fact, we observed lower CCL3, CCL4 and CCL5 fold change in PBMCs from melanoma patients than healthy controls after CpG A stimulation. Despite the lack of statistical significance in some of the cytokines and chemokines production that is due to the low number of patients, similar defect were observed among patients. As chemokines often act in synergy, a reduction of several chemokines with similar functions may impact the function of immune effectors. Since CCL5 acting alone or in combination

with CCL3 and CCL4 could confer protection to T cells from activation-induced cell death, a reduction of these chemokines may indirectly be relevant to a higher susceptibility of T cells to undergo apoptosis in melanoma patients (221).
It has been reported that CCL3, CCL4, CCL5 and CXCL10 are chemokines that display redundant functions in the recruitment of DCs, T cells and NK cells (221-223, 234, 278). Most likely, the production of several chemokines that are able to attract the same type of immune cells represents a mechanism to compensate a deficiency of chemokines (281) and allows the fine-tuning of specific biological responses. Therefore, the lack of pDC activation in melanoma patients that consequently lead to low CCL3, CCL4, CCL5 and CXCL10 release may implicate a defect in recruitment of the respective immune effector cells to site of imflammation. Indeed, a recent study described that the lack of effective T-cell mediated melanoma rejection might be attributable to the absence of key chemokines in these tumours. Lymphocytes-rich melanoma tumours were found to uniquely express CCL2, CCL3, CCL4, CCL5, CCL19, CCL21, CXCL19, CXCL10, CXCL11 and CXCL13 (282).

CCL2 and IL-12p70 secretion as detected in PBMC cultures following CpG A stimulation can be produced by other cell types, which are activated by pDCs. IL-12p70 has been described to represent a key immunoregulatory cytokine produced by immunogenic mDCs and is capable of polarising T cells towards a Th1 phenotype and of optimising NK cell function (55). Treatment of moDCs with IFN-α for example, induces high IL-12p70 production and is associated with a higher capacity in priming antigen specific $CD8^+$ T cells (52). We observed a tendency of reduced IL-12p70 prodcution in PBMCs from melanoma patients after CpG A stimulation. Very often, tumours directly paralyse the capability of mDCs to secrete IL-12p70 through the release of tumour-derived factors such as IL-6, IL-10 and TGF-β, thereby inhibiting efficient $CD8^+$ T cells activation (283, 284). However, since mDC/pDC cooperation confers optimal function of mDCs, it is possible that tumour cells could simply escape from immune recognition by suppressing pDC function, which in turn affects mDC activity. Low CCL2 instead of high concentrations, however, may facilitate the migration of monocytes/macrophages to the tumour and have been previously reported to favour the growth of melanoma (230-

232). These data on the altered PBMC cytokine profile demonstrated in this study may be, at least in part, a consequence of the impaired TLR9 signaling in pDCs from cancer patients.

Interestingly, we observed low CCL2, CCL4 and CCL5 in the sera of melanoma patients. One can not exclude the possibility that the dysregulated chemokine profile observed in melanoma patients may relate to the impaired pDCs function, but the association remains to be established. Although increased IL-6 and CXCL10 levels were observed in the sera of patients, its association with the dysfunctional properties of pDCs is elusive since the tumour itself and endothelial cells may serve as the source for these cytokine and chemokine.

5.5 Reduced NK cell numbers but conserved NK function in melanoma patients

NK cells are one of the key players in preventing growth and spreading of malignant cells. In our study, absolute NK cell numbers were quantified in whole blood from stage IV melanoma patients and age-matched healthy controls. The analysis revealed a reduction in absolute numbers of $CD16^{+}CD56^{+}$ NK cells but not $CD56^{bright}$ NK cells. In fact, a decreased absolute NK cell numbers have been reported for patients diagnosed with HNSCC and with diffuses large B cell lymphoma (285, 286). A low NK cell number may be explained by an impeded maturation and differentiation of NK cells from precursors, which could be induced by tumour growth (287). Another explanation could be that tumours induce apoptosis of NK cells in cancer patients (288).

Tumour associated impairment of NK cell function has been shown in patients with advanced malignancies (289-292). In particular, reduced NK cell numbers, a dysbalance in the activating and inhibitory NK cell receptor repertoire and a dysregulation of the cytotoxic machinery can suppress NK cell function. Moreover, shedding of ligands binding to the activating receptor NKG2D has been reported to down-regulate receptor expression due to chronic ligand engagement (140, 141). Down-regulation of the NKG2D receptor can also be induced by cytokines such as TGF-β derived from tumours (139).

Unexpectedly, despite the reduction of $CD16^{+}CD56^{+}$ NK cells in the circulation of melanoma patients, these cells still displayed a conserved phenotype and function. The expression levels of the NKG2D receptor and the frequency of NKG2D expressing NK cells were comparable for melanoma patients and healthy controls, though the soluble forms of the NKG2D ligands MICA and ULBP2 were elevated in sera of melanoma patients (292). A study by Groh *et al*. suggested that upon prolonged interaction with soluble NKG2D ligands in the sera of cancer patients, the NKG2D receptor was down-regulated on NK and T cells by endocytosis and subsequent degradation (140). In contrast, a down-regulation of the NKG2D receptor was not observed although high concentration of soluble MICA was detected in sera from patients with rheumatoid arthritis (293). Besides, a normal expression of the NKG2D receptor by NK cells has also been reported by Cai *et al.* in hepatocellular carcinoma patients (294), suggesting differential regulation of this receptor in distinct malignancies. On the other hand, defective NK cell function has been associated with aberrant NCR family but not NKG2D receptor expression in acute leukemia (291). NK cells from melanoma patients that were analysed in this study showed an increased expression of the NCR receptors NKp30 and NKp46. Furthermore NKp30 and NKp46 positive NK cells were present at a higher frequency in the peripheral blood from melanoma patients than from controls. In contrast, comparable expression of NKp30 and NKp46 by NK cells from patients and healthy donors were observed in case of metastatic renal cell carcinoma (294). Interestingly, an increased NKp30 and NKp46 expression by NK cells was reported in patients infected with HCV (295). This suggests that the expression profile of NK cell activating receptors is differentially regulated in distinct malignancies and other pathological situations.

Furthermore, the secretory cytolytic machinery of NK cells from melanoma patients was found to be intact since the frequency of perforin expressing NK cells, the ability to degranulate and to secrete IFN-γ by NK cells from melanoma patients were comparable to healthy controls. In agreement, NK cells from metastatic renal cell carcinoma patients display killing activity similar to those from healthy subjects (294). It is tempting to

speculate that an increased NKp30 and NKp46 expression and frequency of $NKp30^+$ and $NKp46^+$ NK cells may play a role in conferring conserved NK cell killing activity although there is decreased NK cell numbers in melanoma patients. In fact, NK cells from patients infected with HCV exhibit increased NKp30 expression and this is accompanied by a conserved cytotoxic activity against all tested targets except hepatoma cells (295). NK cells can also mediate killing through non-secretory mechanisms via the Fas/Fas ligand pathway (131). It remains to be determined if this type of killing is intact in NK cells from melanoma patients.

The present study also demonstrated that in co-cultures of mDC1 and IL-2 activated NK cells, the NK cells purified from melanoma patients induced mDC1 maturation, measured as CD40 up-regulation, similarly to NK cells from normal subjects. This supports the notion that peripheral blood NK cells from melanoma patients possess intact functional properties. However, we could not exclude the possibility that tumour infiltrating NK cells might have different properties compared to blood NK cells, since the tumour microenviroment consists of different immunoregulatory factors with strong suppressive activities.

5.6 Involvement of MyD88, IRF7 and p4E-BP1 in aberrant IFN-α production by pDCs from melanoma patients

A number of factors including the relatively low numbers of pDCs in blood have precluded careful analysis on aberrant functionality of this DC subset in cancer patients. In this study, by using pDCs purified from leukapherasis products of patients, we revealed that TLR9 triggering by CpG A induced a higher IFN-α secretion by pDCs from healthy donors than from patients. Consistently, non-fractionated PBMCs from patients also displayed a marked reduction in IFN-α production after CpG A stimulation in comparison to PBMCs from healthy subjects. Alhough evidence concerning alterations in the IFN-α production by pDCs in several malignancies is rising, the exact mechanism and molecules involved in this process still remain unclear. One explanation for the aberrant function of pDCs could be a dysregulated BDCA2 expression. BDCA2 is a negative regulator of IFN-α signaling and ligation of the BDCA2 receptors inhibits TLR9

induced type I IFN, TNF and IL-6 production (296). In this study, however, investigations on the basal expression of BDCA2 by pDCs from healthy controls and patients revealed no significant differences. Thus, it is unlikely that BDCA2 contributes to the aberrant IFN-α production by pDCs from stage IV melanoma patients. Besides, it is known that BDCA2 is down-regulated when pDCs encounter a maturation signal (245). Interestingly, the reduction in BDCA2 levels on CpG A activated pDCs was greater for pDCs from controls than from melanoma patients, suggesting that the pDCs from patients are somehow defective in their response to CpG A. In addition to BDCA2, the BDCA4 molecule is also involved in the negative regulation of IFN-α production by pDCs. Cross-linking of the BDCA4 receptor on pDCs with magnetic beads has been shown to abrogate IFN-α production (297). However, it is unlikely that BDCA4 down-regulation is responsible for the aberrant IFN-α production by pDCs observed in this study, since pDC purification was performed similarly on cells from patients and controls. This is also supported by a marked reduction in IFN-α production by non-fractionated PBMCs from the patients after CpG A stimulation.

Several signalling pathways are activated in pDCs following TLR9 ligation by CpG A. A major pathway is the TLR9-MyD88-IRF7 signalling cascade that leads to massive IFN-α production by pDCs. Thus, the decreased responsiveness of pDCs to TLR9 stimulation might be related to the TLR9 expression level. Mouse pDCs that lack TLR9 completely lose their ability to produce type I IFN. In particular, tumour-derived factors from patients with HNSCC have been shown to down-regulate intracellular TLR9 expression (298). However, the present analysis revealed similar intracellular TLR9 expression levels in pDCs from melanoma patients and healthy individuals.

Besides TLR9, the aberrant IFN-α secretion by pDCs from patients might be due to defects in the downstream signaling. It has been shown that expression of MyD88 and its recruitment are important for forming signalling complexes with IRAK4 and TRAF6, which in turn are crucial for IRF7 activation (182-185). In murine pDCs deficient of MyD88, type I IFN release upon TLR7/9 ligand stimulation is abolished (182, 186). In this study, TLR9 triggering did not lead to an up-regulation of MyD88 in pDCs from

patients compared to healthy donors, implicating a defect in down-stream signaling for IFN-α production.

In support of this finding, further analysis revealed that CpG A stimulation of PBMCs from patients only slightly up-regulated the mRNA levels of IRF7, the master regulator of IFN-α production. Unlike other immune effector cells, pDCs constitutively express the IRF7 protein and this is partially related to the rapid release of IFN-α by these cells. Upon the stimulation of pDCs with CpG A, it has been shown that the activation of TLR9 signalling leads to a strong transcriptional activation of the IRF7 gene, which is crucial for a high IFN-α production by pDCs (299). Besides, only small changes in IRF7 expression can substantially affect IFN-α production by pDCs (299). With respect to this, the present study suggests that pDCs from melanoma patients were only partially activated by CpG A. Although comparable basal IRF7 protein levels were detected by flow cytometry in gated pDCs from patients and controls, IRF7 up-regulation after TLR9 ligation was significantly lower in patients.

Recently, it has been demonstrated that the expression of IRF7 is also regulated at the level of translation. Colina *et al.* demonstrated that IRF7 mRNA translation is under control of the translational repressor 4E-BP1 (195). The phosphorylation of 4E-BP1 leads to the release of eIF4E and the formation of the eIF4F complex that allows the initiation of eukaryotic cap-dependent mRNA translation to take place. A low p4E-BP1 (Ser65/Thr70) level was detected in pDCs and PBMCs from melanoma patients compared to healthy donors within this study, suggesting that an impaired translation of IRF7 mRNA might contribute to the absense of IRF7 protein up-regulation, despite an increase in IRF7 mRNA. A clear association of nearly constant IRF7 and p4E-BP1 protein levels after CpG A stimulation of PBMCs from patients indicates that the release of eIF4E may inhibited by 4E-BP1, which prevents the increase in translation of IRF7 mRNA. Consistently, Colina *et al.* demonstrated that a deletion of 4E-BP1 and 4E-BP2 in mice enhances the level of IFN-α production in comparison to the corresponding controls (195). The current study can not directly rule out if there is alteration on the total 4E-BP1 protein that may affect the translation efficiency due to limited samples. However, this is

most unlikely the case since there is no significant difference on the basal IRF7 expression between patients and healthy donors. It is reasonable that a deficient IRF7 mRNA translation could affect the IRF7 protein pool, which is essentially required for a robust IFN-α secretion upon TLR9 activation.

IRF7 up-regulation can also occur in response to IFN-α production in an autocrine manner by binding to the IFNAR. Triggering of the IFNAR elicits ISGF3 signalling thereby sustaining IRF7 expression after TLR9 activation (207-209). Since in this study TLR9 stimulation was performed for only 6 hrs, the up-regulation of IRF7 is unlikely to be an effect of autocrine IFN-α signalling because this process needs approximately 10-12 h (300). Besides, we detected similar up-regulation of IRF7 mRNA levels in PBMCs from patients and healthy controls after exogenous IFN-α treatment. The exogenous IFN-α stimulation can activate not only pDCs but also other non-pDCs cells in PBMCs to up-regulate IRF7 expression through the ISGF3 pathway. However, a marked up-regulation of IRF7 mRNA in parallel to increased IRF7 protein levels detected in PBMC gated pDCs from melanoma patients indicates an intact ISGF3 signalling in pDCs from melanoma patients.

Importantly, regulation of type I IFN production upon TLR9 engagement is crucially governed by the translocation of phosphorylated IRF7 to the nucleus. The defective MyD88-IRAK-TRAF complex assembly and their recruitment could contribute to the impairment of IRF7 activation, which is essential for subsequent translocation to the nucleus (301). Confocal microscopy analysis performed within this study demonstrated a lower IRF7 translocation rate in pDCs from melanoma patients than from controls. This impairment likely accounts for the reduced IFN-α production by pDCs from melanoma patients. Moreover, the reduced nuclear translocation of IRF7 detected in cord blood pDCs versus adult pDCs leads to an aberrant IFN-α production, which further supports our finding (302). Besides, the impairment of IRF7 in pDCs from melanoma patients that we observed in our study is unlikely due to prior treatment since a similar defect was observed among all patients included in this analysis. This is further supported by a recent study that has demonstrated an impairment of IFN signalling in lymphocytes from

breast cancer patients was not affected by chemotherapy as similar defect was equally observed in patients received treatment and patients received no treatment (303).

Taken together, these findings underline the impairment of TLR9 signalling accounts for aberrant IFN-α production by pDCs from melanoma patients. Reduced up-regulation of IRF7 mRNA and translation in parallel with an impairment of its nuclear translocation are likely explainations for the alteration of IFN-α release by pDCs from melanoma patients.

6.0 Conclusion

In the present work, we have identified an immune defect in pDCs from stage IV melanoma patients. We have demonstrated that the absolute number of pDCs, mDC2 and $CD16^+CD56^+$ NK cells in the peripheral blood of melanoma patients is reduced. However, functional impairments were observed in pDCs but not NK cells from melanoma patients. The reduced pDC number in melanoma patients is accompanied by a trend of impairment in activating mDC1 during mDC1/pDC interaction upon CpG A stimulation. In addition, pDCs also displayed a defective function in producing pro-inflammatory cytokines and chemokines including IFN-α, CCL5, CCL3 and CCL4. We have further shown that the aberrant function of pDCs in advanced stage melanoma patients was due to an impairment of TLR9 signalling. This defect was further related to a reduced up-regulation of IRF7 mRNA and translation in parallel with an impairment of its nuclear translocation in pDCs from melanoma patients.

In conclusion, our findings provide evidences that pDCs from stage IV melanoma patients display functional defects involving an impairment of TLR9 signalling. These findings represent an important insight into immune dysfunctions in cancer patients. Further analysis on designing strategies to correct this dysfunction may enhance the success of cancer immunotherapeutic strategies.

Reference

1. Hentsche P. (2004). Antitumour effect in solid tumours, tolerance and immune reconstitution after allogeneic haemtopoietic stem cell transplatation.. Thesis. Karolinska University Press.

2. Norell H. (2006). Immunological recognition and tumor escape mechanisms of ovarian carcinoma hesis. Thesis Karolinska University Press.

3. Buzaid AC; Ross MI; Balch CM; Soong S; McCarthy WH; Tinoco L; Mansfield P; Lee JE; Bedikian A; Eton O; Plager C; Papadopoulos N; Legha SS; Benjamin RS. (1997). Critical analysis of the current American Joint Committee on Cancer staging system for cutaneous melanoma and proposal of a new staging system. *J Clin Oncol* 15(3):1039-51.

4. Rigel DS, Carucci JA. (2000). Malignant melanoma: prevention, early detection and treatment in the 21st century. *CA Cancer J Clin* 50:215–30.

5. Davies H, Bignell GR, Cox C, Stephens P, Edkins S, Clegg S, Teague J, Woffendin H, Garnett MJ, Bottomley W, Davis N, Dicks E, Ewing R, Floyd Y, Gray K, Hall S, Hawes R, Hughes J, Kosmidou V, Menzies A, Mould C, Parker A, Stevens C, Watt S, Hooper S, Wilson R, Jayatilake H, Gusterson BA, Cooper C, Shipley J, Hargrave D, Pritchard-Jones K, Maitland N, Chenevix-Trench G, Riggins GJ, Bigner DD, Palmieri G, Cossu A, Flanagan A, Nicholson A, Ho JW, Leung SY, Yuen ST, Weber BL, Seigler HF, Darrow TL, Paterson H, Marais R, Marshall CJ, Wooster R, Stratton MR, Futreal PA. (2002). Mutations of the BRAF gene in human cancer. *Nature* 417: 949–954.

6. Tsao H, Zhang X, Fowlkes K, Haluska FG. (2000). Relative reciprocity of NRAS and PTEN/MMAC1 alterations in cutaneous melanoma cell lines. *Cancer Res* 60:1800–4

7. Guldberg P, thor Straten P, Birck A, Ahrenkiel V, Kirkin AF, Zeuthen J. (1997). Disruption of the MMAC1/PTEN gene by deletion or mutation is a frequent event in malignant melanoma. *Cancer Res* **57**: 3660–3663

8. Stahl JM, Cheung M, Sharma A, Trivedi NR, Shanmugam S, Robertson GP. (2003). Loss of PTEN promotes tumor development in malignant melanoma *Cancer Res* **63**: 2881–2890.

9. Bajetta E, Del Vecchio M, Bernard-Marty C, Vitali M, Buzzoni R, Rixe O, Nova P, Aglione S, Taillibert S, Khayat D. (2002). Metastatic melanoma: chemotherapy. *Semin Oncol* 29:427–445.

10. Al-Sarraf M, Fletcher W, Oishi N, Pugh R, Hewlett JS, Balducci L, McCracken J, Padilla F. (1982). Cisplatin hydration with and without mannitol diuresis in refractory disseminated malignant melanoma: a southwest oncology group study. *Cancer Treat Rep*, 66:31–35.

11. Glover D, Glick JH, Weiler C, Fox K, Guerry D. (1987). WR-2721 and high-dose cisplatin: an active combination in the treatment of metastatic melanoma. *J Clin Oncol* 5:574–578.

12. Middleton MR, Grob JJ, Aaronson N, Fierlbeck G, Tilgen W, Seiter S, Gore M, Aamdal S, Cebon J, Coates A, Dreno B, Henz M, Schadendorf D, Kapp A, Weiss J, Fraass U, Statkevich P, Muller M, Thatcher N.(2000). Randomized phase III study of temozolomide versus dacarbazine in the treatment of patients with advanced metastatic malignant melanoma. *J Clin Oncol* 18:158.

13. Lattanzi SC, Tosteson T, Chertoff J, Maurer LH, O'Donnell J, LeMarbre PJ, Mott L, DelPrete SA, Forcier RJ, Ernstoff MS. (1995). Dacarbazine, cisplatin and carmustine, with or without tamoxifen, for metastatic melanoma: 5-year follow-up. *Melanom Res* 5:365–369.

14. Hwu WJ, Krown SE, Menell JH, Panageas KS, Merrell J, Lamb LA, Williams LJ, Quinn CJ, Foster T, Chapman PB, Livingston PO, Wolchok JD, Houghton AN. (2003). Phase II study of temozolomide plus thalidomide for the treatment of metastatic melanoma. *J Clin Oncol* 21:3351–3356.

15. Hauschild A, Garbe C, Stolz W, Ellwanger U, Seiter S, Dummer R, Ugurel S, Sebastian G, Nashan D, Linse R, Achtelik W, Mohr P, Kaufmann R, Fey M, Ulrich J, Tilgen W. (2001). Dacarbazine and interferon-α with or without interleukin 2 in metastatic melanoma: a randomized phase III multicentre trial of the Dermatologic Cooperative Oncology Group (DeCOG) *Br J Cancer*. 84(8):1036-42

16. Ollila DW, Hsueh EC, Stern SL, Morton DL. (1999): Metastasectomy for recurrent stage IV melanoma. *J Surg Oncol* 71:209–213.

17. Hyunh NT, Veness MJ. Radiotherapy for Lentigo Maligna. (2002). *Arch Derm* 138:581-586.

18. Lavine SD, Petrovich Z, Cohen-Gadol AA, Masri LS, Morton DL, O'Day SJ, Essner R, Zelman V, Yu C, Luxton G, Apuzzo ML. (1999). Gamma knife radiosurgery for metastatic melanoma: an analysis of survival, outcome, and complications. *Neurosurgery* 44:59–64.

19. Kirkwood J. (2002). Cancer immunotherapy: The interferon-alpha experience. *Semin Oncol* 29:18-26.

20. Legha SS. (1997). The role of IFN-α in the treatment of metastatic melanoma. *Semin Onco l*24:24–31.

21. Kirkwood JM, Strawderman MH, Ernstoff MS, Smith TJ, Borden EC, Blum RH. (1996). Interferon alfa-2b adjuvant therapy of high-risk resected cutaneous melanoma: The Eastern Cooperative Oncology Group Trial EST 1684. *J Clin Oncol* 14:7-17.

22. Atkins MB, Kunkel L, Sznol M, Rosenberg SA. (2000). High-dose recombinant interleukin-2 therapy in patients with metastatic melanoma: Long-term survival update. *Cancer J Sci Am* 6:S11-S14.

23. O'Rourke MG, Johnson M, Lanagan C, See J, Yang J, Bell JR, Slater GJ, Kerr BM, Crowe B, Purdie DM, Elliott SL, Ellem KA and Schmidt CW. (2003). Durable complete clinical responses in a phase I/II trial using an autologous melanoma cell/dendritic cell vaccine. *Cancer Immunol Immunother* 52: 387-95.

24. Panelli MC, Wunderlich J, Jeffries J, Wang E, Mixon A, Rosenberg SA and Marincola FM. (2000). Phase 1 study in patients with metastatic melanoma of immunization with dendritic cells presenting epitopes derived from the melanoma-associated antigens MART-1 and gp100. *J Immunother* 23: 487-98.

25. Phan GQ, Yang JC, Sherry RM, Hwu P, Topalian SL, Schwartzentruber DJ, Restifo NP, Haworth LR, Seipp CA, Freezer LJ, Morton KE, Mavroukakis SA, Duray PH, Steinberg SM, Allison JP, Davis TA, Rosenberg SA. (2003). Cancer regression and autoimmunity induced by cytotoxic T lymphocyte-associated antigen 4 blockade in patients with metastatic melanoma. *Proc. Natl. Acad. Sci. USA* 100(14): 8372–8377.

26. Weber JS. (2006). The clinical utility of cytotoxic T lymphocyte antigen 4 abrogation by human antibodies. *Melanoma Res*.16(5):379-83

27. Rosenberg SA, Dudley ME. (2004). Cancer regression in patients with metastatic melanoma after the transfer of autologous antitumour lymphocytes. *Proc Natl Acad Sci USA*. 101 (suppl 2): 14639-14645.

28. Nathan, C. (2006). Neutrophils and immunity: challenges and opportunities. *Nat. Rev. Immunol.* 6173-182.

29. Cassatella MA, Meda L, Gasperini S, D'Andrea A, Ma X, Trinchieri G. (1995). Interleukin-12 production by human polymorphonuclear leukocytes. *Eur J Immunol* 25:1-5

30. Benjamini E, Coico R, and Sunshine G. Immunology: A short course. 4th Edition. New York: A John Wiley & Sons, INC; 2000

31. Pier GB, Lyczak JB, Wetzler LM. (2004). *Immunology, Infection, and Immunity*. ASM Press.

32. Steinman RM, Cohn ZA. (1973). Identification of a novel cell type in peripheral lymphoid organs of mice. I. Morphology, quantitation, tissue distribution. *J Exp Med* 137:1142-1162.

33. Banchereau J, Brier F, Caus C, Davoust J, Lebecque S, Liu YJ, Pulendran B and Palucka K. (2000). Immunobiology of dendritic cells. *Annu. Rev. Immunol* 18: 767-811.

34. Lotze MT and Thomson AW. Dendritic cells. 2nd Edition. London: Academic Press; 2001

35. Ardavin C. (2003). Origin, precursors and differentiation of mouse dendritic cells. *Nat Rev Immunol* 3: 582-90.

36. Grouard G., Rissoan M.-C, Filgueira L, Durand I, Banchereau J, Liu Y-J. (1997). The enigmatic plasmacytoid T cells develop into dendritic cells with IL-3 and CD40-ligand. *J. Exp. Med* 185:1101-1111.

37. Fitzgerald-Bocarsly P, Dai JH and Singh S. (2008). Plasmacytoid dendritic cells and type I IFN: 50 of convergent history. *Cytokine & Growth Factors Reveiws* 19: 3-19.

38. Chicha L, Jarrossay D, Manz MG. (2004). Clonal type I interferon-producing and dendritic cell precursors are contained in both human lymphoid and myeloid progenitor populations. *J. Exp. Med* 200: 1519-24.

39. van Kooyk Y, Geijtenbeek TB. (2002). DC-SIGN: escape mechanism for pathogens. *Nat Rev Immunol* 3(9):697-709.

40. Keir ME, Sharpe AH. (2005). The B7/CD28 costimulatory family in autoimmunity. *Immunol. Rev* 204: 128–143.

41. Haenssle H, Buhl T, Knudsen S, Krueger U, Rosenberger A, Reich K, Neumann C. (2008). CD40 ligation during dendritic cell maturation reduces cell death and prevents interleukin-10-induced regression to macrophage-like monocytes. *Exp Dermatol* 7(3):177-87.

42. Steinman RM and Nussenzweig MC. (2002). Avoiding horror autotoxicus: the importance of dendritic cells in peripheral T cell tolerance. *Proc. Natl Acad. Sci. USA* 99: 351–358.

43. Steinman RM, Hawiger D, Nussenzweig MC. (2003). Tolerogenic dendritic cells. *Annu. Rev. Immunol* 21: 685–711.

44. Albert M.L, Jegathesan M, Darnell RB (2001). Dendritic cell maturation is required for the cross-tolerization of $CD8^+$ T cells. *Nature Immuno* 2: 1010–1017.

45. Menges M, Rössner S, Voigtländer C, Schindler H, Kukutsch NA, Bogdan C, Erb K, Schuler G, Lutz MB. (2002). Repetitive injections of dendritic cells matured with tumor necrosis factor-α induce antigen-specific protection of mice from autoimmunity. *J. Exp. Med* 195: 15–21.

46. Dzionek A, Fuchs A, Schmidt P, Cremer S, Zysk M, Miltenyi S, Buck DW, Schmitz J. (2000). BDCA-2, BDCA-3, and BDCA-4: three markers for distinct subsets of dendritic cells in human peripheral blood. *J Immuno.* 165(11):6037-4.

47. Kim R, Emi M, Tanabe K, Arihiro K. (2007). Potential functional role of plasmacytoid dendritic cells in cancer immunity. *Immunology* 121(2):149-57.

48. Piccioli D, Tavarini S, Borgogni E, Steri V, Nuti S, Sammicheli C, Bardelli M, Montagna D, Locatelli F, Wack A.(2007). Functional specialization of human circulating CD16 and CD1c myeloid dendritic-cell subsets. *Blood* 109:5371-9.

49. Ito T, Inaba M, Inaba K, Toki J, Sogo S, Iguchi T, Adachi Y, Yamaguchi K, Amakawa R, Valladeau J, Saeland S, Fukuhara S, Ikehara S. (1999). A $CD1a^+/CD11c^+$ subset of human blood dendritic cells is a direct precursor of Langerhans cells. *J. Immunol.* 163:1409-19.

50. Lindstedt M, Lundberg K, Borreckbaeck CA. (2005). Gene family clustering identifies functionally associated subsets of human in vivo blood and tonsillar dendritic cells. *J Immunol* 175: 4839 – 4846.

51. Cavanagh LL, Saal RJ, Grimmett KL and Thomas R. (1998). Proliferation of monocyte-derived dendritic cells cultures is caused by progenenitor cells capable of myeloid differentiation. *Blood* 92: 1598 – 1607.

52. Mailliard RB, Wankowicz-Kalinska A, Cai Q, Wesa A, Hilkens CM, Kapsenberg ML, Kirkwood JM, Storkus WJ, Kalinski P. (2004). Alpha-type-1 polarized dendritic cells: a novel immunization tool with optimized CTL-inducing activity. *Cancer Res* 64(17):5934-7.

53. Dubsky P, Saito H, Leogier M, Dantin C, Connolly JE, Banchereau J, Palucka AK.(2007). IL-15-induced human DC efficiently prime melanoma-specific naive CD8+ T cells to differentiate into CTL. *Eur J Immunol*. 37(6):1678-90

54. Fernandez NC, Lozier A, Flament C, Ricciardi-Castagnoli P, Bellet D, Suter M, Perricaudet M, Tursz T, Maraskovsky E, Zitvogel L. (1999). Dendritic cells directly trigger NK cell functions: cross-talk relevant in innate anti-tumor immune responses in vivo. *Nat Med.* 5(4):405-11.

55. Degli-Esposti MA, Smyth MJ. (2005). Close encounters of different kinds: dendritic cells and NK cells take centre stage. *Nat Rev Immunol*. 5(2):112-24

56. Ferlazzo G, Tsang ML, Moretta L, Melioli G, Steinman RM, Münz C. (2002). Human dendritic cells activate resting natural killer (NK) cells and are recognized via the NKp30 receptor by activated NK cells. *J. Exp. Med.* 195, 343–351.

57. Facchetti F, Vergoni F. (2000). The plasmacytoid monocyte: from morphology to function. *Advances in Clinical Pathology: the Official Journal of Adriatic Society of Pathology* 4 : 187

58. Dzionek A, Sohma Y, Nagafune J, Cella M, Colonna M, Facchetti F, Günther G, Johnston I, Lanzavecchia A, Nagasaka T, Okada T, Vermi W, Winkels G, Yamamoto T, Zysk M, Yamaguchi Y, Schmitz J. (2001). BDCA-2, a novel plasmacytoid dendritic cell-specific type II C-type lectin, mediates antigen capture and is a potent inhibitor of interferon alpha/beta induction. *J Exp Med* 194:1823–1834.

59. Penna G, Vulcano M, Sozzani S, Adorini L. (2002). Differential migration behavior and chemokine production by myeloid and plasmacytoid dendritic cells. *Hum. Immunol* 63(12):1164-71.

60. Siegal FP, Kadowaki N, Shodell M, Fitzgerald-Bocarsly PA, Shah K, Ho S, Antonenko S, Liu YJ.(1999). The nature of the principal type 1 interferon-producing cells in human blood [see comment]. *Science* 284:1835-7.

61. Decalf J, Fernandes S, Longman R, Ahloulay M, Audat F, Lefrerre F, Rice CM, Pol S, Albert ML. (2007). Plasmacytoid dendritic cells initiate a complex chemokine and cytokine network and are a viable drug target in chronic HCV patients. *J. Exp. Med*. 204(10):2423-37.

62. Chuang TH, Lee J, Kline L, Mathison JC, Ulevitch RJ. (2002). Toll-like receptor 9 mediates CpG-DNA signaling. *J. Leukocyte Biol* 71:538 – 44.

63. Gilliet M, Liu YJ. (2002). Generation of human $CD8^+$T regulatory cells by CD40 ligand-activated plasmacytoid dendritic cells. *J. Exp. Med* 195:695-704.

64. Ito T, Yang M, Wang YH, Lande R, Gregorio J, Perng OA, Qin XF, Liu YJ, Gilliet M. (2007). Plasmacytoid dendritic cells prime IL-10-producing T regulatory cells by inducible costimulator ligand. *J. Exp. Med* 204:105-115.

65. Kawamura K, Kadowaki N, Kitawaki T, Uchiyama T. (2006). Virus-stimulated plasmacytoid dendritic cells induce CD4+ cytotoxic regulatory T cells. *Blood* 107:1031-1038.

66. Manches O, Munn D, Fallahi A, Lifson J, Chaperot L, Plumas J, Bhardwaj N.J Clin Invest. (2008). HIV-activated human plasmacytoid DCs induce Tregs through an indoleamine 2,3-dioxygenase–dependent mechanism. *J Clin Invest.* 118(10):3431-9.

67. Moseman EA, Liang X, Dawson AJ, Panoskaltsis-Mortari A, Krieg AM, Liu YJ, Blazar BR, Chen W. (2004). Human plasmacytoid dendritic cells activated by CpG oligodeox1ynucleotides induce the generation of CD4+CD25+ regulatory T cells. J Immunol. 173(7):4433-42.

68. Palmer P, Charley B, Rombaut B, Daeron M, Lebon P. (2000). Antibody-dependent induction of type 1 interferons by poliovirus in mononuclear blood cells requires the type II Fcγ receptor (CD32). *Virol* 278: 86–94.

69. Feldman SB, Ferraro M, Zheng HM, Patel N, Gould-Fogerite S, Fitzgerald-Bocarsly P. (1994). Viral induction of low frequency interferon-alpha producing cells. *Virology* 204: 1–7.

70. Wang JP, Asher DR, Chan M, Kurt-Jones EA, Finberg RW. (2007). Cutting edge: antibody-mediated TLR7-dependent recognition of viral RNA. *J Immunol* 178: 3363–3367.

71. Gerosa F, Gobbi A, Zorzi P, Burg S, Briere F, Carra G, Trinchieri G. (2005). The reciprocal interaction of NK cells with plasmacytoid or myeloid dendritic cells profoundly affects innate resistance functions. *J. Immunol* 174: 727–734.

72. Vanbervliet B, Bendriss-Vermare N, Massacrier C, Homey B, de Bouteiller O, Brière F, Trinchieri G, Caux C. (2003). The inducible CXCR3 ligands control plasmacytoid dendritic cell responsiveness to the constitutive chemokine stromal cell-derived factor 1 (SDF-1)/CXCL12. *J Exp Med* 198: 823–830.

73. Fonteneau JF, Larsson M, Beignon AS, McKenna K, Dasilva I, Amara A, Liu YJ, Lifson JD, Littman DR, Bhardwaj N. (2004). Human immunodeficiency virus type 1 activates plasmacytoid dendritic cells and concomitantly induces the bystander maturation of myeloid dendritic cells. *J. Virol* 78: 5223–5232.

74. Mailliard RB, son YI, Redlinger R, Coates PT, Giermasz A, Morel PA, Storkus WJ, Kalinski P. (2003). Dendritic cells mediate NK cell help for Th1 and CTL responses: two signal requirements for the induction of NK cell helper function. *J Imnunol.* 171(5):2366-73.

75. Yoneyama H, Matsuno K, Toda E, Nishiwaki T, Matsuo N, Nakano A, Narumi S, Lu B, Gerard C, Ishikawa S, Matsushima K. (2005). Plasmacytoid DCs help lymph node DCs to induce anti-HSV CTLs. *J. Exp. Med* 202: 425–435.

76. Piccioli D, Sammicheli C, Tavarini S, Nuti S, Frigimelica E, Manetti AG, Nuccitelli A, Aprea S, Valentini S, Borgogni E, Wack A, Valiante NM. (2009). Human plasmacytoid dendritic cells are unresponsive to bacterial stimulation and require a novel type of cooperation with myeloid dendritic cells for maturation. *Blood* 113:4232-9.

77. Le Bon A, Etchart N, Rossmann C, Ashton M, Hou S, Gewert D, Borrow P, Tough DF. (2003). Cross-priming of $CD8^+$ T cells stimulated by virus-induced type I interferon. *Nature Immunol* 4: 1009–1015.

78. Kolumam G A, Thomas S, Thompson LJ, Sprent J, Murali-Krishna K. (2005). Type I interferons act directly on CD8 T cells to allow clonal expansion and memory formation in response to viral infection. *J. Exp. Med* 202: 637–650.

79. Hibbert L, Pflanz S, De Waal Malefyt R, Kastelein RA. (2003). IL-27 and IFN-α signal via Stat1 and Stat3 and induce T-Bet and IL12R-β2 in naive T cells. *J. Interferon Cytokine Res* 23: 513–522.

80. Hoeffel G, Ripoche AC, Matheoud D, Nascimbeni M, Escriou N, Lebon P, Heshmati F, Guillet JG, Gannagé M, Caillat-Zucman S, Casartelli N, Schwartz O, De la Salle H, Hanau D, Hosmalin A, Marañón C. (2007). Antigen crosspresentation by human plasmacytoid dendritic cells. *Immunity*: 481-92.

81. Jego G, Palucka AK, Blanck JP, Chalouni C, Pascual V, Banchereau J. (2003). Plasmacytoid dendritic cells induce plasma cell differentiation through type I interferon and interleukin 6. *Immunity* 19: 225–234.

82. Proietti E, Bracci L, Puzelli S, Di Pucchio T, Sestili P, De Vincenzi E, Venditti M, Capone I, Seif I, De Maeyer E, Tough D, Donatelli I, Belardelli F. (2002). Type I IFN as a natural adjuvant for a protective immune response: lessons from the influenza vaccine model. *J Immunol* 169: 375–383.

83. Almand B, Resser JR, Lindman B, Nadaf S, Clark JI, Kwon ED, Carbone DP, Gabrilovich DI. (2000). Clinical significance of defective dendritic cell differentiation in cancer, *Clin Cancer Res* 6: 1755–1766.

84. Lissoni P, Vigore L, Ferranti R, Bukovec R, Meregalli S, Mandala M, Barni S, Tancini G, Fumagalli L, Giani L. (1999). Circulating dendritic cells in early and advanced cancer patients: diminished percent in the metastatic disease. *J Biol Regul Homeost Agents* 13: 216–219.

85. Della Porta M, Danova M, Rigolin GM, Brugnatelli S, Rovati B, Tronconi C, Fraulini C, Russo Rossi A, Riccardi A, Castoldi G. (2005). Dendritic cells and vascular endothelial growth factor in colorectal cancer: correlations with clinicobiological findings. *Oncology* 68:276–284.

86. Bellone G, Carbone A, Smirne C, Scirelli T, Buffolino A, Novarino A, Stacchini A, Bertetto O, Palestro G, Sorio C, Scarpa A, Emanuelli G, Rodeck U. (2006). Cooperative

induction of a tolerogenic dendritic cell phenotype by cytokines secreted by pancreatic carcinoma cells. *J Immunol* 177:3448–3460.

87. Hasebe H, Nagayama H, Sato K, Enomoto M, Takeda Y, Takahashi TA, Hasumi K, Eriguchi M. (2000). Dysfunctional regulation of the development of monocyte-derived dendritic cells in cancer patients. *Biomed Pharmacother* 54:291–298.

88. Orsini E, Guarini A, Chiaretti S, Mauro FR, Foa R.(2003).The circulating dendritic cell compartment in patients with chronic lymphocytic leukemia is severely defective and unable to stimulate an effective T-cell response. *Cancer Res* 63 (15):4497-506

89. Bell D, Chomarat P, Broyles D, Netto G, Harb GM, Lebecque S, Valladeau J, Davoust J, Palucka KA, Banchereau J. (1999). In breast carcinoma tissue, immature dendritic cells reside within the tumor, whereas mature dendritic cells are located in peritumoral areas, *J.Exp.Med.* 190(10):1417-26.

90. Ishida T, Oyama T, Carbone DP, Gabrilovich DI. (1998). Defective function of Langerhans cells in tumor-bearing animals is the result of defective maturation from hematopoietic progenitors. *J Immunol* 161: 4842–4851.

91. Gabrilovich D, Ishida T, Oyama T, Ran S, Kravtsov V, Nadaf S, Carbone DP. (1998). Vascular endothelial growth factor inhibits the development of dendritic cells and dramatically affects the differentiation of multiple hematopoietic lineages in vivo. *Blood* 92:4150–4166.

92. Gabrilovich DI, Ishida T, Nadaf S, Ohm JE, Carbone DP. (1999). Antibodies to vascular endothelial growth factor enhance the efficacy of cancer immunotherapy by improving endogenous dendritic cell function. *Clin Cancer Res* 5: 2963–2970.

93. Aspord C, Pedroza-Gonzalez A, Gallegos M, Tindle S, Burton EC, Su D, Marches F, Banchereau J, Palucka AK. (2007). Breast cancer instructs dendritic cells to prime interleukin 13-secreting CD4+ T cells that facilitate tumor development. *J Exp Med*. 204(5):1037-47.

94. DeNardo DG, Barreto JB, Andreu P, Vasquez L, Tawfik D, Kolhatkar N, Coussens LM. (2009). CD4(+) T cells regulate pulmonary metastasis of mammary carcinomas by enhancing protumor properties of macrophages. *Cancer Cell* 16: 91–102.

95. Berzofsky JA, Terabe MA. (2008). Novel immunoregulatory axis of NKT cell subsets regulating tumor immunity. *Cancer Immunol Immunother* 57:1679–1683.

96. Kukreja A, Hutchinson A, Dhodapkar K, Mazumder A, Vesole D, Angitapalli R, Jagannath S, Dhodapkar MV. (2006). Enhancement of clonogenicity of human multiple myeloma by dendritic cells. *J. Exp. Med* 203:1859–1865.

97. Bahlis NJ, King AM, Kolonias D, Carlson LM, Liu HY, Hussein MA, Terebelo HR, Byrne GE Jr, Levine BL, Boise LH, Lee KP. (2007). CD28-mediated regulation of multiple myeloma cell proliferation and survival. *Blood* 109:5002–5010.

98. Liu Y, Bi X, Xu S, Xiang J. (2005). Tumor-Infiltrating Dendritic Cell Subsets of Progressive or Regressive Tumors Induce Suppressive or Protective Immune Responses. *Cancer Res*. 65(11): 4955-62.

99. Treilleux I, Blay JY, Bendriss-Vermare N, Ray-Coquard I, Bachelot T, Guastalla JP, Bremond A, Goddard S, Pin JJ, Barthelemy-Dubois C, Lebecque S. (2004). Dendritic cell infiltration and prognosis of early stage breast cancer. *Clin Cancer Res* 10: 7466–7474.

100. Cox K, North M, burke M, Singhal H, Renton S Aqel N, Islam S, Knight SC. (2005). Plasmacytoid dendritic cells (PDC) are the major DC subset innately producing cytokines in human lymph nodes. *J Leukoc Biol* 78: 1142-1152.

101. Hartmann E, Wollenberg B, Rothenfusser S, Wagner M, Wellisch D, Mack B, Giese T, Gires O, Endres S, Hartmann G. (2003). Identification and functional analysis of tumor-infiltrating plasmacytoid dendritic cells in head and neck cancer. *Cancer Res* 63: 6478–6487.

102. Gerlini G, Urso C, Mariotti G, Di Gennaro P, Palli D, Brandani P, Salvadori A, Pimpinelli N, Reali UM, Borgognoni L. (2007). Plasmacytoid dendritic cells represent a major dendritic cell subset in sentinel lymph nodes of melanoma patients and accumulate in metastatic nodes. *Clin Immunol* 125:184-93.

103. Robertson MJ, Ritz J. (1990). Biology and clinical relevance of human natural killer cells. *Blood* 76: 2421–2438.

104. Lanier LL, Le AM, Civin CI, Loken MR, Phillips JH. (1986). The relationship of CD16 (Leu-11) and Leu-19 (NKH-1) antigen expression on human peripheral blood NK cells and cytotoxic T lymphocytes. *J. Immunol* 136: 4480–4486.

105. Leibson PJ. (1997). Signal transduction during natural-killer-cell activation: inside the mind of a killer. *Immunity* 6: 655–661.

106. Cooper MA, Fehniger TA, Turner SC, Chen KS, Ghaheri BA, Ghayur T, Carson WE, Caligiuri MA. (2001). Human natural killer cells: a unique innate immunoregulatory role for the CD56bright subset. *Blood* 97: 3146–3151.

107. Campbell JJ, Qin S, Unutmaz D, Soler D, Murphy KE, Hodge MR, Wu L, Butcher EC. (2001). Unique subpopulations of CD56+ NK and NK-T peripheral blood lymphocytes identified by chemokine receptor expression repertoire. *J. Immunol* 166: 6477–6482.

108. Ljunggren HG, Karre K. (1990). In search of the "missing self": MHC molecules and NK cell recognition. *Immunol Today* 11: 237.

109. Fauci AS, Mavilio D, Kottilil S. (2005). NK cells in HIV infection: Paradigm for protection or targets for ambush. *Nat Rev Immunol*. 5: 835-843

110. Vivier E, Tomasello E, Baratin M, Walzer T, Ugolini S. (2008). Functions of natural killer cells. *Nature Immunol* 9: 503–510.

111. Long E. (1999). Regulation of immune responses through inhibitory receptors. *Annu. Rev. Immunol.* 17: 875–904.

112. Wu J, Song Y, Bakker AB, Bauer S, Spies T, Lanier LL, Phillips JH. (1999). An activating immunoreceptor complex formed by NKG2D and DAP10. *Science* 285: 730–732.

113. Bauer S, Groh V, Wu J, Steinle A, Phillips JH, Lanier LL, Spies T (1999). Activation of NK cells and T cells by NKG2D, a receptor for stress-inducible MICA. *Science* 285: 727–729.

114. Long EO. (2002). Versatile signaling through NKG2D. *Nat Immunol* 3(12): 1119-20.

115. Groh V, Rhinehart R, Randolph-Habecker J, Topp MS, Riddell SR, Spies T. (2001). Costimulation of CD8alphabeta T cells by NKG2D via engagement by MIC induced on virus-infected cells. *Nat Immunol* 2(3): 255-60.

116. Eagle RA, Trowsdale J. (2007). Promiscuity and the single receptor: NKG2D. *Nat Rev Immunol* 7: 737–44.

117. Hayakawa Y, Smyth MJ. (2006). NKG2D and cytotoxic effector function in tumor immune surveillance. *Semin Immunol* 18:176–85.

118. Schwinn N, Vokhminova D, Sucker A, Textor S, Striegel S, Moll I, Nausch N, Tuettenberg J, Steinle A, Cerwenka A, Schadendorf D, Paschen A. (2009). Interferon-gamma down-regulates NKG2D ligand expression and impairs the NKG2D-mediated cytolysis of MHC class I-deficient melanoma by natural killer cells. *Int J Cancer*. 124(7):1594-604.

119. Conejo-Garcia JR, Benencia F, Courreges MC, Gimotty PA, Khang E, Buckanovich RJ, Frauwirth KA, Zhang L, Katsaros D, Thompson CB, Levine B, Coukos G. (2004). Ovarian carcinoma expresses the NKG2D ligand Letal and promotes the survival and expansion of CD28- antitumor T cells. *Cancer Res* 64(6): 2175-82.

120. Eisele G, Wischhusen J, Mittelbronn M, Meyermann R, Waldhauer I, Steinle A, Weller M, Friese MA. (2006). TGF-beta and metalloproteinases differentially suppress NKG2D ligand surface expression on malignant glioma cells. *Brain. Sep* 129(Pt 9): 2416-25.

121. Coudert JD, Held W. (2006). The role of the NKG2D receptor for tumor immunity. *Semin. Cancer Biol* 16: 333-43.

122. Guerra N, Tan YX, Joncker NT, Choy A, Gallardo F, Xiong N, Knoblaugh S, Cado D, Greenberg NM, Raulet DH. (2008). NKG2D-deficient mice are defective in tumor surveillance in models of spontaneous malignancy. *Immunity* 28: 571–580.

123. Raulet DH, Guerra N. (2009). Oncogenic stress sensed by the immune system: role of natural killer cell receptors. *Nat Rev Immunol* 9(8): 568-80.

124. von Lilienfeld-Toal M, Nattermann J, Feldmann G, Sievers E, Frank S, Strehl J, Schmidt-Wolf IG. (2006). Activated γδT cells express the natural cytotoxicity receptor natural killer p 44 and show cytotoxic activity against myeloma cells. *Clin. Exp. Immunol.* 144: 528–533.

125. Mandelboim O, Lieberman N, Lev M, Paul L, Arnon TI, Bushkin Y, Davis DM, Strominger JL, Yewdell JW, Porgador A. (2001). Recognition of haemagglutinins on virus-infected cells by NKp46 activates lysis by human NK cells. *Nature* 409: 1055–1060.

126. Bloushtain N, Qimron U, Bar-Ilan A, Hershkovitz O, Gazit R, Fima E, Korc M, Vlodavsky I, Bovin NV, Porgador A. (2004). Membrane-associated heparan sulfate proteoglycans are involved in the recognition of cellular targets by NKp30 and NKp46. *J. Immunol.* 173: 2392–2401.

127. Pessino A, Sivori S, Bottino C, Malaspina A, Morelli L, Moretta L, Biassoni R, Moretta A. (1998). Molecular cloning of NKp46: a novel member of the immunoglobulin superfamily involved in triggering of natural cytotoxicity. *J. Exp. Med.* 188: 953–960.

128. Sivori S, Pende D, Bottino C, Marcenaro E, Pessino A, Biassoni R, Moretta L, Moretta A. (1999).NKp46 is the major triggering receptor involved in the natural cytotoxicity of fresh or cultured human NK cells. Correlation between surface density of NKp46 and natural cytotoxicity against autologous, allogeneic or xenogeneic target cells. *Eur. J. Immunol.* 29, 1656–1666.

129. Kägi D, Ledermann B, Bürki K, Seiler P, Odermatt B, Olsen KJ, Podack ER, Zinkernagel RM, Hengartner H. (1994). Cytotoxicity mediated by T cells and natural killer cells is greatly impaired in perforin-deficient mice. *Nature* 369(6475): 31-7.

130. Bryceson YT, March ME, Ljunggren HG, Long EO. (2006). Activation, coactivation, and costimulation of resting human natural killer cells. *Immunol. Rev*. 214: 73.

131. Screpanti V, Wallin RP, Ljunggren HG, Grandien A. (2001). A central role for death receptor-mediated apoptosis in the rejection of tumors by NK cells. *J Immunol*. 167(4): 2068-73.

132. Kayagaki N, Yamaguchi N, Nakayama M, Takeda K, Akiba H, Tsutsui H, Okamura H, Nakanishi K, Okumura K, Yagita H. (1999). Expression and function of TNF-related apoptosis-inducing ligand on murine activated NK cells. *J Immunol* 163(4):1906-13.

133. Ljunggren HG, Malmberg KJ. (2007). Prospect for the use of NK cells in immunotherapy of human cancer. *Nat Rev Immunol.* 7(5):329-39.

134. Dasgupta S, Bhattacharya-Chatterjee M,. O'Malley BW, Chatterjee Jr SK. (2004). Reversal of immune suppression following vaccination with recombinant vaccinia virus expressing IL-2 in an orthotopic murine model of head and neck squamous cell carcinoma. *Cancer Ther* 2: 375.-388.

135. Long EO. (2002). Tumor cell recognition by natural killer cells. *Semin. Cancer Biol*. 12: 57-61.

136. Ishigami S, Natsugoe S, Tokuda K, Nakajo A, Che X, Iwashige H, Aridome K, Hokita S, Aikou T. (2000). Prognostic value of intratumoral natural killer cells in gastric carcinoma. *Cancer* 88: 577.

137. Divino CM, Chen SH, Yang W, Thung S, Brower ST, Woo SL. (2000). Anti-tumor immunity induced by interleukin-12 gene therapy in a metastatic model of breast cancer is mediated by natural killer cells. *Breast Cancer Res Treat* 60: 129.

138. llavena PF, Zanaboni S, Rossini A, Merendino C, Bonazzi L, Vassena C, Mangioni A, Mantovani A. (1986). Lymphokine-activated killer activity of tumor-associated and peripheral blood lymphocytes isolated from patients with ascites ovarian tumors. *J. Natl. Cancer Inst.* 77: 863-868.

139. Dasgupta S, Bhattacharya-Chatterjee M, O'Malley BW Jr, Chatterjee SK. (2005). Inhibition of NK cell activity through TGF-beta 1 by down-regulation of NKG2D in a murine model of head and neck cancer. *J Immunol* 175(8): 5541-50.

140. Groh V, Wu J, Yee C, Spies T. (2002). Tumour-derived soluble MIC ligands impair expression of NKG2D and T-cell activation. *Nature* 419*:* 734–8.

141. Waldhauer I, Goehlsdorf D, Gieseke F, Weinschenk T, Wittenbrink M, Ludwig A, Stevanovic S, Rammensee HG, Steinle A. (2008). Tumor-associated MICA is shed by ADAM proteases. *Cancer Res* 68*:*6368–76.

142. Lemaitre B, Nicolas E, Michaut L, Reichhart JM, Hoffmann JA. (1996). The dorsoventral regulatory gene cassette spätzle/Toll/cactus controls the potent antifungal response in Drosophila adults. *Cell* 86 (6): 973–83.

143. Akira S, Uematsu S, Takeuchi O. (2006). Pathogen recognition and innate immunity, *Cell* 124: 783–801.

144. Medzhitov R. (2001). Toll-like receptors and innate immunity. *Nature Rev. Immunol*. 1:135-145.

145. Guiducci C, Coffman RL, Barrat FJ. (2008). Signalling pathways leading to IFN-α production in human plasmacytoid dendritic cell and the possible use of agonist of TLR7 and TLR9 in clinical indications. *Journal of internal medicine*. 265: 43-57.

146. Akira S, Takeda K. (2004). Toll-like receptor signaling. *Nat Rev Immunol* 4: 499–511.

147. Colona M. (2007). TLR pathways and IFN-regulatory facrots: To each its own. *Eur. J. Immunol.* 37: 306-309.

148. Honda K, Taniguchi T. (2006). IRFs: master regulators of signalling by Toll-like receptors and cytosolic pattern-recognition receptors. *Nat Rev Immunol* 6: 644-58.

149. Yamamoto M, Sato S, Hemmi H, Hoshino K, Kaisho T, Sanjo H, Takeuchi O, Sugiyama M, Okabe M, Takeda K, Akira S. (2003). Role of adaptor TRIF in the MyD88-independent toll-like receptor signaling pathway. *Science* 301: 640–643.

150. Perry AK, Chow EK, Goodnough JB, Yeh WC, Cheng G. (2004). Differential requirement for TANK-binding kinase-1 in type I interferon responses to Toll-like receptor activation and viral infection. *J. Exp. Med.* 199: 1651–1658.

151. Kawai T, Adachi O, Ogawa T, Takeda K, Akira S. (1999). Unresponsiveness of MyD88-deficient mice to endotoxin. *Immunity* 11: 115–122.

152. Liu-Y-J. (2005). IPC: professional type I interferon-producing cells and plasmacytoid dendritic cells precursors. *Annu Rev. Immunol*. 23: 275-306.

153. Hornung V, Rothenfusser S, Britsch S, Krug A, Jahrsdörfer B, Giese T, Endres S, Hartmann G. (2002).Quantitative expression of toll-like receptor 1-10 mRNA in cellular subsets of human peripheral blood mononuclear cells and sensitivity to CpG oligodeoxynucleotides. *J Immunol*. 168(9):4531-7.

154. Rothenfusser S, Hornung V, Krug A, Towarowski A, Krieg AM, Endres S, Hartmann G. (2001). Distinct CpG oligonucleotide sequences activate human gamma delta T cells via interferon-alpha/-beta. *Eur J Immunol.* 31(12):3525-34.

155. Colonna M, Trinchieri G, Liu YJ. (2004). Plasmacytoid dendritic cells in immunity. *Nature Immunol*. 5: 1219–1226.

156. Jarrossay D, Napolitani G, Colonna M, Sallusto F, Lanzavecchia A. (2001). Specialization and complementarity in microbial molecule recognition by human myeloid and plasmacytoid dendritic cells. *Eur. J. Immunol*. 31: 3388–3393.

157. Iwasaki A, Medzhitov R. (2004). Toll-like receptor control of the adaptive immune responses. *Nature Immunology* 5: 987-995.

158. Krieg AM, Yi AK, Matson S, Waldschmidt TJ, Bishop GA, Teasdale R, Koretzky GA Klinman DM. (1995). CpG motifs in bacterial DNA trigger direct B-cell activation. *Nature* 374 (6522): 546–9.

159. Dalpke AH, Zimmermann S, Albrecht I, Heeg K. (2002). Phosphodiester CpG oligonucleotides as adjuvants: polyguanosine runs enhance cellular uptake and improve immunostimulative activity of phosphodiester CpG oligonucleotides in vitro and in vivo. *Immunology* 106 (1): 102–12.

160. Wu CC, Lee J, Raz E, Corr M, Carson DA. (2004). Necessity of oligonucleotide aggregation for toll-like receptor 9 activation. *The Journal of biological chemistry* 279 (32): 33071–8.

161. Marshall JD, Fearon K, Abbate C, Subramanian S, Yee P, Gregorio J,. Coffman RL Van Nest G. (2003). Identification of a novel CpG DNA class and motif which optimally stimulate B cell and plasmacytoid dendritic cell functions. *J. Leukoc. Biol.* 73:781–792.

162. HartmannG, Battiany J, Poeck H, Wagner M, Kerkmann M, Lubenow N, Rothenfusser S, Endres S. (2003). Rational design of new CpG oligonucleotides that combine B cell activation with high IFN-α induction in plasmacytoid dendritic cells. *Eur. J. Immunol.* 33:1633–1641.

163. Krug, A., Rothenfusser, S., Hornung, V., Jahrsdorfer, B., Blackwell, S., Ballas, Z. K., Endres, S., Krieg, A. M., Hartmann, G. (2001). Identification of CpG oligonucleotide sequences with high induction of IFN-α/β in plasmacytoid dendritic cells. *Eur. J. Immunol.* 31, 2154–2163.

164. Kerkmann M, Costa LT, Richter C, Rothenfusser S, Battiany J, Hornung V, Johnson J, Englert S, Ketterer T, Heckl W, Thalhammer S, Endres S, Hartmann G. (2005). Spontaneous formation of nucleic acid-based nanoparticles is responsible for high interferon-α induction by CpG-A in plasmacytoid dendritic cells. *J. Biol. Chem.* 280: 8086–8093.

165. Krieg AM. (2002). CpG motifs in bacterial DNA and their immune effects. *Annu. Rev. Immunol.* 20:709–760.

166. Noppert SJ, Fitzgerald KA, Hertzog PJ. (2007). The role of type I interferons in TLR responses. *Immunol Cell Biol*. 85(6): 446-57.

167. Chawla-Sarkar M, Lindner DJ, Liu YF, Williams BR, Sen GC, Silverman RH, Borden EC. (2003). Apoptosis and interferons: role of interferon-stimulated genes as mediators of apoptosis. *Apoptosis* 8: 237–249.

168. Clemens MJ. (2003). Interferons and apoptosis. *J Interferon Cytokine Res* 23: 277–292.

169. Cheng WF, Hung CF, Lin KY, Ling M, Juang J, He L, Lin CT, Wu TC. (2003). CD8+ T cells, NK cells and IFN-γ are important for control of tumor with downregulated MHC class I expression by DNA vaccination. *Gene Ther.* 10(16): 1311-20.

170. Lee JJ, Foon KA, Mailliard RB, Muthuswamy R, Kalinski P. (2008) Type 1-polarized dendritic cells loaded with autologous tumor are a potent immunogen against chronic lymphocytic leukemia *J Leukoc Biol.*84(1):319-25.

171. Honda K, Takaoka A, Taniguchi T. (2006a). Type I gene induction by the interferon regulatory factor family of transcription factors. *Immunity* 25: 349-60.

172. Akira S, Takeda K. (2004). Toll-like receptor signalling. *Nat Rev Immunol* 4:499-511.

173. Yoneyama M, Kikuchi M, Natsukawa T, Shinobu N, Imaizumi T, Miyagishi M, Taira K, Akira S, Fujita T. (2004). The RNA helicase RIG-I has an essential function in double-stranded RNA-induced innate antiviral responses. *Nat Immunol* 5: 730 – 746.

174. Yoneyama M, Kikuchi M, Matsumoto K, Imaizumi T, Miyagishi M, Taira K, Foy E, Loo YM, Gale M Jr, Akira S, Yonehara S, Kato A, Fujita T. (2005). Shared and unique functions of the DExD/H-box helicases RIG-I, MDA5, and LGP2 in antiviral innate immunity. *J Immunol* 175: 2851-8.

175. Kato H, Sato S, Yoneyama M, Yamamoto M, Uematsu S, Matsui K, Tsujimura T, Takeda K, Fujita T, Takeuchi O, Akira S. (2005). Cell type specific involvement of RIG-I in antiviral response. *Immunity* 23: 19-28.

176. Takeda K, Akira S. (2005). Toll-like receptors in innate immunity. *Int Immunol* 17: 1-14.

177. Hornung V, Ellegast J, Kim S, Brzózka K, Jung A, Kato H, Poeck H, Akira S, Conzelmann KK, Schlee M, Endres S, Hartmann G. (2006). 5'-Triphosphate RNA is the ligand for RIG-I. *Science* 314: 994–997.

178. Pichlmair A, Schulz O, Tan CP, Näslund TI, Liljeström P, Weber F, Reis e Sousa C. (2006). RIG-I-mediated antiviral responses to single-stranded RNA bearing 5' phosphates. *Science* 314: 997–1001.

179. Gitlin L, Barchet W, Gilfillan S, Cella M, Beutler B, Flavell RA, Diamond MS, Colonna M. (2006). Essential role of mda-5 in type I IFN responses to polyriboinosinic:polyribocytidylic acid and encephalomyocarditis picornavirus. *Proc. Natl. Acad. Sci. USA* 103: 8459–8464.

180. Baccala R, Hoebe K, Kono DH, Beutler B, Theofilopoulos AN. (2007). TLR-dependent and TLR-independent pathways of type I interferon induction in systemic autoimmunity *Nat Med*. 3(5):543-51.

181. Edwards AD, Diebold SS, Slack EM, Tomizawa H, Hemmi H, Kaisho T, Akira S, Reis e Sousa C. (2003). Toll-like receptor expresssion in murine DC subsets: lack of TLR7 expression by CD8α DC correlates with unresponsiveness imidazoquilines. *Eur J Immunol.*33(4):827-33.

182. Kawai T, Sato S, Ishii KJ, Coban C, Hemmi H, Yamamoto M, Terai K, Matsuda M, Inoue J, Uematsu S, Takeuchi O, Akira S. (2004). Interferon-alpha induction through Toll-like receptors involves a direct interaction of IRF7 with MyD88 and TRAF6. *Nat Immunol* 5: 1061–8.

183. Kim TW, Staschke K, Bulek K, Yao J, Peters K, Oh KH, Vandenburg Y, Xiao H, Qian W, Hamilton T, Min B, Sen G, Gilmour R, Li X .(2007). A critical role for IRAK4 kinase activity in Toll-like receptor-mediated innate immunity. *J Exp Med*: 204: 1025–36.

184. Yang K, Puel A, Zhang S, Eidenschenk C, Ku CL, Casrouge A, Picard C, von Bernuth H, Senechal B, Plancoulaine S, Al-Hajjar S, Al-Ghonaium A, Maródi L, Davidson D, Speert D, Roifman C, Garty BZ, Ozinsky A, Barrat FJ, Coffman RL, Miller RL, Li X, Lebon P, Rodriguez-Gallego C, Chapel H, Geissmann F, Jouanguy E, Casanova JL. (2005). Human TLR-7-, -8-, and -9-mediated induction of IFN-alpha/beta and -lambda Is IRAK-4 dependent and redundant for protective immunity to viruses. *Immunity* 23: 465–78.

185. Gohda J, Matsumura T, Inoue J. (2004). Cutting edge: TNFR-associated factor (TRAF) 6 is essential for MyD88-dependent pathway but not toll/IL-1 receptor domain-containing adaptor-inducing IFN-beta (TRIF)-dependent pathway in TLR signalling. *J Immunol* 173: 2913–7.

186. Hemmi H, Kaisho T, Takeda K, Akira S. (2003). The roles of Toll-like receptor 9, MyD88, and DNA-dependent protein kinase catalytic subunit in the effects of two distinct CpG DNAs on dendritic cell subsets. *J. Immunol*. 170: 3059–3064.

187. Taniguchi T, Ogasawara K, Takaoka A, Tanaka N. (2001). IRF family of transcription factors as regulators of host defense. *Annu. Rev. Immunol*. 19: 623–55.

188. Marie I, Durbin JE, Levy DE. (1998). Differential viral induction of distinct interferon-alpha genes by positive feedback through interferon regulatory factor-7. *EMBO J* 17: 6660 – 9.

189. Sato M, Suemori H, Hata N, Asagiri M, Ogasawara K, Nakao K, Nakaya T, Katsuki M, Noguchi S, Tanaka N, Taniguchi T. (2000). Distinct and essential roles of transcription factors IRF-3 and IRF-7 in response to viruses for IFNalpha/beta gene induction. *Immunity* 13: 539 – 48.

190. Kawai T, Takeuchi O, Fujita T, Inoue J, Mühlradt PF, Sato S, Hoshino K, Akira S. (2001). Lipopolysaccharide stimulates the MyD88-independent pathway and results in activation of IFN-regulatory factor 3 and the expression of a subset of lipopolysaccharide-inducible genes. *J. Immunol.* 167: 5887–5894.

191. Ogawa S, Lozach J, Benner C, Pascual G, Tangirala RK, Westin S, Hoffmann A, Subramaniam S, David M, Rosenfeld MG, Glass CK. (2005). Molecular determinants of crosstalk between nuclear receptors and Toll-like receptors. *Cell* 122: 707–721.

192. Honda K, Yanai H, Mizutani T, Negishi H, Shimada N, Suzuki N, Ohba Y, Takaoka A, Yeh WC, Taniguchi T. (2004). Role of a transductional-transcriptional processor complex involving MyD88 and IRF-7 in Toll-like receptor signaling. *Proc. Natl. Acad. Sci. USA* 101:15416–21.

193. Kawai T, Sato S, Ishii KJ, Coban C, Hemmi H, Yamamoto M, Terai K, Matsuda M, Inoue J, Uematsu S, Takeuchi O, Akira S. (2004). Interferon-α induction through Toll-like receptors involves a direct interaction of IRF7 with MyD88 and TRAF6. *Nat. Immunol.* 5:1061–68.

194. Honda, K., Yanai, H., Negishi, H., Asagiri, M., Sato, M., Mizutani, T., Shimada, N.,Ohba, Y., Takaoka, A., Yoshida, N. and Taniguchi, T. (2005). IRF-7 is the master regulator of type-I interferon-dependent immune responses. *Nature* 434: 772-7.

195. Colina R, Costa-Mattioli M, Dowling RJ, Jaramillo M, Tai LH, Breitbach CJ, Martineau Y, Larsson O, Rong L, Svitkin YV, Makrigiannis AP, Bell JC, Sonenberg N. (2008). Translational control of the innate immune response through IRF-7. *Nature*. 452 (7185):323-8.

196. Yan H, Frost P, Shi Y, Hoang B, Sharma S, Fisher M, Gera J, Lichtenstein A. (2006). Mechanism by which mammalian target of rapamycin inhibitors sensitize multiple myeloma cells to dexamethasone-induced apoptosis. *Cancer Res* 66: 2305–2313.

197. Pause A, Belsham GJ, Gingras AC, Donzé O, Lin TA, Lawrence JC Jr, Sonenberg N. (1994). Insulin-dependent stimulation of protein synthesis by phosphorylation of a regulator of 5'-cap function. *Nature* 371: 762-767.

198. Sonenberg N, Hinnebusch AG. (2007). New modes of translational control in development, behavior, and disease. *Mol Cell* 28:721–729.

199. Gingras AC, Gygi SP, Raught B, Polakiewicz RD, Abraham RT, Hoekstra MF, Aebersold R, Sonenberg N. (1999a). Regulation of 4E-BP1 phosphorylation: a novel two-step mechanism. *Genes Dev* 13: 1422–1437.

200. Gingras AC, Raught B, Gygi SP, Niedzwiecka A, Miron M, Burley SK, Polakiewicz RD, Wyslouch-Cieszynska A, Aebersold R, Sonenberg N. (2001). Hierarchical phosphorylation of the translation inhibitor 4E-BP1 Genes Dev 15: 2852–2864.

201. Darnell JE,Kerr IM Jr, Stark GR. (1994). Jak-STAT pathways and transcriptional activation in response to IFNs and other extracellular signaling proteins. *Science* 264: 1415-21.

202. van Boxel-Dezaire AH, Rani MR, Stark GR. (2006). Complex modulation of cell type-specific signaling in response to type I interferons. *Immunity* 25: 361-72.

203. Stark GR, Kerr IM, Williams BR, Silverman RH, Schreiber RD. (1998). How cells respond to interferons. *Annu Rev Biochem* 67: 227-64.

204. Meurs E, Chong K, Galabru J, Thomas NS, Kerr IM, Williams BR, Hovanessian AG. (1990). Molecular cloning and characterization of the human double-stranded RNA-activated protein kinase induced by interferon. *Cell* 62: 379-90.

205. Rebouillat D, Hovanessian AG. (1999). The human 2',5'-oligoadenylate synthetase family: interferon-induced proteins with unique enzymatic properties. *J Interferon Cytokine Res* 19: 295-308.

206. Staeheli P. (1990). Interferon-induced proteins and the antiviral state. *Adv Virus Res* 38: 147-200.

207. van den Broek MF, Muller U, Huang S, Zinkernagel RM Aguet M. (1995). Immune defence in mice lacking type I and/or type II interferon receptors.*Immunol Rev* 148: 5-18.

208. Luker GD, Prior JL, Song J, Pica CM, Leib DA. (2003). Bioluminescence imaging reveals systemic dissemination of herpes simplex virus type 1 in the absence of interferon receptors. *J Virol* 77: 11082 – 93.

209. Harada H, Matsumoto M, Sato M, Kashiwazaki Y, Kimura T, Kitagawa M, Yokochi T, Tan RS, Takasugi T, Kadokawa Y, Schindler C, Schreiber RD, Noguchi S, Taniguchi T. (1996). Regulation of IFN-alpha/beta genes: evidence for a dual function of the transcription factor complex ISGF3 in the production and action of IFN-alpha/beta. *Genes Cells* 1: 995-1005.

210. Hwang SY, Hertzog PJ, Holland KA, Sumarsono SH, Tymms MJ, Hamilton JA, Whitty G, Bertoncello I, Kola I. (1995). A null mutation in the gene encoding a type I interferon receptor component eliminates antiproliferative and antiviral responses to interferons alpha and beta and alters macrophage responses. *Proc Natl Acad Sci U S A* 92: 11284 – 8.

211. Zlotnik A, Yoshie O. (2000). Chemokines: a new classification system and their role in immunity. *Immunity* 12: 121-127.

212. Zhou Y, Kurihara T, Ryseck RP, Yang Y, Ryan C, Loy J, Warr G, Bravo R. (1998). Impaired macrophage function and enhanced T cell-dependent immune response in mice lacking CCR5, the mouse homologue of the major HIV-1 coreceptor. *J Immunol* 160: 4018 – 4025.

213. Esche C, Stellato C, Beck LA. (2005). Chemokines: key players in innate and adaptive immunity. *J Invest Dermatol*.125 (4):615 – 28.

214. Mrowietz U, Schwenk U, Maune S, Bartels J, Küpper M, Fichtner I, Schröder JM, Schadendorf D. (1999). The chemokine RANTES is secreted by human melanoma cells and is associated with enhanced tumour formation in nude mice. *Br J Cancer* 79: 1025–1031.

215. Mellado M, de Ana AM, Moreno MC, Martinez C, Rodriguez-Frade JM. (2001). A potential immune escape mechanism by melanoma cells through the activation of chemokine-induced T cell death. *Curr Biol* 11: 691 – 696.

216. Algeciras-Schimnich A, Vlahakis SR, Villasis-Keever A, Gomez T, Heppelman CJ, Bou G, Paya CV. (2002). CCR5 mediates Fas- and caspase-8 dependent apoptosis of both uninfected and HIV infected primary human CD4 T cells. *Aids* 16: 1467 – 1478.

217. Pinto LA, Williams MS, Dolan MJ, Henkart PA, Shearer GM. (2000). Beta-chemokines inhibit activation-induced death of lymphocytes from HIV-infected individuals. *Eur J Immunol* 30: 2048 – 2055.

218. Taub DD, Turcovski-Corrales SM, Key ML, Longo DL, Murphy WJ. (1996). Chemokines and T lymphocyte activation: I. Beta chemokines costimulate human T lymphocyte activation in vitro. *J Immunol* 156: 2095 – 2103.

219. Makino Y, Cook DN, Smithies O, Hwang OY, Neilson EG, Turka LA, Sato H, Wells AD, Danoff TM. (2002). Impaired T cell function in RANTES deficient mice. *Clin Immunol* 102: 302 – 309.

220. Bacon KB, Schall TJ, Dairaghi DJ. (1998). RANTES activation of phospholipase D in Jurkat T cells: requirement of GTP-binding proteins ARF and RhoA. *J Immunol* 160: 1894 – 1900.

221. Murooka TT. (2009). The role of CCL5/CCR5 signal transduction in T cell function and breast cancer. Thesis Toronto. University Press.

222. Caux C, Ait-Yahia S, Chemin K, de Bouteiller O, Dieu-Nosjean MC, Homey B, Massacrier C, Vanbervliet B, Zlotnik A, Vicari A. (2000) Dendritic cell biology and regulation of dendritic cell trafficking by chemokines. *Sermin immunopathol* 22(4):345–369.

223. Uguccioni M, D'Apuzzo M, Loetscher M, Dewald B, Baggiolini M. (1995). Actions of the chemotactic cytokines MCP-1, MCP-2, MCP-3, RANTES, MIP-1 alpha and MIP-1 beta on human monocytes *Eur. J. Immunol*. 25: 64–68.

224. Taub DD, Conlon K, Lloyd AR, Oppenheim JJ, Kelvin DJ. (1993). Preferential migration of activated CD4+ and CD8+ T cells in response to MIP-1 alpha and MIP-1 beta. Science 260, 355–358.

225. Nobile C, Lind M, Miro F, Chemin K, Tourret M, Occhipinti G, Dogniaux, Amigorena S, Hivroz C. (2008). Cognate CD4+ T-cell-dendritic cell interactions induce migrationof immature dendritic cells through dissolution of their podosomes. *Blood.* 111(7):3579-90.

226. Cittera E, Leidi M, Buracchi C, Pasqualini F, Sozzani S, Vecchi A, Waterfield JD, Introna M, Golay J. (2007). The CCL3 family of chemokines and innate immunity

cooperates in vivo in the eradication of an established lymphoma xenograft by rituximab. J Immunol. 178 (10):6616-23.

227. Castellino F, Huang AY, Altan-Bonnet G, Stoll S, Scheinecker C, Germain RN. (2006). Chemokines enhance immunity by guiding naive CD8+ T cells to sites of CD4+ T cell–dendritic cell interaction. *Nature* 440: 890–895.

228. Allavena P, Bianchi D, Zhou D, van Damme J, Jilek P, Sozzani S, Mantovani A. (1994). Induction of natural killer cell migration by monocyte chemoattractant protein-1, -2 and -3. *Eur J Immunol* 24: 3233–3236.

229. Torisu H, Ono M, Kiryu H, Furue M, Ohmoto Y, Nakayama J, Nishioka Y, Sone S, Kuwano M. (2000). Macrophage infiltration correlates with tumor stage and angiogenesis in human malignant melanoma: possible involvement of TNF-alpha and IL-1alpha. *Int J Cancer* 85: 182–188.

230. Nesbit M, Schaider H, Miller T H, Herlyn M. (2001). Low-level monocyte chemoattractant protein-1 stimulation of monocytes leads to tumor formation in nontumorigenic melanoma cells. *J Immunol* 166: 6483–6490.

231. Carr MW, Rioth SJ, Luther E, Rose SS & Springer A. (1994). Monocyte chemoattractant protein 1 acts as a T-lymphocyte chemoattractant. *Proc Natl Acad Sci USA* 91:3652–3656.

232. Bottazzi B, Walter S, Govoni D, Colotta F, Mantovani A. (1992). Monocyte chemotactic cytokine gene transfer modulates macrophage infiltration, growth, and susceptibility to IL-2 therapy of a murine melanoma. *J Immunol* 148(4):1280- 5.

233. Zou W, Borvak J, Marches F, Wei S, Galanaud P, Emilie D, Curiel TJ. (2000). Macrophage-derived dendritic cells have strong Th1-polarizing potential mediated by beta-chemokines rather than IL-12. *J. Immunol*. 165: 4388.

234. Moser B, Wolf M, Walz A, Loetscher P. (2004). Chemokines: multiple levels of leukocyte migration control. *Trends Immunol*. 25: 75.

235. Bendriss-Vermare N, Burg S, Kanzler H, Chaperot L, Duhen T, de Bouteiller O, D'agostini M, Bridon JM, Durand I, Sederstrom JM, Chen W, Plumas J, Jacob MC, Liu YJ, Garrone P, Trinchieri G, Caux C, Brière F. (2005). Virus overrides the propensity of human CD40L-activated plasmacytoid dendritic cells to produce Th2 mediators through synergistic induction of IFN-{gamma} and Th1 chemokine production. *J. Leukoc. Biol.* 78: 954-66.

236. Paschen A, Sucker A, Hill B, Moll I, Zapatka M, Nguyen XD, Sim GC, Gutmann I, Hassel J, Becker JC, Steinle A, Schadendorf D, Ugurel S. (2009). Differential clinical significance of individual NKG2D ligands in melanoma: soluble ULBP2 as an indicator of poor prognosis superior to S100B. *Clin Cancer Res.* 15 (16):5208-15.

237. Mazariegos GV, Zahorchak AF, Reyes J, Ostrowski L, Flynn B, Zeevi A, Thomson AW. (2003). Dendritic cell subset ratio in peripheral blood correlates with successful withdrawal of immunosuppresion in liver transplant patients. *AM J Transplant* 3: 689-696.

238. Athanassopoulos P, Vaessen LM, Balk AH, Takkenberg JJ, Maat AP, Weimar W, Bogers AJ. (2005). Impaired circulating dendritic cell reconstitution identifies rejecting recipients after clinical heart transplantation independent of rejection. *Eur J Cardiothorac Sur.* 27:783-789.

239. Hashizume H, Horibe T, Yagi H, Seo N, Takigawa M.. (2005). Compartmental imbalance and aberrant immune function of blood CD123+ (Plasmacytoid) and CD11c+ (Myeloid) dendritic cells in atoipic dermatitis. *J Immunol.* 174: 2396-2403.

240. Lou Y, Liu C, Kim GJ, Liu YJ, Hwu P, Wang G. (2007). Plasmacytoid dendritic cells synergize with myeloid dendritic cells in the induction of antigen-specific antitumor immune responses. *J Immunol* 178:1534-41.

241. Byrnes AA, Li DY, Park K, Thompson D, Mocilnikar C, Mohan P, Molleston JP, Narkewicz M, Zhou H, Wolf SF, Schwarz KB, Karp CL. (2007) Modulation of the IL-12/IFN-γ axis by IFN-α therapy for hepatitis C. *J Leukoc Biol.* 81(3):825-34.

242. Paquette RL. (1998). Intereferon-α and granulocyte-macrophage colony-stimulating factor differentiate peripheral blood monocytes into potent antigen-presenting cells. *J Leukoc. Biol*. 64,358-367.

243. Angiolillo AL, Sgadari C, Angiolillo A, Taub DD, Liao F, Farber JM., Maheshwari, S., Kleinman, H. K., osato, G. (1995). Human interferon-inducible protein 10 is a potent inhibitor of angiogenesis in vivo. *J. Exp. Med.*. 182:155–162.

244. Strieter RM, Kunkel SL, Arenberg DA, Burdick M D, Polverini PJ. (1995). Interferon g-inducible protein 10 (IP-10), a member of the -C-X-C- chemokine family, is an inhibitor of angiogenesis. *Biochem.Biophys. Res. Comm.*. 210:51–57.

245. Gibson SJ, Lindh JM, Riter TR, Gleason RM, Rogers LM, Fuller AE, Oesterich JL, Gorden KB, Qiu X, McKane SW, Noelle RJ, Miller RL, Kedl RM, Fitzgerald-Bocarsly P, Tomai MA, Vasilakos JP. (2002).Plasmacytoid dendritic cells produce cytokines and mature in response to the TLR7 agonists, imiquimod and resiquimod. Cell immunol. 218 (1-2):74-86.

246. Peters PJ, Borst J, Oorschot V, Fukuda M, Krähenbühl O, Tschopp J, Slot JW, Geuze HJ. (1991). Cytotoxic T lymphocyte granules are secretory lysosomes, containing both perforin and granzymes. *J Exp Med*. 173(5):1099-109.

247. Alter G, Malenfant JM, Altfeld M. (2004).CD107a as a functional marker for the identification of natural killer cell activity.*J Immunol Methods*. 294(1-2):15-22

248. Hoffmann TK., Müller-Berghaus J, Ferris RL., Johnson, J T, Storkus, W J, and Whiteside TL. (2002). Alterations in the frequency of dendritic cell subsets in the peripheral circulation of patients with squamous cell carcinomas of the head and neck. *Clin. Cancer Res*. 8:1787-93.

249. Almand B, Clark JI., Nikitina E, van Beynen J, English NR, Knight SC, Carbone DP, Gabrilovich DI (2000). Clinical significance of defective dendritic cell differentiation in cancer. *Clin. Cancer Res*. 6:1755-66.

250. Pinzon-Charry A, Ho CS, Maxwell T, McGuckin MA, Schmidt C, Furnival C, Pyke C M, and López JA. (2007). Numerical and functional defects of blood dendritic cells in early- and late-stage breast cancer. *Br. J. Cancer*. 97:1251-59.

251. Tabarkiewicz. J., Rybojad, P., Jablonka, A., and Rolinski, J. (2008). CD1c+ and CD303+ dendritic cells in peripheral blood, lymph nodes and tumor tissue of patients with non-small cell lung cancer. *Oncol. Rep.* 19:237-243.

252. Della Bella S, Gennaro M, Vaccari M, Ferraris C, Nicola S, Riva A, Clerici M, Greco M, and Villa ML. (2003). Altered maturation of peripheral blood dendritic cells in patients with breast cancer. *Br. J. Cancer* .89:1463-72.

253. Nestle FO, Conrad C, Tun-Kyi A, Homey B, Gombert M, Boyman O, Burg G, Liu YJ, Gilliet M. (2005). Plasmacytoid predendritic cells initiate psoriasis through interferon-alpha production. *J Exp Med.* 202(1):135-43.

254. Cederblad BS. Blomberg H, Vallin A, Perers G, AlmV and Ronnblom L. (1998). Patients with systemic lupus erythematosus have reduced numbers of circulating natural interferon-alpha-producing cells. *J. Autoimmun.* 11:465–470.

255. Cravens PD, Hayashida K, Davis LS, Nanki T, Lipsky PE. (2007). Human Peripheral Blood Dendritic Cells and Monocyte Subsets Display Similar Chemokine Receptor Expression Profiles with Differential Migratory Responses. *Scand J Immunol*. 65(6):514-24.

256. Pinzon-Charry A, Maxwell T, McGuckin MA, Schmidt C, Furnival C, Lopez JA. (2006). Spontaneous apoptosis of blood dendritic cells in patients with breast cancer. *Breast Cancer Res*. 8:R5.

257. Palucka AK, Blanck JP, Bennett L, Pascual V, Banchereau J. (2005). Cross-regulation of TNF and IFN-a in autoimmune diseases. *PNAS* 102 (9): 3372-3377.

258. Gerlini G, Tun-Kyi A, Dudli C, Burg G, Pimpinelli N, Nestle FO. (2004). Metastatic Melanoma Secreted IL-10 Down-Regulates CD1 Molecules on Dendritic Cells in Metastatic Tumor Lesions. *Am J Pathol*. 165(6):1853-63.

259. Balkwill F. (2002). Tumor necrosis factor or tumor promoting factor? *Cytokine Growth Factor Rev 13*:135–41.

260. Ito M, Minamiya Y, Kawai H, Saito S, Saito H, Nakagawa T, Imai K, Hirokawa M, and Ogawa J. (2006). Tumor-derived TGFbeta-1 induces dendritic cell apoptosis in the sentinel lymph nodes. *J. Immunol.* 176, 5637-43.

261. Lissoni P, Vigore L, Ferranti R, Bukovec R, Meregalli S, Mandala M, Barni S, Tancini G, Fumagalli L, Giani L. (1999). Circulating dendritic cells in early and advanced cancer patients: diminished percent in the metastatic disease. *J Biol Regul Homeost Agents.* 13:216–219.

262. Lou Y, Liu C, Kim GJ, Liu YJ, Hwu P, Wang G. (2007). Plasmacytoid dendritic cells synergize with myeloid dendritic cells in the induction of antigen-specific antitumor immune responses. *J Immunol.* 178:1534-41.

263. Jongbloed SL, Lebre MC, Fraser AR, Gracie JA, Sturrock RD,Tak PP.(2006) Enumeration and phenotypical analysis of distinct dendritic cell subsets in psoriatic arthritis and rheumatoid arthritis. *Arthritis Res Ther.*8*:*R15.*3*248.

264. Peng R, Li Y, Brezner K, Litherland S, Clare-Salzler MJ. (2003). Abnormal peripheral blood dendritic cell populations in type 1 diabetesю *Ann N Y Acad Sci*. 1005:222-5.

265. Demedts IK, Bruselle GG, Vermaelen KY, Pauwels RA. (2005). Identification of human pulmonary dendritic cells. *Am J Respir Cell Mol Biol.* 32*:*177–84.

266. Demedts IK, Bracke KR, Maes T, Joos GF, Brusselle GG. (2006). Different roles for human lung dendritic cell subsets in pulmonary immune defense mechanisms. *Am J Respir Cell Mol Biol.*35*:*387–93.

267. Fiore N, Castellano G, Blasi A, Capobianco C, Loverre A, Montinaro V, Netti S, Torres D, Manno C, Grandaliano G, Ranieri E, Schena FP, Gesualdo L. (2008). Immature myeloid and plasmacytoid dendritic cells infiltrate renal tubulointerstitium in patients with lupus nephritis. *Mol Immunol.* 45*:*259–65.

268. Vogelsang P, Brun JG, Oijordsbakken G, Skarstein K, Jonsson R, Appel S. (2009). Levels of plasmacytoid dendritic cells and type-2 myeloid dendritic cells are reduced in peripheral blood of patients with primary Sjogren's syndrome. *Ann Rheum Dis* doi:10.1136/ard.2009.118158.

269. Blanco P, Palucka AK, Gill M, Pascual S, Banchereau J. (2001). Induction of dendritic cells differentiation by IFN-a in systemic lupus erythematosus. *Science* 294:1540-1543.

270. Yoneyama H, Matsuno K, Toda E, Nishiwaki T, Matsuo N, Nakano A, Narumi S, Lu B, Gerard C, Ishikawa S, Matsushima K.. (2005). Plasmacytoid DCs help lymph node DCs to induce anti-HSV CTLs. *J Exp Med.* 202(3):425-35.

271. Ratta M, Fagnoni F, Curti A, Vescovini R, Sansoni P, Oliviero B, Fogli M, Ferri E, Della Cuna GR, Tura S, Baccarani M, Lemoli RM. (2002). Dendritic cells are functionally defective in multiple myeloma: the role of interleukin-6. *Blood.* 100(1):230-7.

272. Perez VL, Van Parijs L, Biuckians A, Zheng XX, Strom TB, Abbas AK. (1997). Induction of peripheral T cell tolerance *in vivo* requires CTLA-4 engagement. *Immunity* **6**, 411–417.

273. Banchereau J, Briere F, Caux C, Davoust J, Lebecque S, Liu YJ, Pulendran B, Palucka K. (2000). Immunobiology of denderitic cells. *Annu Rev Immunol.*; 18:787-811.

274. Marrack P, Kappler J, Mitchell T. (1999). Type I interferons keep activated T cells alive. *J. Exp. Med.* 189:521-530.

275. Luft T, Pang KC, Thomas E, Hertzog P, Hart DN, Trapani J, Cebon J. (1998) Type I IFN enhance the terminal differentiation of dendritic cells. *J. Immunol*. 161:1947-1953.

276. Liu, Y.J. 2005. IPC: professional type 1 interferon-producing cells and plasmacytoid dendritic cell precursors. *Annu. Rev. Immunol.* 23:275–306

277. Colonna, M., G. Trinchieri, and Y.J. Liu. (2004). Plasmacytoid dendritic cells in immunity. *Nat. Immunol.* 5:1219–1226

278. Megjugorac, N.J., H.A. Young, S.B. Amrute, S.L. Olshalsky, and P. Fitzgerald-Bocarsly. (2004). Virally stimulated plasmacytoid dendritic cells produce chemokines and induce migration of T and NK cells. *J. Leukoc. Biol.* 75:504–514

279. Piqueras, B., J. Connolly, H. Freitas, A.K. Palucka, and J. Banchereau. (2006). Upon viral exposure, myeloid and plasmacytoid dendritic cells produce 3 waves of distinct chemokines to recruit immune effectors. *Blood.* 107:2613–2618

280. Jego G, Palucka AK, Blanck JP, Chalouni C, Pascual V, and Banchereau J. (2003). Plasmacytoid dendritic cells induce plasma cell differentiation through type I interferon and interleukin 6. *Immunity.* 19:225–234

281. Seet BT, Mcfadden G. (2002). Viral chemokine-binding proteins. *J Leukoc Biol*. 72:24-34

282. Harlin H, Meng Y, Peterson AC, Zha Y, Tretiakova M, Slingluff C, McKee M, Gajewski TF. (2009). Chemokine expression in melanoma metastases associated with CD8+ T-cell recruitment *Cancer Res*. 69(7):3077-85

283. Bellone G, Carbone A, Smirne C, Scirelli T, Buffolino A, Novarino A, Stacchini A, Bertetto O, Palestro G, Sorio C, Scarpa A, Emanuelli G, and Rodeck U. (2006). Cooperative induction of a tolerogenic dendritic cell phenotype by cytokines secreted by pancreatic carcinoma cells. *J. Immunol*. 177: 3448-60.

284. Shurin MR, and Gabrilovich DI. (2001). Regulation of dendritic cell system by tumor. *Cancer Res. Ther. Control*. 11: 65-78.

285. Molling JW, Langius JA, Langendijk JA, Leemans CR, Bontkes HJ, van der Vliet HJ, von Blomberg BM, Scheper RJ, van den Eertwegh AJ.. (2007). Low levels of circulating invariant natural killer T cells predict poor clinical outcome in patients with head and neck squamous cell carcinoma. *J Clin Oncol.* 25: 862-868

286. Plonquet A, Haioun C, Jais JP, Debard AL, Salles G, Bene MC, Feugier P, Rabian C, Casasnovas O, Labalette M, Kuhlein E, Farcet JP, Emile JF, Gisselbrecht C, Delfau-Larue MH; Groupe d'étude des lymphomes de l'adulte. (2007). Peripheral blood natural killer cell count is associated with clinical outcome in patients with aaIPI 2-3 diffuse large B-cell lymphoma. *Ann Oncology*. 18: 1209-1215

287. Richards JO, Chang X, Blaser BW, Caligiuri MA, Zheng P, Liu Y. (2006) Tumour growth impedes natural-killer-cell maturation in the bone marrow. *Blood.* 108:246-252.

288. Vujanovic, N. L., Basse, P., Herberman, R. B., Whiteside, T. L. (1996) Antitumor functions of natural killer cells and control of metastases. *Methods* 9: 394–408.

289. Lee JC, Lee KM, Kim DW, Heo DS. (2004) Elevated TGF-β1 secretion and down-modulation of NKG2D underlies impaired cytotoxicity in cancer patients. *J Immunol*, 172:7335-7340.

290. Krockenberger M, Dombrowski Y. (2008). Macrophage migration inhibitory factors contributes to the immune escape of ovarian cancer by down-regulating NKG2D. *J Immunol*. 180: 7338-7348.

291. Costello RT, Sivori S, Marcenaro E, Lafage-Pochitaloff M, Mozziconacci MJ, Reviron D, Gastaut JA, Pende D, Olive D, Moretta A. (2002). Defective expression and function of natural killer cell-triggering receptors in patients with acute myeloid leukemia. *Blood*. 99: 3661-3667.

292. Cai L, Zhang Z, Zhou L, Wang H, Fu J, Zhang S, Shi M, Zhang H, Yang Y, Wu H, Tien P, Wang FS. (2008). Functional impairment in circulating and intrahepatic NK cells and relative mechanism in hepatocellular carcinoma patients. *Clinical Immunology*. 129:428-437.

293. Groh V, Bruhl A, El-Gabalawy H, Nelson JL, Spies T. (2003). Stimulation of T cell autoreactivity by anomalous expression of NKG2D, its MIC ligands in rheumatoid arthritis. *Proc Natl Acad Sci U S A*.100:9452–7

294. Gati A, Da Rocha S, Guerra N, Escudier B, Moretta A, Chouaib S, Angevin E, Caignard A. (2004). Analysis of the natural killer mediated immune response in metastatic renal cell carcinoma patients. *Int. J. cancer.* 109:393-401.

295. De Maria A, Fogli M, Mazza S, Basso M, Picciotto A, Costa P, Congia S, Mingari MC Moretta L. (2007). Increased natural cytotoxicity receptor expression and relevant IL-10 production in NK cells from chronically infected viremic HCV patients. *Eur. J, Immunol*. 37: 445-455.

296. Dzionek A, Sohma Y, Nagafune J, Cella M, Colonna M, Facchetti F, Günther G, Johnston I, Lanzavecchia A, Nagasaka T, Okada T, Vermi W, Winkels G, Yamamoto T, Zysk M, Yamaguchi Y, Schmitz J.. (2001) BDCA-2, a novel plasmacytoid dendritic cell-specific type II C-type lectin, mediates antigen capture and is a potent inhibitor of interferon alpha/beta induction. *J Exp Med* 194:1823–1834.

297. Grage-Griebenow E, Löseke S, Kauth M, Gehlhar K, Zawatzky R, Bufe A. (2007). Anti-BDCA-4 (neuropilin-1) antibody can suppress virus-induced IFN-alpha production of plasmacytoid dendritic cells. *Immunol Cell Biol*. 85(5):383-90

298. Hartmann E, Wollenberg B, Rothenfusser S, Wagner M, Wellisch D, Mack B, Giese T, Gires O, Endres S, Hartmann G. (2003). Identification and functional analysis of tumour infiltrating plasmacytid dendritic cells in head and neck cancer. *Cancer Res*. 63:6478-6487.

299. Izaguirre A, Barnes BJ, Amrute S, Yeow WS, Megjugorac N, Dai J, Feng D, Chung E, Pitha PM, Fitzgerald-Bocarsly P. (2003). Comparative analysis of IRF and IFN-alpha expression in human plasmacytoid and monocyte-derived dendritic cells. *J Leukoc Biol*. 74(6):1125-38.

300. Osawa Y, Iho S, Takauji R, Takatsuka H, Yamamoto S, Takahashi T, Horiguchi S, Urasaki Y, Matsuki T, Fujieda S. (2006).Collaborative action of NF-kappaB and p38 MAPK is involved in CpG DNA-induced IFN-alpha and chemokine production in human plasmacytoid dendritic cells. *J Immunol*. 177(7):4841-52.

301. Honda, K., Y. Ohba, H. Yanai, H. Negishi, T. Mizutani, A. Takaoka, C. Taya, and T. Taniguchi. (2005). Spatiotemporal regulation of MyD88-IRF-7 signalling for robust type-I interferon induction. *Nature.* 434:1035–1040.

302. Danis B, George TC, Goriely S, Dutta B, Renneson J, Gatto L, Fitzgerald-Bocarsly P, Marchant A, Goldman M, Willems F, De Wit D. (2008). Interferon regulatory factor 7-mediated responses are defective in cord blood plasmacytoid dendritic cells. *Eur J Immunol* 38(2):507-17.

303. Critchley-Thorne RJ, Simons DL, Yan N, Miyahira AK, Dirbas FM, Johnson DL, Swetter SM, Carlson RW, Fisher GA, Koong A, Holmes S, Lee PP. (2009). Impaired interferon signaling is a common immune defect in human cancer. *Proc Natl Acad Sci USA*. 106(22):9010-5.

8.0 Appendix

8.1 Buffers

Blood DC Enumeration Buffer
0.5% BSA: 0.01% NaN_3; 1x PBS

1X BD FACS™ lysing solution
5mL of 10X BD FACS™ lysing solution in 45mL distilled H_2O

FACS Buffer
10% FCS; 1x PBS without Ca^{2+}/Mg^{2+} (pH7.2-7.4) (PAA); 0.1% NaN_3

3.75% PFA
5mL of 37.5% Formaldehyde solution (Microscopy grade) in 45mL distilled H_2O

MACS Buffer
0.5% BSA; 2mM EDTA; sterile 1xPBS without Ca^{2+}/Mg^{2+} (pH 7.4);

Dead Cell Removal Binding Buffer
25 mL of 20X dead cell removal binding buffer; 475 mL sterile double distilled H_2O

Fixation Solution for Immunofluorescence
1.0% Formaldehyde in PBS

Permeabilisation Buffer for Immunofluoresence
0.25% Triton-X (v/v); 1x PBS without Ca^{2+}/Mg^{2+} (pH7.4); 3% FCS

Wash Buffer for Immunofluorescence
0.1% BSA; 1x PBS without Ca^{2+}/Mg^{2+} (pH 7.2-7.4)

ELISA Coating buffer
PBS without Ca^{2+}/Mg^{2+} (pH 7.2-7.4)

ELISA Wash Buffer
0.05% Tween-20 (v/v); 1x PBS without Ca^{2+}/Mg^{2+} (pH 7.2-7.4)

Blocking Buffer for ELISA (IFN-α)
0.05% Tween-20 (v/v); 0.1% BSA; 1x PBS without Ca^{2+}/Mg^{2+} (pH 7.2-7.4)

Assay diluent for ELISA (IFN-α)
0.05% Tween-20 (v/v); 0.1% BSA (w/v); 1x PBS without Ca^{2+}/Mg^{2+} (pH 7.2-7.4)

Blocking Buffer for ELISA (IL-10)
5.0% BSA (w/v); 1x PBS without Ca^{2+}/Mg^{2+} (pH 7.2-7.4)

Assay diluent for ELISA (IL-10)
1.0% BSA (w/v); 1x PBS without Ca^{2+}/Mg^{2+} (pH 7.2-7.4)

ELISA Stop Solution
1N H_2SO_4 in H_2O

Complete Cell Culture Medium
RPMI 1640 (with Glutamine) (PAA) ; 10% FCS; 1% Penicillin/streptomycin
IMDM (with Glutamine) (PAA); 10% Human AB Serum; 1% Penicillin/streptomycin

Freezing Medium
10% DMSO; 90% FCS

Trypan blue
3.6 mL diluted with 6.4 mL 1X PBS.

50X TAE Buffer
242 g/L Tris base
37.2 g/L Na2EDTA*2H2O
57.1 mL/L glacial acetic acid
in ddH2O, pH 8.5, storage at room temperature

SDS poly-acrylamide gel electrophoresis

5X Sample buffer
5ml glycerol (99% v/v); 1.5g SDS; 2.5ml β-mercaptoethanol; 1mL bromophenol blue (0.25% w/v); Adjust with H_2O to 7.5 mL and store at 4 °C

4X Upper Buffer, pH 6.8
3.03 g Tris-base (0.5 M); 0.2ml SDS (20 %); Adjust pH to 6.8 and with H_2O to 100 mL

4X Lower Buffer, pH 8.8
18.17 g Tris-base (1.5 M); 2ml SDS (20 %); Adjust pH to 8.8 and with H_2O to 100 mL
Separating gel (10 %)
4.0 mL ddH2O
3.3 mL 30% acrylamide/bis-acrylamide solution
2.5 mL Tris HCl (1,5 M, pH 8.8)
0.1 mL SDS (10 %)
0.1 mL APS (10%)
4 µL TEMED

Stacking gel 3 mL ddH2O
1.72 mL ddH2O
0.5 mL 30% acrylamide/bis-acrylamide solution
0.76 mL Tris HCl (0.5 M, pH 6.8)
30 µL SDS (10 %)
30 µL APS (10%)
3 µL TEMED

10X Electrophoresis Running Buffer
30g Tris-Base; 144g Glycine; 10g SDS; Adjust with H_2O to 1 L; store at room temperature

10X Western blot Transfer Buffer
30g Tris-Base; 145g Glycine; 3.74g SDS; Adjust with H_2O to 1 L; store at room temperature

PBS-T Washing Solution for Western Blot
1x PBS without Ca^{2+}/Mg^{2+} (pH 7.2-7.4); 0.1 % (v/v) Tween 20

Blocking buffer
(5 %) 5 % (w/v) powdered milk or BSA in PBS-T solution

8.2 MyD88 and IRF7 expression by pDCs from melanoma patients upon NDV stimulation

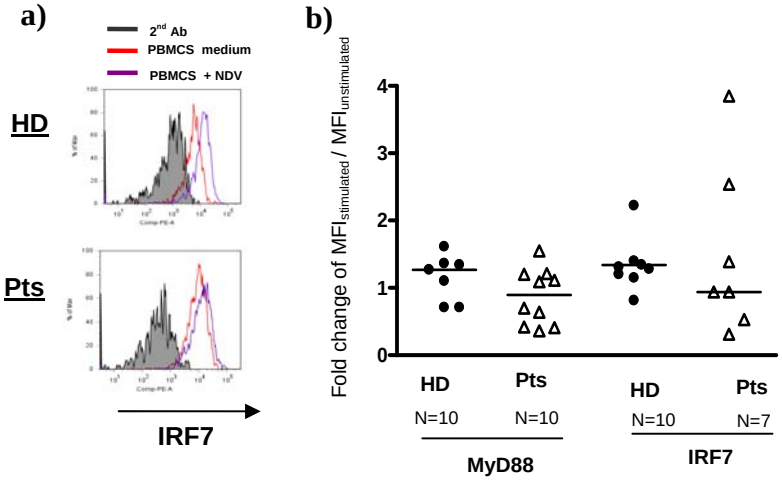

Figure 30: MyD88 and IRF7 expression in pDCs from melanoma patients after NDV infection. PBMCs from melanoma patients (Pts) and healthy donors (HD) were incubated with either UV-inactivated NDV or in medium for 6 h. The cells were then harvested and stained with antibodies against surface antigens CD123, CD11c and BDCA-2 followed by intracellular staining of MyD88 or IRF7. (a) The expression levels of IRF7 on $CD123^+BDCA2^+CD11c^-$ pDC are shown in histograms, the fluorescence intensity is determined as median fluorescence intensity (MFI). (b) The fold changes ($MFI_{stimulated}$ / $MFI_{unstimulated}$) of MyD88 and IRF7 on $CD123^+BDCA2^+CD11c^-$ pDCs are presented in scatter plot, bars indicate median value of expression. *P<0.05.

Activation of TLR7 signalling, which sense the ssRNA of virus triggers the type I IFN production via the recruitment MyD88 with downstream complexes including TRAF6 and IRAK1. In this study, when we stimulated PBMCs with UV-inactivated NDV, a ssRNA type virus that can activate TLR7 signalling and TLR independent pathway (RIG-I and MDA-5), some tendency of reduced fold changes ($MFI_{stimulated}/MFI_{unstimulated}$) of MyD88 expression was noted in $CD123^+BDCA2^+$ gated pDCs from patients compared to healthy controls. Subsequent analysis on NDV stimulated PBMCs revealed a tendency of lower fold change of IRF7 expression in PBMCs from patients (Appendix 7.2, Figure 30). Statistic analysis revealed no significant difference on the fold changes of MyD88 and IRF7 expression between healthy controls and patients.